Effect of Loading Frequency on Dynamic Properties of Soils Using Resonant Column

by

Soheil Moayerian

A thesis

presented to the University of Waterloo

in fulfillment of the

thesis requirement for the degree of

Master of Applied Science

in

Civil Engineering

Waterloo, Ontario, Canada, 2012

AUTHOR'S DECLARATON

I hereby declare that I am the sole author of this thesis. This is a true copy of the thesis, including any required final revisions, as accepted by my examiners.

I understand that my thesis may be made electronically available to the public.

ABSTRACT

Dynamic properties of soils (shear stiffness and damping ratio) are critical for the design of structures subjected to vibrations. The dynamic properties of a benchmark standardized laboratory sand (Ottawa silica sand) were evaluated with two different resonant column devices, utilising software with different analytical approaches for the evaluation of soil properties. The dynamic properties (shear modulus and damping ratio) are evaluated as a function of the shear strain level. The results are compared to evaluate the effect of the type of equipment and the form of the data analysis on the measured dynamic properties of the samples. The results are discussed in light of the applicability of the procedures in practice, the ease of the testing methods, and the errors they introduced into analysis and design. In general, the shear wave velocities obtained from the two different devices are in good agreement. However, the damping ratios they give show considerable differences as strains increase.

Dynamic properties are typically measured by curve fitting of the transfer function between the excitation and the response using the resonant column device. However, the force function generated by sinusoidal sweep or random noise excitations induce different shear strain levels at different frequencies. Consequently, the shape of the measured transfer function is distorted and differs from the theoretical transfer function for an equivalent single-degree-of-freedom system. The difference between the measured and theoretical transfer functions as well as the bias in the computed dynamic properties

becomes more pronounced with the increase in shear strain. This study presents a new methodology for the evaluation of dynamic properties from an equivalent constant-strain transfer function. The soil specimen is excited simultaneously using a sinusoidal excitation (carrier signal) at the required strain level and small amplitude, narrow band random noise. The strain level induced by the fixed sine is shown to control the resonant frequency of the specimen; whereas the random noise introduces the required frequency bandwidth to determine the transfer function and hence the dynamic properties at a constant strain level. The new methodology also shows a good potential for the evaluation of frequency effects on the dynamic properties of soils in resonant column testing.

ACKNOWLEDGEMENTS

First and foremost, I would like to thank my supervisor: Prof. Giovanni Cascante for his guidance and patience. Without his help and encouragement this thesis would not exist.

I would to thank all members in NDT group. Especially thanks to Yen Wu and Zahid Khan for Their help through my study. My thanks are also due to Fernando Tallavo , Hassan Ali, Serhan kirlangic, Antonin Du Tertre and Paul Groves. I would like to also thank Shahriar Ofavezi for his supports and advices.

I would like to thank Professor Timothy A. Newson for his guidance and helps and also Lisa Katherine Reipas for her helps.

I am forever indebted to my parents and my sister for their understanding, endless patient and love.

Finally, Many thanks to my patient and loving wife, who gave me strength trough this work and she support me and encourage me whenever I was tired. Thanks to my lovely Kian and Nika for their motivation.

TABLE OF CONTENTS

CHAPTER 6

CONCLUSIONS AND RECOMMENDATIONS

LIST OF TABLES

LIST OF FIGURES

CHAPTER 1

INTRODUCTION

1.1 DEFINITION OF THE PROBLEM

The evaluation of soil properties by sampling methods is a powerful tool in geotechnical engineering. Dynamic properties of soils are used to solve problems such as response of foundations and structures to earthquake loads, machine excitations and wind and wave loads (Humar 2005). Soil characteristics are required before any geotechnical design. Shear wave velocity and damping ratios are dynamic properties required for soil characterization. The new National Building Code of Canada (NRC 2010) and allows the use wave velocity and acceleration factors for different soil classes; which are selected based on the average shear wave velocity of the top 30 m of the site profile.

Wave-based methods are well suited for lower depth measurements and the induced strain is small enough to assume that the medium responds in the elastic range (Cevic 2009). When a detailed space distribution of properties is needed, seismic methods provide unique complementary information not only to extrapolate data from boreholes but also to monitor processes (Groves et al. 2011). Seismic methods were used in the past decades to evaluate interfaces and structures in hydrocarbon exploration. Currently, wave-based methods are also used to infer properties of geomaterials such as

porosity, mineralogy, saturation and pore pressure (Cao et al. 2010, Crow et al. 2011, Tallavo et al. 2011).

The dynamic properties of soils can be measured either in the field or in the laboratory. In-situ testing facilitates determination of dynamic properties of soil in undisturbed state, and involves a large mass of soil (Groves et al. 2011, Crow et al. 2011).

In-situ measurement of dynamic properties may be affected by many sources of errors such as soil layering, inclusions, reflections from layers interfaces, and depth limitations of the testing technique. Wave propagation occurs during in-situ measurements, which introduces radiation damping; making it more difficult to quantifying the material damping ratio in-siu (Yang et al. 2010; Jiang et al. 2011; Das and Ramana 2011, Tsui 2009). On the other hand, laboratory determination of the dynamic properties is convenient and allows easy and precise control on different parameters that affect the soil properties. Laboratory determination of the dynamic properties is also affected by unknown sources of errors and unverified assumptions used in the analysis of data (Khan et al. 2008; Park 2010; Naggar 2008; Cascante et al. 2005) .

Resonant column and cyclic triaxial testing are ASTM standard tests and are widely used for the evaluation of dynamic properties of soils (ASTM 2000; Cascante et al. 2005). Having results from both these tests helps geotechnical engineers to know the behavior of sample in a wide frequency range between 0.01 Hz to 200 Hz. The resonant column is capable of determining dynamic properties at shear strain levels from very low ($\gamma < 10^{-6}$) to mid shear strain level ($\gamma < 10^{-3}$). Moreover, shear modulus and damping ratio

are measured independently of each other, contrary to the principle of causality and excessive number of cycles are imposed. To address some of these issues, a non-resonance method based on simultaneous evaluation of dynamic properties at different frequencies has been recently developed and tested at only very low strain levels. (Khan et al. 2008)

For large strain dynamic characterization of soils, the cyclic triaxial device have limitations in attainable strains and loading frequencies. Therefore, an appropriate set of devices may be needed to evaluate dynamic properties at wider range of strains and frequencies (Khan et al. 2011; Tsui 2009). Models predicting dynamic properties as a function of shear strain and frequency should only be reliable if they are developed based on reliable laboratory results. The resonant column device, RCD, provides more consistent test results; and it is considered one of the most accurate ways to determine the dynamic properties of soils at low to mid shear strain levels (ASTM 2000; Park 2010; Cascante et al. 2005; Khan et al. 2008). Resonant column (RC) tests are accurate and reliable; however, the effect of the excitation frequency and of different equipment characteristics on the results has not yet been evaluated. This is especially true in the damping measurements, which are significantly affected by the electro-motive force (EMF) (Cascante et al. 2003; Wang et al. 2003, Rix and Meng 2005).

The RC tests can vary in their configuration and the analytical methods used for the computation of the dynamic properties. While many testing programs were used to measure the dynamic properties of soils on a single resonant column apparatus (Stokoe et al. 1994, Dobry and Vucetic 1987; Cascante and Santamarina 1997, Khan et al. 2005,

Camacho et al. 2008), very few have evaluated the dynamic properties of the same soils as function of frequency and on different RC equipment. In most cases, in which a soil was tested on two different RC equipment, the tests were for calibration purposes, when the RC had been modified to accommodate different samples (e.g. stiffened base, Avramidis and Saxena 1990; Khan 2008). In this case, however, the same test method and data analysis are used in the initial and modified state of the RCDs. Fewer comparisons have been conducted with two RCDs that use different testing methods and different data analysis.

The standard RC testing method is based on harmonic excitation, sweeping the frequency around resonance. The transfer function is determined with small frequency increments in order to get precise values of damping and resonant frequency. This procedure is time consuming, especially for low damping materials that present sharp resonant peak. To overcome this limitation, random noise and sinusoidal sweep excitations were used (Park 2010, Prange 1981, Aggour et al. 1989, Cascante and Santamarina 1997). However, these excitations do not impose a constant strain on all frequencies; thus the reliability of the measurement rests on the definition of an equivalent strain level.

Previous studies have discussed the effect of different strain levels in frequency sweep tests (e.g. Cascante et al. 1997; Khan et al. 2008, Tsui 2009, Turan et al. 2009). These studies concluded that the error in the measured damping ratio increases with the increase in strain level because of the non-symmetrical shape of the measured transfer function. Although the measured transfer function can be curve fitted within acceptable

error at low strain levels, the goodness of the fit declines with the increase in shear strain level (Khan et al. 2008). Moreover, the effect of frequency on the dynamic properties is difficult to evaluate in the conventional RC testing and the recently proposed non-resonance (NR) method.

1.2 RESEARCH OBJECTIVES AND METHODOLOGY

The overall goal of this research is to investigate the effect of frequency on the dynamic properties of soils. The main objectives of this work are to develop a new method for the evaluation of dynamic properties of soils as a function of frequency and shear strain levels in the resonant column; and to evaluate the effects of different reonant column equipment and data analysis procedures on the dynamic characterization of sands and clays. For the first objective, a modified, Stokoe-type resonant-torsional column apparatus is used in this study. The calibration probes of lower resonant frequencies were selected to avoid the effects of base fixidity (Khan et al. 2008b). RC tests were performed on a sand specimen at a two confinements. The tests were performed using conventional RC method, NR method (using equal strains), and the proposed methodology (FN) at different shear strain levels. The details of test setup and methodology for each method are presented in the following sub-sections. The proposed new method is based on the novel idea of applying simultaneously sinuandal and random noise excitatiobns. Controlled sand samples are used to assess the validity of the proposed method. For the second objective, two different resonant columns are used: the resonant column developed at the University of Waterloo, and a resonant column device

that is commercially available (GDS Instruments). The effects of different equipment are evaluated by comparing resonant column tests on sands and clays. Excatly the same sample preparation techniques were used to enhance the difference in wave velocity and damping rations introduced because of the differences in the equipment and the data analysis procedures.

1.3 THESIS ORGANIZATION

Chapter 1 presents an introduction, the objectives and the general outline of the thesis. Chapter 2 provides the general background and review of the wave propagation, discusses the important factors affecting the dynamic properties, and the experimental techniques used for the measurement of dynamic properties. Chapter 3 evaluates two key assumptions in the analysis of resonant column results. The assumptions of the linearity of the first mode of vibration and fixed base are investigated. A new model based on the two-degree-of-freedom system instead of conventional single-degree-of-freedom is presented for the analysis of the resonant column measurements. Chapter 4 presents the evaluation of dynamic properties using two different resonant column devices to evaluate the effect of different instrumentation analysis methods on the measured dynamic properties. Controlled conditions are used for testing dry sand with constant density and confinement. Chapter 5 presents the evaluation of the frequency-dependent dynamic properties in the resonant column. This is usually difficult to assess in conventional resonant column tests. A new technique is proposed to measure the shear modulus and damping ratio simultaneously at a single frequency. Moreover, the non-resonance

methods, as well as the resonant method, are evaluated at larger frequency range and shear strain levels for comparison with our result from proposed techniques. Degradation of dynamic properties with shear strains using one frequency is included, which enables the comparison of results from resonant column using different methods.

Finally, the main conclusions and recommendations for further research are discussed in Chapter 6.

CHAPTER 2

DYNAMIC BEHAVIOR OF SOILS

2.1 INTRODUCTION

Shallow shear-wave velocity (VS) profiles are used in a variety of earthquake engineering applications, including site response in sedimentary basins, liquefaction analyse sand soil–structure Interaction evaluations. It is an important parameter in building codes and the engineering community widely uses VS in design applications. Hazard mapping methodology, particularly in urbanized areas, advances with the incorporation of more accurate local VS information. This trend is expected to accelerate with future expansion of these efforts. VS velocity has become the standard property from which in-situ shear modulus is determined because of its relative ease of measurement with seismic prospecting. (Raptakis, 2011)

Dynamic properties of soils are used to evaluate the dynamic response of soils at different strain levels in geotechnical engineering. Shear modulus and material damping ratio are the most important dynamic properties of soils. Wave propagation theory has been widely used to measure material properties. This chapter starts with a brief discussion on wave propagation modes and velocity, followed by a review of energy loss mechanisms in materials. Then, the factors that affect the dynamic response and the laboratory procedures used to measure damping are reviewed.

2.2 MECHANICAL WAVES

There are mainly two types of waves: body waves (compression and shear) and Rayleigh waves. Their features are described next.

2.2.1 Compression Waves

Compression waves, also known as P-waves, can propagate through the soil media generating particle motions that are parallel to the direction of propagation. Essentially, a particle is deformed (compressed) by the propagating wave, transferring its energy to an adjacent particle; similar to a linear arrangement of particles interconnected with springs.

Wave velocity is the ratio of the stiffness and the inertia of a material. The velocity of P-waves in an isotropic full-space is given by (Achenbach, 1984)

$$V_P = \sqrt{\frac{\eta + 2G}{\rho}} = \sqrt{\frac{M}{\rho}} \tag{2-1}$$

where η and G are Lame's constants, G is also called the shear modulus, ρ is the mass density of the medium, and M is the constrained modulus. The compressional wave velocity in an elastic-circular rod, when the wave length is much greater than the radius of the rod, is given by (Achenbach, 1984)

$$V_E = \sqrt{\frac{E}{\rho}} \tag{2-2}$$

where E is Young's modulus. Equations 2-1 and 2-2 indicate that compressional waves travel faster in the infinite space than in a rod (Poisson's ratio ≠ 0), because the lateral displacements are constrained in the infinite medium, leading to higher stiffness. P-waves are subjected to "geometric dispersion" as implied by Equation 2-1 and 2-2.

There are two types of compressional waves in saturated soils (Biot, 1956): compressional waves of the 1st and 2nd kind. Waves of the 1st kind have low attenuation and propagate with very little dispersion. In this case, the liquid and the solid tend to move in-phase. Compressional waves of the 2nd kind attenuate very rapidly and have significantly lower velocity. They are also called diffusional waves (Stoll, 1978); the liquid and the solid tend to move out-of-phase. A comprehensive study of wave propagation in saturated media was reviewed by Bourbie et al. (1987).

2.2.2 Shear Waves

The particle motion in shear waves is perpendicular to the direction of propagation. Shear waves are not subjected to geometric dispersion as P-waves are. Thus, the velocity of propagation in either an infinite space or a rod is the same, and it's given by (Humar J.L., 1970)

$$V_s = \sqrt{\frac{G}{\rho}} \tag{2-3}$$

Shear waves can be polarized in any given plane. This property has been used in many experimental studies (e.g., Stokoe and Hoar 1977; Auld 1977). There is only one

type of shear wave in saturated porous media that can travel through the rigid skeleton, affected only by the soil inertia and fluid viscosity.

2.2.3 Rayleigh Waves

Rayleigh waves (also known as surface waves) travel along the surface of a relatively thick solid material penetrating into a depth of one wavelength. Its particle displacement consists of elliptical motions in the vertical plane and parallel to the direction of propagation. The amplitude decreases with the depth. The material returns to its original shape subsequent to the particle displacement generated by the passing wave. For an input excitation generated at the surface of an elastic half-space, the Rayleigh waves are formed and they propagate outward from the source in a cylindrical wave front. The particle motion appears to be a combination of compression and shear waves, with components parallel and perpendicular to the direction of propagation. The particle displacement perpendicular to the direction of propagation attenuates faster than the longitudinal motion.

2.3 DAMPING RATIO

It is defined as the ratio between the system damping and the critical damping (no oscillatory movement involved). From the equation of motion for a single degree of freedom system with viscous damping, the damping ratio is expressed as (Humar J. L., 2005)

$$D = \frac{C}{C_c} = \frac{C}{2\sqrt{k \cdot m}} \qquad (2\text{-}4)$$

where C_c is the critical damping coefficient, C is the system damping coefficient [N/(m/s)], k and m are the stiffness and the mass of the system, respectively.

The critical damping corresponds to the limit between oscillatory motion and non-oscillatory motion. The system is over-damped for D > 1, critically damped for D=1 and under damped for D < 1.

2.4 DYNAMIC PROPERTIES IN THE LABORATORY

In current practice of geotechnical engineering, the measurement of dynamic shear modulus and damping ratio is performed independently. Different in-situ and laboratory techniques are used for this purpose. In general, laboratory techniques provide more accurate measurements compared to in-situ measurements; however, there are limitations and assumptions associated with laboratory techniques. Laboratory measurements are very difficult to operate at very low strain levels. Only resonant column and pulse velocity techniques (bender elements, ultrasonics) offer the very small strain level measurements. Figure 2.1 illustrates the strain levels achieved in most common in-situ and laboratory techniques.

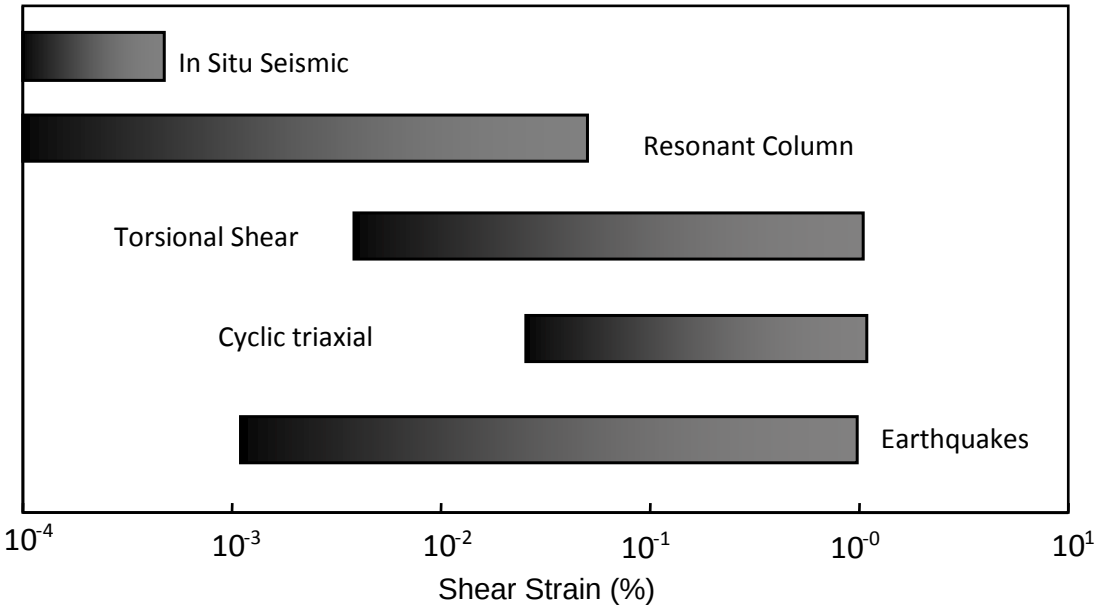

Figure 2.1: Shear strains mobilized in in-situ and common laboratory techniques (Ishihara 1996)

The resonant column device permits testing a specimen under axi-symmetric loading in steady state vibration and in free vibration (Fig. 2-2). There are different types of resonant columns, depending on boundary conditions and mode of vibration.

Wilson and Dietrich (1960) developed a fixed-free resonant column to measure both longitudinal and torsional vibrations. Hardin and Richart (1963) described two devices with free-free end conditions to measure torsional and longitudinal vibrations. Hardin and Music (1965) developed a resonant column device which allowed the application of deviatoric axial loads. All these devices were designed to operate at small strains (in the range of 10^{-5}). In 1967, Drnevich developed a free-fixed resonant column which allowed for strains greater than 10^{-4}. Later, devices that combine resonant column and torsional shear were designed to measure dynamic properties of soils for shear

strains between 10^{-6} and 10^{-1} (Drnevich, 1978; Drnevich et al., 1978; Isenhower, 1980).

In the resonant column test, a solid or hollow cylindrical specimen is subjected to harmonic excitation by an electromagnetic driving system. In a fixed-free configuration, the specimen is assumed fixed at the base and free at the top. The mass attached to the top of the specimen (driving plate) is driven by sets of coils and magnets. The soil can be excited in torsional, flexural, and axial modes of vibration at different confinements and shear strain levels.

In the fixed-free configuration of the resonant column, the distribution of angular rotation (φ) along the specimen is given by a quarter-sine function if the mass polar moment of inertia of the driving plate tends to zero ($I_o = 0$). Conversely, the distribution of angular rotation approaches a straight line as the ratio of the mass polar moment of inertia of the specimen (I) and the drive plate I/I_o tends to zero (Fig. 2.2).

Two parameters are obtained from resonant column measurements: resonant frequency and damping coefficient. Wave velocity and attenuation are computed from these measurements. The computation of the damping coefficient assumes an equivalent, uniform, linear viscoelastic specimen, i.e. Kelvin-Voigt model (Hardin 1965, Hardin and Scott 1966). This model predicts a response similar to the response observed in sand specimens, even though damping in sands is not necessarily of viscous nature (Hardin, 1965; Hardin and Scott, 1966). The frequency dependency of wave velocity and

attenuation is difficult to obtain with this device because of problems involved in measuring high resonant modes (see Stoll, 1979 for alternative approaches).

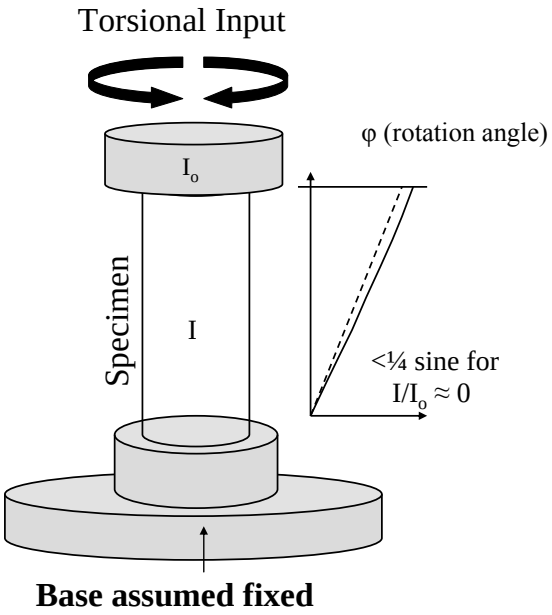

Figure 2.2: Fixed-free resonant column schematic

The effect of the rigid mass at the top of the sample is important for the calculation of shear wave velocity and the shear strain at resonance. If the rigid mass tends to zero, the first mode is a quarter sine wave, hence the shear strain is not constant throughout the height of the sample. If the rigid mass tends to infinity compared with the mass of the sample, the first mode approaches a straight line and the shear strain is constant at a given radius (Woods, 1978).

Several testing effects on resonant column results have been studied including: aging due to number of cycles (Drnevich and Richart, 1970), coupling between the specimen and end platens (Drnevich, 1978), restraint of the sample due to end platens

(Alarcon-Guzman, 1986) and membrane penetration (Frost, 1989; Drnevich, 1985; suggested that the latex membrane should have a thickness less than 1% of the specimen diameter). In general, these effects are negligible when the shear strain amplitude is small ($\gamma < 10^{-4}$). Furthermore, small deformations permit assuming in-plane strain conditions in data interpretation. The shear strain varies radially throughout the specimen; the representative value most often selected is the shear strain at r = 0.707∗R, where R is the radius of the sample. This strain is an average strain for the volume of the sample.

The solution of the motion of resonant column specimen to applied torque is presented in Appendix A. In conventional resonant column tests, the solution is obtained by considering an elastic medium with negligible damping ratio. The equation has the form (Lai et al., 2001)

$$\frac{T_o(\omega)\, e^{-i\phi(\omega)}}{\varphi(\omega)} = J_P\, \rho\, \omega^2\, H \frac{1}{\left[\sqrt{\frac{\rho\, \omega^2 H^2}{G_S}}\, \tan\left(\sqrt{\frac{\rho\, \omega^2 H^2}{G_S}}\right)\right]} - I_o\, \omega^2 \qquad (2.5)$$

where T_o is the applied harmonic torque, φ is the rotation angle of the specimen, ϕ is the phase lag between torque and rotation angle, G_S is the shear modulus, ρ is the density, J_P is the polar moment of inertia, H is the height of the specimen, and ω is the excitation frequency. At resonance, the excitation frequency $\omega = \omega_o$ and due to negligible damping the response of the system (rotation) becomes so large that the left hand side of Eq. 2.5 tends to zero. At this condition the solution becomes (Lai et al., 2001)

$$\frac{I}{I_o} = \sqrt{\frac{\rho\,\omega_o{}^2 H^2}{G_S}}\,\tan\left(\sqrt{\frac{\rho\,\omega_o{}^2 H^2}{G_S}}\right) \tag{2.6}$$

Damping ratio in conventional resonant column tests is defined as the ratio between system damping and critical damping. From the equation of motion of a single degree of freedom system with viscous damping, the damping ratio is expressed as (Humar J. L., 2005)

$$\xi = \frac{C}{C_c} = \frac{C}{2\sqrt{k\,m}} \tag{2.7}$$

where C_c is the critical damping coefficient, C is the viscous damping coefficient [N/(m/s)], k and m are the stiffness and mass of the system, respectively. The critical damping represents the limit between harmonic motion and non harmonic motion; the system is over-damped for $\xi > 1$, critically damped for $\xi = 1$ and under damped for $\xi < 1$.

The solution of Eq. 2.6 yields the elastic shear modulus of specimen material, and its material damping ratio has to be evaluated independently. However, in a viscoelastic medium the dynamic properties are not independent and have to be evaluated simultaneously. A convenient method is to replace the shear modulus in Eq. 2.5 with complex shear modulus using the viscoelastic correspondence principle as discussed before. Solving Eq. 2.5 based on complex modulus allows the determination of frequency dependent dynamic properties. The procedure of determining frequency dependent dynamic properties in resonant column is known as non-resonance method (Lai et al., 2001).

Both conventional and non-resonance methods in resonant column can be performed in voltage based or current based measurements (Cascante et al., 2003). Voltage based measurements yield significantly large damping ratios; therefore, the values have to be corrected. Cascante et al. (2003) present transfer functions for the correct measurement of damping ratio from either voltage or current based measurements.

2.5 FACTORS AFFECTING THE DYNAMIC RESPONSE

The most important factors that affect the dynamic behaviour of soils can be divided into two main categories (Kramer, 1996). Firstly, external variables such as stress/strain path, stress/strain magnitude, stress/strain rate, and stress/strain duration can affect the dynamic property of soils. Secondly, the characteristics of the material, such as soil type, size and shape of soil particles, and void ratio, can affect the response of the material to any dynamic loading.

2.5.1 Cyclic Shear Strain

Experimental results show that the magnitude of applied stress or strain is the most important external variable affecting the soil's dynamic behaviour .The strain level induced in soil mass are measured during dynamic excitation.

The response of soils below the linear cyclic threshold shear strain (Vucetic, 1994) is linear but not elastic, since energy dissipation occurs even at very small strain levels (Lo Presti and Pallara, 1997; Kramer, 1996). The linear response of a soil is

exhibited by constant soil stiffness; whereas, energy dissipation at very small shear strain levels occurs due to the time-lag between cyclic strain and stress (typical of viscoelastic behaviour). Soil properties are also independent of the number of excitation cycles below linear cyclic threshold shear strain level (Ishihara, 1996).

Experimental observations of the soil response in small strain level are characterized by permanent changes in volume in drained tests and development of pore pressure in undrained tests (Vucetic, 1994). The response of soils is non-linear viscoelastic; however, material properties do not change significantly at this stage, and little degradation is measured by way of the number of cycles.

In an intermediate strain level, also called pre-failure, instantaneous energy dissipation/losses occur over a finite period of time in function of the number of cycles. In this level the degradation of soil properties is demonstrated not only within the hysteretic loop but also with the increase of number of cycles (Ishihara, 1996). The behaviour of soils in this shear strain range is characterised as non-linear elasto-visco-plastic.

Energy losses occurring below the volumetric threshold shear strain are considered as viscoelastic in nature, e.g., they only occur over a finite period of time. The value of volumetric threshold shear strain varies with the soil type. The upper region corresponding to this range is 0.005 % for gravels, 0.01 % for sands, and 0.1 % for normally consolidated high plasticity clays (Bellotti et al.,1989; Vucetic and Dobry, 1991).

Table 2.1: Soil behaviour and shear strain level (Ishihara, 1996)

Shear Strain	Very Small $\gamma < 10^{-7}$	Small $10^{-6} < \gamma < 10^{-3}$	Intermediate $10^{-3} < \gamma < 10^{0}$	Large $> 10^{0}$
Soil Behavior	Linar Inelastic	Non Linear Viscoelastic	Non- Linear Viscoplastc	Failure

There are three factors that limit the strain levels that can be obtained in resonant column testing. First, limited torque in the drive system; second, limited travel in the drive system; and third, limits in the deflection measuring system. By decreasing the length of the specimen, a higher strain can be achieved for the same rotation of the drive in a resonant column test. By fabricating taller base platens, shorter specimens can be employed. An additional benefit to using short specimens in torsional shear testing is that the resonant frequency of the specimen and drive plate system will be higher. This allows testing at higher frequencies without inducing significant inertial effects. The third limitation on strain in torsional shear testing is limits in the deflection sensor. The use of shorter specimens largely mitigates this limitation. Micro proximitors are typically employed to measure rotations of the RC/TS drive plate, from which strains can be calculated. The proximitor calibration was performed using a milling machine to obtain an accurate measurement between the proximitor and target . Sasanakul showed that the average linear range for the two proximitors is about 0.216 cm and that strain levels up to about 1.5% can be measured for a soil specimen with an aspect ratio of 2:1. One solution to measure higher strains is to employ a less sensitive proximitor with a large linear

measurement range. Another solution is to make a local strain measurement using a strain gage attached to the specimen membrane. (Bae, Y. S., 2009)

2.5.2 Stress/Strain Rate

Important external variables that affect the soil response are the stress/strain rate (frequency of excitation) and the duration (number of cycles). A number of studies have investigated the frequency effect on the response of soils (Dobry and Vucetic, 1987; Vucetic and Dobry, 1991; Shibuya et al., 1995; Malagnini 1996; Lo Presti et al., 1996). Results from these studies indicate that frequency effect depends on the strain level. The stiffness generally increases with the frequency, and low plasticity soils exhibit the lowest sensitivity to frequency.

Studies have shown that the damping ratio is frequency dependent at certain bandwidths, and frequency independent at others (Hardin and Drnevich, 1972; Shibuya et al., 1995; Lo Presti and Pallara, 1997). Shibuya et al., (1995) suggests the following conceptual diagram:

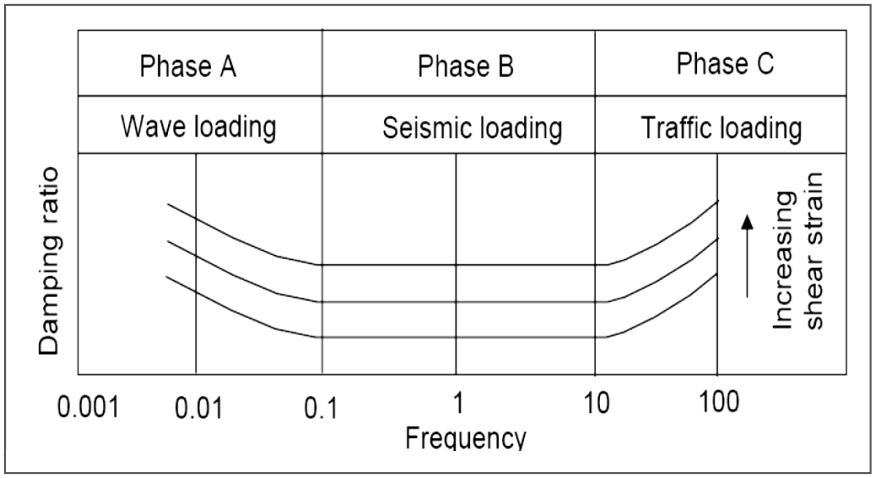

Figure 2.3: Frequency dependence of damping ratio within soil mass (Shibuya et al., 1995).

2.5.3 Duration of Excitation

The duration of excitation (also known as number of cycles) may significantly affect the soil's response to dynamic excitation. Experimental results show that in clayey soils and dry sands, the effect of the number of cycles is negligible at very small strain levels (Shibuya et al., 1995; Lo Presti and Pallara, 1997). The effect of the number of cycles becomes more significant as the shear strain level increases. In the case of sandy soils, as the number of cycles is increased, the stiffness increases in drained conditions; whereas, it decreases under undrained conditions (Dobry and Vucetic, 1997). The lower stiffness is associated to the decrease in the effective stress due to an increase in the pore pressure.

There are several factors, such as cyclic pre straining, creep, relaxation, anisotropy, digenetic processes, degree of saturation, and drainage conditions, that may affect the degradation of dynamic properties.

2.5.4 Moisture Content

When the soil mass is accelerated by the propagating wave, the fluid and the soil particles are subjected to different inertial forces. Viscous shear stresses develop within the pore fluid, decreasing away from the pore wall. (Winkler and Nur, 1982). Strong coupling of the solid and liquid phases exists for compressional waves; conversely, a lack of coupling is exhibited for shear waves.

Dynamic stiffness and damping characteristic were found to be substantially in dependent of saturation ratio in the range of 25-75%. However, by approaching the full saturation state, the values of modulus fall sharply and damping of loose samples increases dramatically from corresponding values of unsaturated levels. Results of drained tests revealed that most of increase in shear modulus and decrease in damping take place in the first 30 cycles. It was found that vertical consolidation stress is the most important parameter which affects shear modulus and damping ratio of sand. Similarly, relative density or void ratio significantly affects dynamic stiffness and damping under undrained conditions. Moreover, the influence of shears strain amplitude should be considered for both drained and undrained tests. (Jafarzadeh, 2011)

The attenuation and dispersion of low strain waves ($\gamma < 10^{-6}$) is controlled by the degree of fluid saturation and the frequency content of the wave (Murphy 1983; Winkler and Nur 1982). The strain amplitude dependence increases in water-saturated rocks (Winkler et al., 1979). Other mechanisms, such as the flow of droplets and the compression of the gaseous phase, participate in partially saturated media. These mechanisms specify the increase in attenuation with saturation, and the final reduction in attenuation when the medium reaches 100% saturation (Winkler and Nur, 1979).

The attenuation of compressional and shear waves responds differently in fully saturated and partially saturated media. In fully saturated media, the cracks and pores are compressed uniformly by the traversing P-wave producing no substantial fluid flow. Pure shear causes compression in some regions and dilation in others, enhancing the fluid flow. Thus, attenuation in fully saturated media is expected to be higher in shear than in compression. In the case of compression, the energy lost can be twice as great as the energy lost in shear. Furthermore, the large compressibility of the gas-water mixture enhances the fluid-flow mechanisms in the compressional mode (White, 1975; Murphy et al., 1982).

At low strains, the low saturation slightly increases the attenuation (fluid-flow mechanism); however, it generates a large increase at high strains when frictional losses prevail (Winkler and Nur, 1982). Hornby and Murphy (1987) considered the change in both bulk and shear moduli due to saturation with heavy hydrocarbon, and suggested the use of the ratio V_P/V_S to distinguish between oil saturated sands ($V_P/V_S < 2.5$) and

shales ($V_P/V_S > 2.5$). The change in attenuation for compressional and shear modes with saturation leads to an important diagnostic tool: $Q_P/Q_S > 1$ indicate full saturation and $Q_P/Q_S < 1$ indicates partial saturation (Winkler and Nur, 1979). This tool is very important for field measurements, particularly when the absolute values of the attenuation are difficult to determine. Thus, the attenuation provides information that is independent to the velocity, and in function of the saturation condition in the medium.

2.5.5 Confinement

The decrease in attenuation with an increased confining pressure within the near-surface pressure range is one of the most stable patterns that can be observed in the laboratory. At high pressure, attenuation remains constant, and it does not change with frequency or saturation condition (Johnston, 1981). This observation can be explained by the increase in the number and stability of contacts, and by the reduction of fluid flow and elastic dispersion as pores and cracks close with increased pressure (Winkler and Nur, 1982; Jones, 1986).

In the case of clays, the increase in confinement generates higher shear wave velocities, and decreases attenuation. The latter is mainly due to the reduction in void ratio during primary consolidation, and the strengthening of particle bonding after primary consolidation (Stokoe, 1980). The effect of time is more significant on the attenuation than on the shear wave velocity (Stokoe ,1980; Lodde, 1982).

2.5.6 Frequency

Stoll (1978) showed that the attenuation in saturated soils is frequency dependent. This study considered that the energy dissipation can be accounted by the inelasticity of the soil skeleton, and the viscous interaction of the fluid in the pore space. The soil-skeleton losses dominate at low frequencies, while the viscous losses prevail at high frequencies. "High" and "low" frequencies are relative to the physical properties of the soil under investigation. The attenuation peak of shear waves in a sand (porosity = 40%) changes from 500 Hz to 5000 Hz when the intrinsic permeability is reduced from 10^{-6} cm^2 to 10^{-7} cm^2. Stoll (1984) found that the attenuation in dry Ottawa sand was almost constant from 2 Hz to 1000 Hz. However, the attenuation increased with frequency in saturated Ottawa sand, reaching a maximum in the low kilohertz range. These results were well predicted by Biot's model. Nevertheless, Biot's theory failed to predict the frequency dependency of attenuation (1/Q) for low permeability silts (Stoll, 1985). Kim et al. (1991) used a torsional shear device and a resonant column (shear strain < 10^{-5}) to discover that the damping effects in dry sand are independent of frequency (0.1 Hz to 100 Hz). This was not the case for compacted clay beyond 10 Hz.

Table 2-2 presents a summary of the attenuation trends for increasing strain, confinement and frequency. The identification of parameters that affect attenuation is a fundamental stage in the investigation of the physical laws that control wave propagation.

Table 2.2: General Trends in Attenuation (After Badali and Santamarina, 1992).

	Material condition	Attenuation Parameter	Attenuation Trend	Measurement Device	Material	References
Strain	Dry	Damping Ratio	Increase	Longitudinal Oscillations	Clean Sand	Hardin, Drnevich 1972
		Logarithmic Decrement	Increase	Torsional Column	Ottawa Sand	Bae, 2009
			Increase	Longitudinal Oscillations	Ottawa Sand	Bae, 2009
	Saturated		Increase (Saturant Glycerin)	Longitudinal Oscillations	Ottawa Sand Test 19	Bae, 2009
			Increase	Torsional Column	Ottawa Sand	Jafarzadeh, 2011
			Increase	Torsional Column	Siltt	Jafarzadeh, 2011
Confinement	Dry	Damping Ratio	Decrease	Longitudinal Oscillation	Clean Sand	Drnevich Hardin,
		Logarithmic Decrement	Decrease	Torsional Column	Ottawa Sand	Cabalar, 2009
			Decrease	Torsional Column	Soil	Cabalar, 2009
			Decrease	Longitudinal Oscillation	Ottawa Sand	Cabalar, 2009
	Saturated		Decrease (Saturant Glycerin)	Longitudinal Oscillation	Ottawa Sand Test 19	Hall, Richart 1963
Frequency	Dry	Amplitude Ratio	Increase	Transmission Line	Sandstone Limestone	Khan , 2005
		Logarithmic Decrement	Increase then Decrease	Torsional Column	Sand and Silts	Khan, 2011
			Increase	Torsional Column	Fire Island Sand	Khan, 2011
	Saturated		Parabolic Downward	Resonance Column	Sand	Khan, 2011

2.6 CHAPTER SUMMARY

Wave propagation theory has been extensively used to measure material properties. Earlier work focused primarily on propagation velocity, due to difficulties in measuring attenuation. Recent developments in analysis procedures and electronics, together with the increased need for full-wave data interpretation, stimulated further studies in attenuation.

The dynamic properties of soils are essentially viscoelastic in nature when the mobilized shear strains are below the volumetric threshold shear strain level. Depending upon the shear strain level, the behaviour of soils can change from linear viscoelastic to non-linear viscoplastic. Different laboratory techniques are used to evaluate the dynamic properties at different frequencies and shear strain levels. The most common laboratory techniques, such as the resonant column, ultrasonic, and cyclic triaxial tests, can be used to model the behaviour of soils under dynamic excitation. These techniques excite the soil specimens in different modes and employ various analysis approaches to characterize the soils in viscoelastic range as far as the damping ratio is concerned.

CHAPTER 3

RESONANT COLUMN TESTING

3.1 INTRODUCTION

The resonant column device (RC) is used to measure the low and mid strain shear modulus and damping ratio of soils. In order to determine the resonant frequency of soil specimen, the resonant column device was used to measure the specimen response to different excitation frequencies (frequency sweep).

The solution of the equation of motion for a single degree of freedom (SDOF) system is used to determine shear wave velocity from the resonant frequency. Furthermore, material damping ratio can be measured by curve fitting the frequency (transfer function) or time domain (free vibration decay) data with the corresponding theoretical equations, or by the half-power bandwidth method (Cascante et al., 2003).

During a frequency sweep (constant excitation voltage), the imposed shear strain levels are not constant for all frequency components. Measurements of the variation of dynamic properties of soils (shear wave velocity and damping ratio) with frequency are difficult to perform in conventional RC tests.

The non-resonance (NR) method has been recently used to measure the dynamic properties of soils as a function of frequency (Lai et al., 2001; Rix and Meng, 2005). The NR method is based on the solution of the equation of motion governing the forced

vibrations of a continuous, homogeneous, and linear viscoelastic cylinder representing a soil specimen. The method allows determining simultaneously the shear wave velocity and material damping ratio at the same frequency of excitation (Khan, 2011). Since these parameters can be determined at different frequencies of excitation, the NR method is well suited to investigate the frequency dependence laws of these important soil parameters. The NR method founds its roots on viscoelasticity theory through the application of the elastic-viscoelastic correspondence principle The quantity determined experimentally is the complex shear modulus, which allows the simultaneous measurement of the shear wave velocity and shear damping ratio as a function of frequency.

The NR method has been used for low frequencies ($f < 30Hz$) and at low strain levels in cohesive soils (Lai et al., 2001; Rix and Meng, 2005). Meza and Lai (2006) showed that NR data from two cohesive soils are well described by the Kramers-Kroning relationships (Booij and Thoone, 1982), which constitute the necessary and sufficient conditions for a mechanical disturbance, propagating in a linear viscoelastic medium, to satisfy the fundamental principle of physical causality.

Results indicate that the NR and the RC methods give the same results at the resonant frequency of the specimen if the shear strain levels are the same. The NR method can be significantly affected by participation of flexural modes of vibration.

3.2 BACKGROUND

In a fixed-free RC configuration, the base of the specimen is assumed fixed and torsional loads are applied at the top of specimen. In the standard interpretation of the resonant-column test, the shear modulus and damping ratio of the specimen are computed by solving the equation of motion of a column-mass system (Richart et al., 1970). The torsional excitation should be perfectly perpendicular to the top surface of the specimen. However, from an experimental point of view, deviations from orthogonality occur and flexural modes are excited in addition to torsional modes (Cascante et al., 1998).

The analytical solution for a resonant-column test is obtained using a viscoelastic Kelvin–Voigt model for a material characterized by weak energy dissipation i.e., low material damping ratio. The shear stress in a slice of a specimen under torsional excitation is given by the following relation Hardin (1965):

$$T(Z,r,t) = G\,r\,\frac{d\,\theta}{d\,z} + c\,r\,\frac{d^2\,\theta}{dz\,dt} \tag{3-1}$$

Where $d\,\theta/d\,z$ angle of twist per unit length; r radial distance from the center of the specimen; z position along the height of the specimen; c viscous damping coefficient; and G elastic shear modulus. Therefore, the torque T along an arbitrary cross section of the specimen is given by:

$$T(Z,t) = G\,J_P\,\frac{d\,\theta}{d\,z} + c\,J_P\,\frac{d^2\,\theta}{dz\,dt} \tag{3-2}$$

where J_p area polar moment of inertia. Thus, the basic equation of motion for a rod undergoing torsional oscillations is given by Hardin (1965):

$$\frac{d^2\theta}{dt^2} = \frac{G}{\rho}\frac{d^2\theta}{dz^2} + \frac{c}{\rho}\frac{d^3\theta}{dz^2\,dt} \tag{3-3}$$

where ρ is the mass density. The solution of Eq. 3-3 is obtained using the separation of variables method and appropriate boundary conditions, which are (1) zero rotation at the fixed end of the soil column; (2) at the top of the specimen $z = H$; the torque must be equal to the applied torsional excitation Lai et al. (2001).

$$\frac{T_0}{\varphi\,(H)} = J_P\,\frac{\rho\omega^2 H}{\beta\tan(\beta)} - I_0\,\omega^2 \tag{3-4}$$

where I_o is the mass polar moment of inertia of the driving plate; V_s shear wave velocity; H height of the specimen; β rotation angle at z = H; and is given by Hardin (1965).

$$\beta = \frac{\omega H}{V_S}\sqrt{\frac{q+1}{2q^2}} \tag{3-5}$$

where q = $\sqrt{(1 + c\,\omega/G)^2}$. At the resonant frequency (i. e., ω_o) the amplitude of twist (rotation angle) approaches infinity for a zero damping material; thus , equation 3.4 become equation 3.6. (stokoe et al., 1994)

$$\frac{I}{I_0} = \beta\tan\beta \tag{3-6}$$

where I is mass polar moment of inertia of the specimen $I = \rho\,J_p\,H$; and for zero

value of damping ratio, $\beta = \omega H/V_S$ Eq. 3-6 is used in conventional RC testing to compute the shear wave velocity V_S of the material. The standard analysis of resonant-column results is then based on the continuum theory of elastic wave propagation; only when $I_0 >> I$ the fundamental frequency predominates and the approximation of a SDOF model can be used e.g., Richart et al. (1970).

The material damping ratio and resonant frequency is typically obtained by measuring the transfer function between induced current and resulting rotation of the top of the specimen during a frequency sweep. Figure 3.1 presents the typical measured transfer function during RC testing. The measured transfer function is curve fitted with a theoretical acceleration transfer function (TF(ω)) to obtain the resonant frequency and the damping ratio (e.g. Cascante et al., 2003).

$$TF(\omega) = \frac{-(\omega / \omega_o)^2 \left[\frac{B1 r_m r_a}{J} \right]}{\left[(1-(\omega / \omega_o)^2 + (c_E r_m{}^2 + d_s) \frac{(\omega / \omega_o) i}{\omega_o J} \right]} \qquad (3\text{-}7)$$

where B_1 (the effective product of the magnetic-field induction and the length of wire in the coils) is the magnetic force factor of the coils (N/A); J is the mass moment of inertia of the specimen and driving plate (kg•m^2); c_E is the damping coefficient that represents energy losses resulting from the eddy-current forces (N/(m/s)); d_S is the viscous damping coefficient that represents energy losses in the specimen (N•m^2/(m/s)); r_m is the distance from the centre of the specimen to the magnets (m); and r_a is the distance from the centre of the specimen to the accelerometer (m). The theoretical transfer function assumes that

the shear strains induced by all the frequencies in a frequency sweep are constant. At large strains; however, the goodness of fit deteriorates and the damping ratio is over estimated (Figure 3.1).

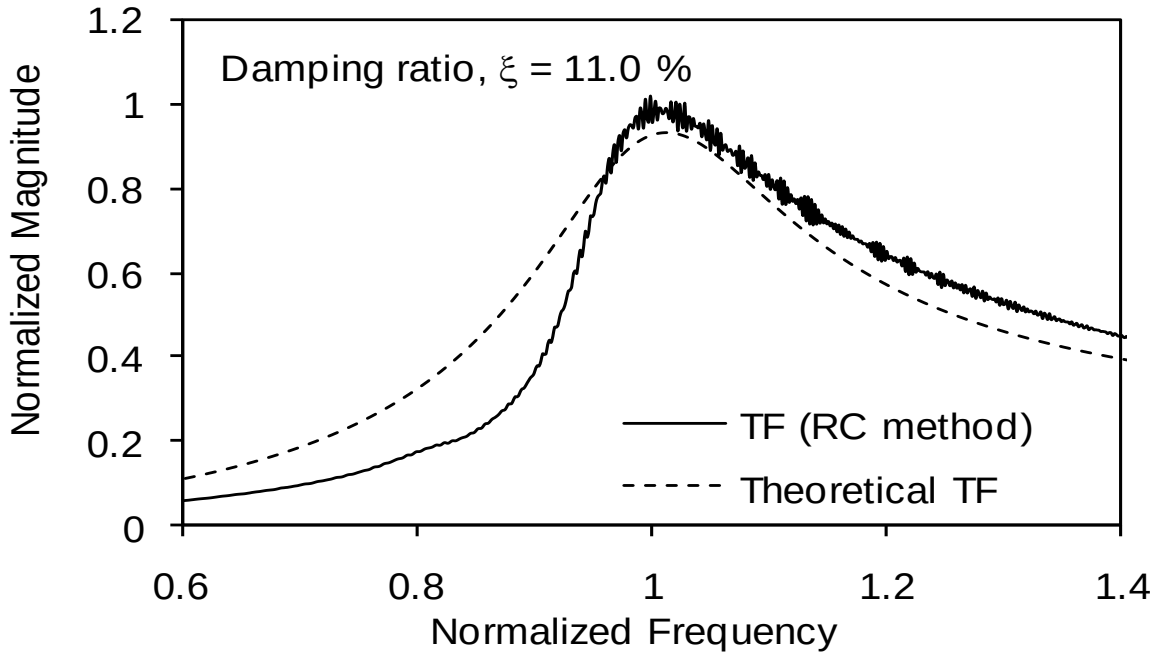

Figure 3.1: Transfer functions from RC measurements fitted with theoretical TF (f_o = 42 Hz, $\gamma = 5.27 \times 10^{-4}$).

The current in the coil system of resonant column is controlled by either a power amplifier or current amplifier. Irrespective of the type of amplifier used in the RC tests, shear strains at different frequencies are difficult to control. The shear strain associatedwith a measured resonant frequency is typically computed from the peak-to-peak acceleration response of the specimen in time domain by (Cascante et al., 2003)

$$\gamma = \frac{d\ g\ 0.71 V_{out}}{\pi^2\ 16\ r_a\ S\ H\ f_o\ 10^{\left(\frac{Amp}{20}\right)}} \tag{3-8}$$

where d is the diameter, g is acceleration due to gravity, V_{out} is the amplitude of response in volts, S is the sensitivity of the accelerometer, and Amp is the amplification in the filter amplifier. This equation can also be used to compute the shear strains at any frequency of excitation during equal strain testing.

Khan et al. (2008) presented the effect of unequal strains in a transfer function on the computation of dynamic properties. They proposed a new procedure of constructing the equal strain transfer function. The procedure is based on exciting the specimen with sinusoids inducing similar strains in the specimen and measurement of discrete values of transfer function (TF). The resulting transfer function (Figure 3.2) has a symmetrical shape even at large strains that improves the error in curve fitting of theoretical TF. The method; however, is time consuming and induces undesirable number of cycles to the specimen in calculating the Transfer Function which is critical at mid to large strain levels in loose sands and saturated soils.

Non-resonance (NR) methods involving single frequency excitation are based on elastic-viscoelastic correspondence principle (Christensen 1971, Lai et al., 2001, Lai and Rix 1998) which replaces elastic shear modulus with the complex-valued shear modulus. Khan et al. (2008) presented another non-resonance model based on transfer function approach. Solution for non resonant method is presented in appendix C .The substitution of elastic shear modulus with complex shear modulus allows the simultaneous

determination of dynamic properties but implicitly forces one of the property to be function of frequency even for a hypothetical response of an elastic material. Khan et al (2008) showed that the damping ratio of a hypothetical specimen with frequency independent damping (as assumed in RC testing) increases linearly with frequency.

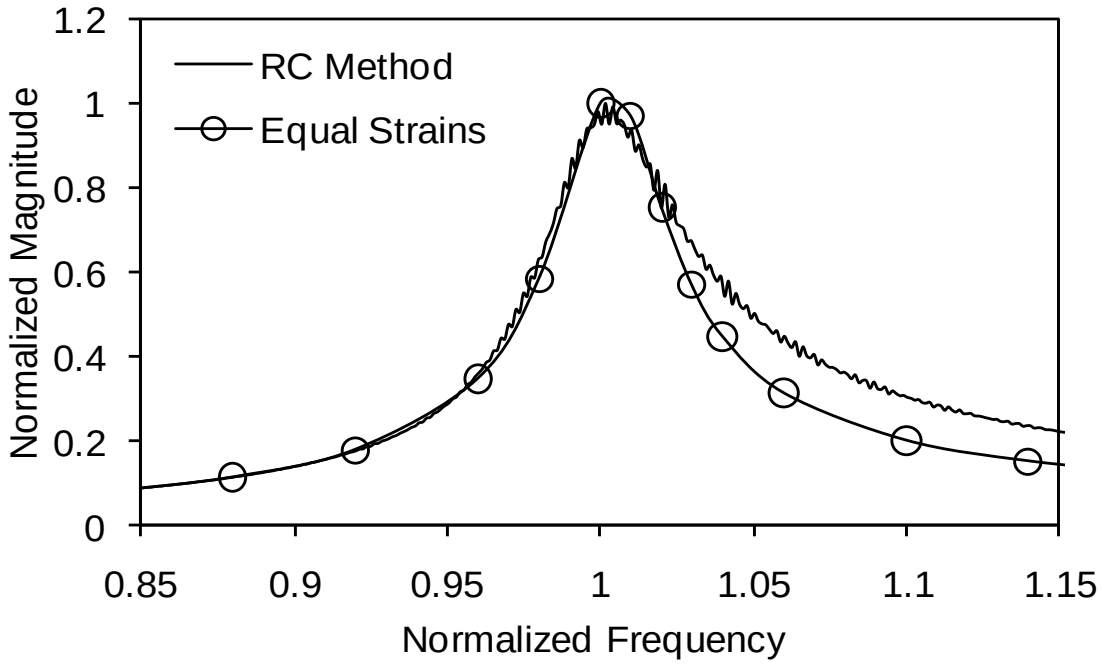

Figure 3.2: Transfer functions from equal strain and frequency sweep (RC) measurements (f_o = 51 Hz, $\gamma = 9.54 \times 10^{-5}$).

Material damping ratio could be determined from Eq. 3-4 written for q = 1 i.e., perfectly elastic material by using the elastic - viscoelastic correspondence principle Christensen 1971; Lai et al. 2001; thus, assuming that soil behavior at low-strain levels can be represented by a linear viscoelastic model. Meza-Fajardo and Lai (2007) derived a

closed-form solution for the Kramers– Kronig relationships and showed that experimental measurements 0 – 30 Hz for kaolin and natural clay are well described by the viscoelastic model. By replacing the elastic shear modulus with the complex-valued shear modulus $G_s^*(\omega)$, which is expressed in terms of the real, $G_1(\omega)$, and the imaginary, $G_2(\omega)$, components as: (Christensen, 1971)

$$Gs(\omega) = G_1(\omega) + i\, G_2(\omega) \tag{3-9}$$

thus, the complex value of the parameter β* is given by

$$\beta^* = \sqrt{\frac{\rho\, \omega^2 H^2}{G^*_S}} \tag{3-10}$$

Substitution of Eq. 3-10 in Eq. 3-4 yields an equation that can be solved iteratively for the complex shear modulus as a function of frequency, if the torque and rotation angle at the top of the specimen are known for a given excitation frequency. The torque and the angle of twist are in general out of phase because of energy dissipation, thus Eq. 3-4 can be rewritten as (Lai et al., 2001; Lai and Rix, 1998).

$$\frac{T_0(\omega)e^{-i\,\theta\,(\omega)}}{\varphi(\omega)} = \frac{I\,\omega^2}{[\sqrt{\rho\,\omega^2H^2\,/G^*_S\,(\omega)}\,tan(\sqrt{\rho\,\omega^2H^2\,/G^*_S\,(\omega)})]} - I_0\omega^2 \tag{3-11}$$

Using the equation of motion for a cylindrical specimen subjected to a torsional excitation, the Lorentz force equation proportionality between the force applied to the system by the magnetic field in coils and the current in the coils, and representing the soil specimen in a resonant-column test by a SDOF system, the transfer function between the

torque and the angle of twist can be computed as (Khan et al., 2008)

$$\frac{T_0(\omega)e^{-i\,\theta\,(\omega)}}{\varphi(\omega)} = \left(I_0 + \frac{I}{3}\right)\ {\omega_0}^2\ [\,1 - \left(\frac{\omega}{\omega_0}\right)^2 + \ i\,2\,\xi\ \left(\frac{\omega}{\omega_0}\right)] \tag{3-12}$$

Eddy current damping, which is significant at low frequencies, can be easily incorporated into this equation (Cascante et al., 2005). Once the material damping ratio (ξ) and the resonant frequency (ω) are obtained from Eq. 3-12, the shear wave velocity is computed by solving Eq. 3-6. The dynamic properties computed by using Eq. 3-12 are referred to here as properties from the NTF method. Dynamic soil properties obtained from Eq. 3-11 are referred to as properties from the NR method. Finally, soil properties determined from the standard resonant-column method using a sinusoidal chirp excitation will be referred to herein as properties from the standard RC method (Eq. 3-6 and the half-power bandwidth method).

A hypothetical specimen with frequency-independent damping (as assumed in RC) testing is tested using the non-resonant method (frequency-dependent dynamic properties) to show the expected NR test results for the standard assumptions. The response of this hypothetical specimen in terms of the applied torque and the corresponding angle of twist are computed by using the transfer function approach proposed by Cascante et al. (2003, 2005). The hypothetical soil specimen has a resonant frequency $f_o = 29\ Hz$, shear wave velocity V_S = 257.7 m/s, and a damping ratio of ξ = 0.68%. The hypothetical specimen is used to show the expected results if a specimen

with constant damping (as assumed in the standard resonant-column test) is tested using the non-resonant method (frequency-dependent dynamic properties). The response of this hypothetical specimen was simulated by using the transfer function approach proposed by Cascante et al. (2003, 2005).

Figure 3.3 shows the soil dynamic properties obtained from the NR and the NTF methods for the simulated specimen. As expected, the shear wave velocity and shear damping ratio from the NTF method are constant. The shear wave velocity from the NR method is also constant for the frequency bandwidth of the simulation. However, the damping ratio increases linearly with frequency to fulfill the causality principle (i.e., Kramers–Kronig relationships) at the resonant frequency, both the NTF and NR methods predict the same value of the material damping ratio because the strain level is the same at this frequency. The SDOF approximation commonly used in the interpretation of RC tests does not fulfill the physical principle of causality for a linear viscoelastic material. This approximation linearly underestimates the damping ratio above resonance and overestimates it below resonance.

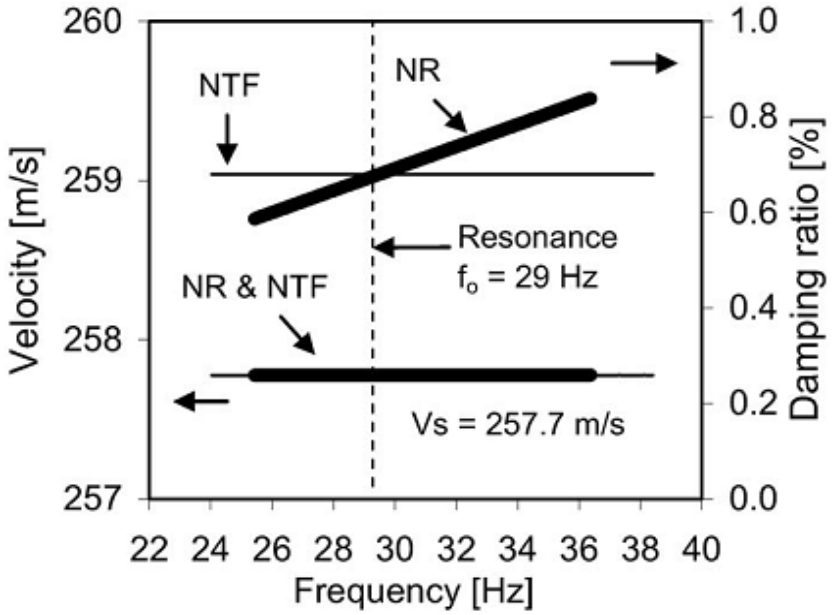

Figure 3.3: Comparison of simulated NR and the NTF tests results for a soil specimen: $f_o = 29$ Hz, $\xi = 0.68\%$, and $V_S = 257.7$ m /s (Khan et al., 2008)

3.3 THE UNIVERSITY OF WATERLOO DEVICE

A Stokoe resonant-torsional column device was used in this research (SBEL D1128). The cell and sample pressures are independently controlled by a Brainard & Kilman pneumatic pressure control panel. The air pressure system allows confining pressures up to 700 kPa. The axial deformation of the specimen is measured with a LVDT (Schaevitz 500HR) mounted inside the confining chamber. The input signal for the driving coils is generated by a function/arbitrary waveform generator (HP-33120A or the built-in signal generator in HP-35665A) through a power amplifier (Krohn-Hite 7500). During resonant testing, the response of the sample to torsional vibrations is monitored with one accelerometer mounted at the top, and one on the base (Columbia

Research 8402, and charge amplifier 1035). The output signal from these transducers is monitored and processed in a digital storage oscilloscope (HP-54600A with a HP-54657A Module), a universal counter (HP-53131A), a dynamic signal analyzer (HP-35665A), and by software developed as part of this research, running in a 486 computer. Figure 3.4 shows a general view of the setup and instrumentation; required components are boxed in full-lines, while optional devices are boxed in dashed-lines.

The driving system is 15 cm in diameter, which is close to the height of the sample. The solution neglecting the inertia of the driving system in the transverse direction is a good approximation just for the first mode of vibration, even in the extreme case when the radius of gyration is computed assuming the mass of the driving system concentrated at the position of the four magnets (h = 0.4; Fig. 3.5). For this device with $c=m_T/m$ smaller than 4, approximate Eqs. 3-6 and 3-7 have less than 0.3% error with respect to the theoretical values obtained with Eqs. 3-4 and 3-5. For typical soils, levels of confinement (10 kPa to 700 kPa), and standard specimen size (H=13 cm, R=3.5 cm), the torsional frequency is about 60% higher than the flexural frequency ($\omega_T \approx 1.6\ \omega_f$). Thus, mode coupling can be neglected for the expected damping coefficient at low strain.

Figure 3.4: Typical setup and instrumentation.

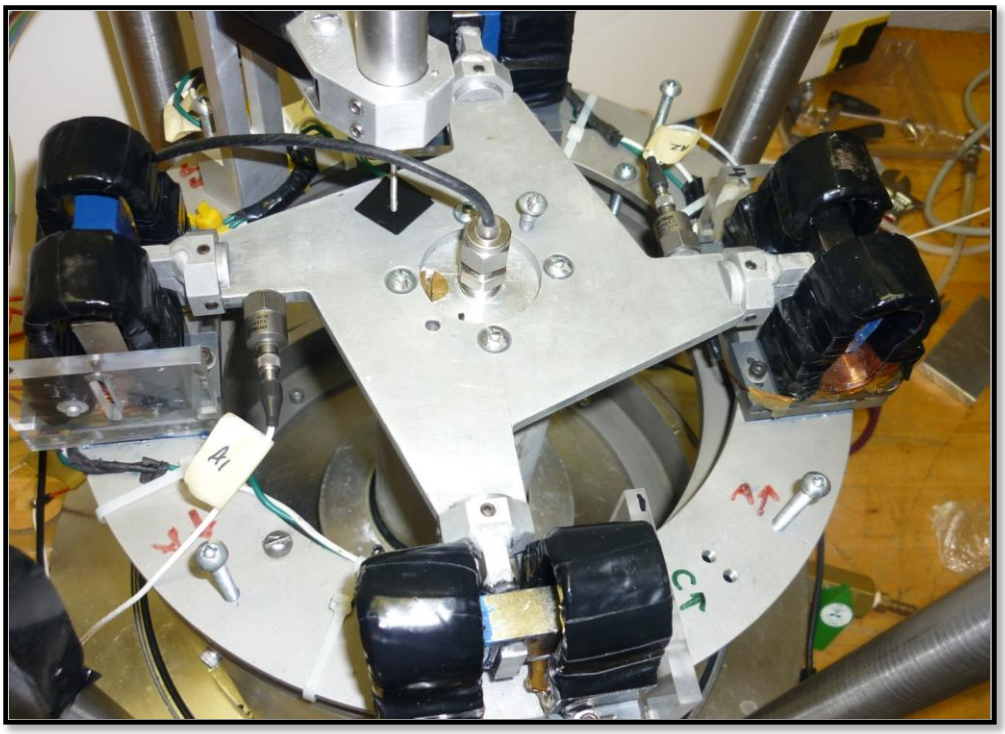

Figure 3.5: Sample position and magnets.

3.4 CALIBRATION – DRIVING SYSTEM

The computation of the shear wave velocity in the resonant column test requires the mass polar moment of inertia of the driving system I_o. In general, due to the complex geometry of driving systems, the experimental determination of I_o is preferred. A metal calibration specimen (Figure 3.6) and a mass are used to measure I_o assuming a single degree of freedom system with total mass equal to the mass of the driving system plus any additional mass attached to the system (Figure 3.7). Several aluminum and steel probes were manufactured to verify calibration in different frequency ranges. Equipment modes in the range of frequency of interest were assessed with a solid stiff steel sample. No spurious modes were detected. Characteristics of the calibration probes are summarized in Table 3.1.

Table 3.1 Characteristics of calibration bars

Device	Prob	Diameter (cm)		Length (cm)	Resonant Frequency (Hz)
		Outside	Inside		
RCD - 1	AL 1	0.955	0.701	22.54	12
RCD - 1	AL 2	2.534	1.901	22.54	97
RCD - 2	AL 3	1	0	10	40.7
RCD - 2	AL 4	1.5	0	10	90

The mass polar moment of inertia of the driving system must be re-calibrated whenever changes are made, e.g. transducers added to the top cap. Errors in the measurement of frequencies have a significant effect in the computation of I_o, for

example, a 5% error in frequency can produce a 50% error in the computed inertia of the driving system.

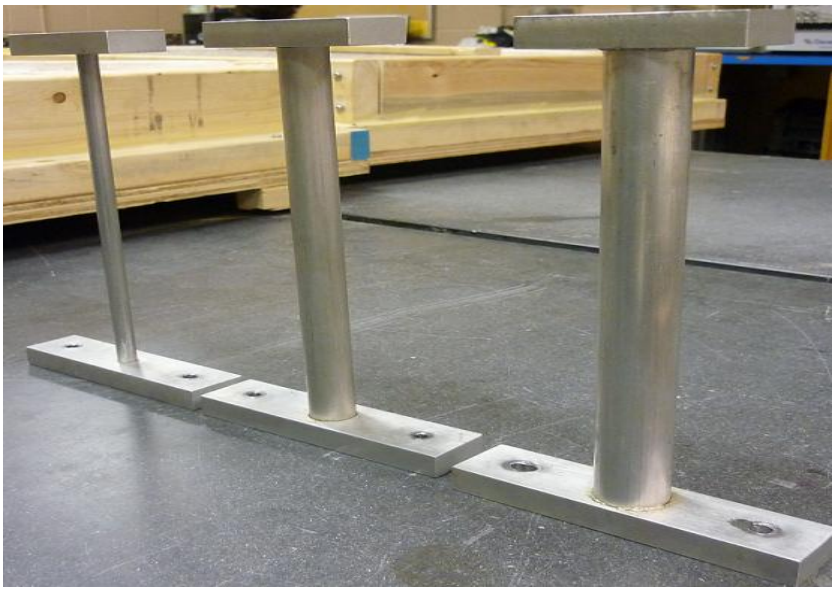

Figure 3.6: Calibration bars.

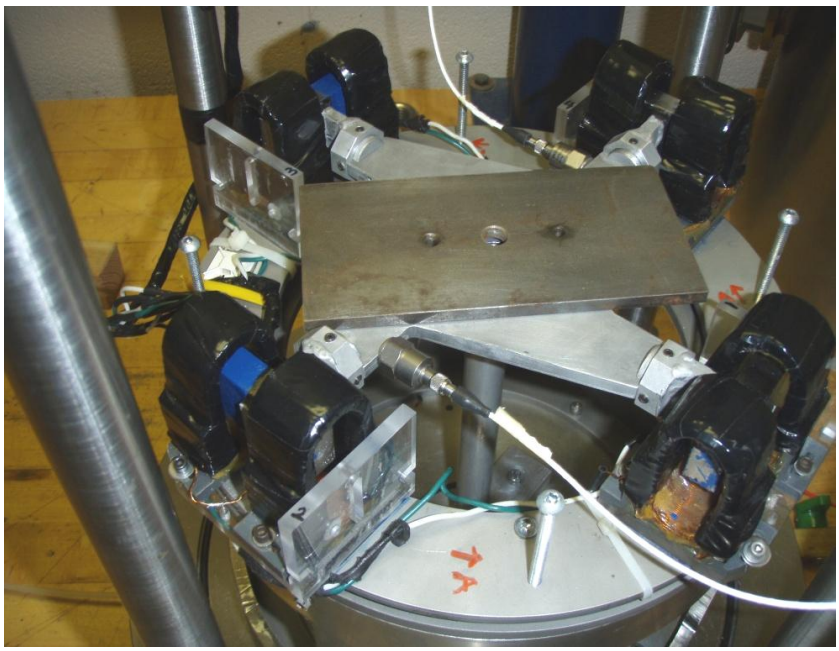

Figure 3.7: Additional mass for I_0 calculation.

3.5 REDUCTION OF EQUIPMENT GENERATED DAMPING

Equipment-generated damping in the resonant column (RC) test due to interaction between the magnets and solenoids in the drive system causes a bias error in measured values of material damping ratio. Calibration and post-measurement corrections have been used to address this problem.

Another error in RC measurements of material damping ratio arises from the use of solenoids and magnets [Fig.3.8(a)] to provide the torsional excitation (Kim, 1991; Hwang, 1997; d'Onofrio et al., 1999; Cascante et al., 2003; Wang et al., 2003). An AC current passing through the solenoids generates a uniform magnetic field that interacts with the permanent magnets. The resulting mechanical motion of the magnets applies a torque to the test specimen via the drive plate shown in Figure 3.8(b). An oscillating torque can be produced by switching the poles of the generated magnetic field. Simultaneously, the motion of the magnets results in a magnetic field that induces an electromagnetic force (EMF) in the solenoids according to Faraday's law. Furthermore, according to Lenz's law the induced EMF opposes the motion that produces it and is termed back-EMF. This back- EMF is an additional means of dissipating energy in the system above and beyond the intrinsic losses occurring in the test specimen and results in equipment-generated damping.

Back-EMF causes negligible errors in measured values of shear modulus (Wang et al., 2003). Previous studies (Kim, 1991; Hwang, 1997; Wang et al., 2003) have sought to quantify the magnitude of the equipment-generated damping and to develop correction

procedures. The results summarised in Figure 3.9 indicate that the equipment-generated damping may be as large as 4% at low resonant frequencies and decreases with increasing frequency. Errors of this magnitude are significant in the context of the material damping ratio of most soils, particularly at very small strains. These studies have recommended subtracting the equipment-generated damping from measured values to correct for the error.

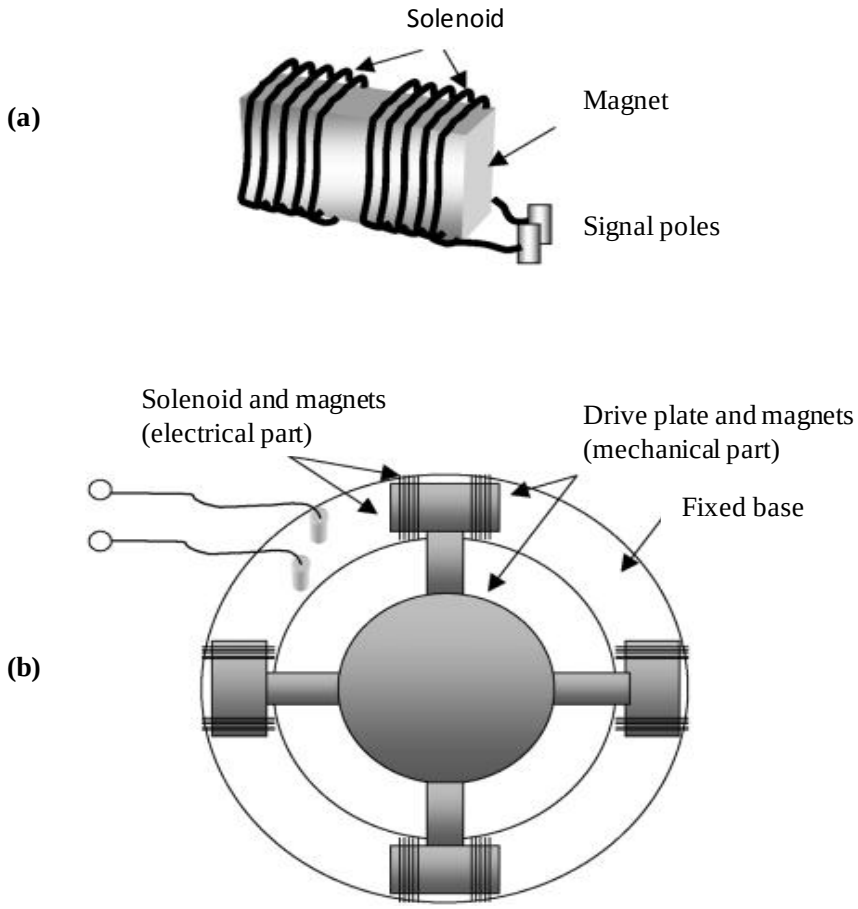

Figure 3.8: (a) Schematic diagram of the solenoid-magnet unit; **(b)** the drive system (top view) (Rix and Meng, 2005)

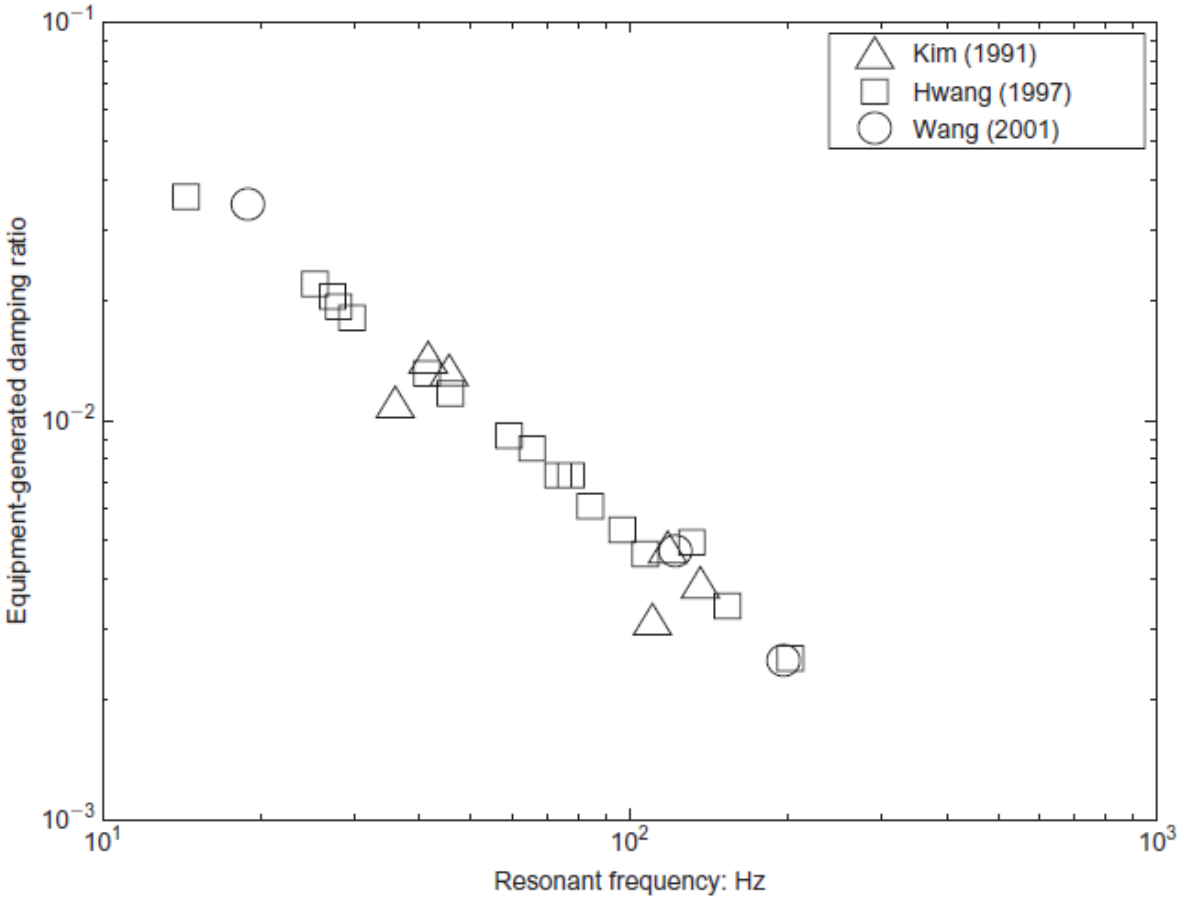

Figure 3.9: Equipment-generated damping ratio from RC measurements in previous research. (Tallavo, Cascante, Pandy, & Narasimhan, 2011)

3.6 EXPERIMENTAL METHODOLOGY

This study is consisted of three different projects. First we study the effect loading frequency on dynamic property of Mine paste at different strain level, confinement and age. Then a comparison study was conducted on sand between two different RC device to understand the equipment effect on our RC measurements. At the end of study we proposed new testing technique in RC measurements and compare it with previous method of testing.

The transfer function between the excitation force and the acceleration is computed by using both the top accelerometer and the miniature accelerometer. Random noise as well as burst chirp is used as excitation force (Cascante and Santamarina, 1997). For the evaluation of the torsional mode shape, a sinusoidal excitation is used at the resonant frequency of the specimen. The responses of the accelerometers are measured with a dynamic signal analyzer (HP 35670A). The driving plate is assumed rigid; therefore, the acceleration measured on the driving plate is only corrected by the location of the accelerometer with respect to the radius of the specimen. This procedure is repeated for different isotropic confinements to understand the effect of confinement on dynamic property measurement.

3.7 VOLTAGE-MODES AND CURRENT-MODE SOURCES

3.7.1 Voltage Source

An important factor to consider in studying equipment generated damping is the difference between voltage-mode and current-mode sources depicted in Figure 3.10. An ideal voltage-mode source maintains a specified output voltage regardless of the load impedance and the current through it. Theoretically, this is possible only if the internal resistance approaches zero, but all actual voltage sources have a finite internal resistance, Rs, typically about 50 Ω. When Rs is non-zero, the source voltage, Es, is subject to the voltage division rule. The load voltage is given as (Rix and Meng, 2005)

$$E_1 = \frac{R_1}{R_S + R_1} E_S \quad (3\text{-}13)$$

where R_1 is the load impedance. In the case of the RC apparatus, $R_1 = R_C$, where R_C is the resistance of solenoids. When the source resistance and the load impedance are comparable, a significant portion of the source voltage will be restricted to the source, and it will load itself. This is termed source–load mismatch, and is generally undesirable.

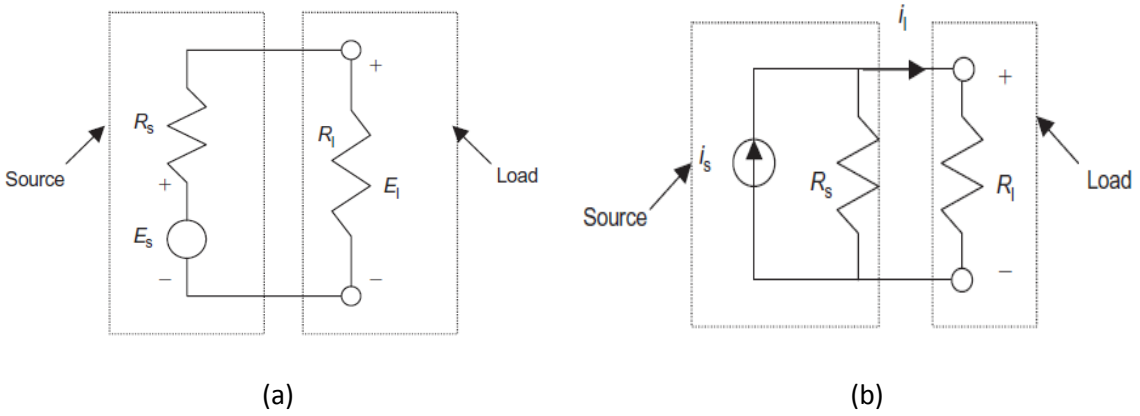

Figure 3.10: (a) Voltage-mode and (b) current-mode sources (Rix and Meng, 2005)

3.7.2 Current Source

An ideal current source provides a specified output current regardless of the load impedance and the voltage across it. This implies that the internal resistance of the source must be infinite, but all actual current sources have some finite internal resistance, typically several hundred kilo-ohms or greater. In this case, the source current, is, is subject to the current division rule. The load current is expressed as (Rix and Meng, 2005)

$$i_1 = \frac{R_S}{R_S + R_1} i_S \quad (3\text{-}14)$$

This implies that, when the source resistance is much higher than the load impedance, the load current is minimally affected by the load impedance.

3.8 EQUIPMENT EFFECTS

Both of the resonant column devices (RCDs) used in this study have a similar general configuration, where the base of the sample is fixed and the applied torsional excitation is at the top of the sample as shown in Figure 3.11 (Stokoe type resonant column). The two devices are referred as RCD-1 and RCD-2. The RCD-1 is a custom-made device (Cascante et al. 2003); whereas the RCD-2 is a commercially available system (GDS-RCA, 2009). The primary differences between the two devices relate to their geometry, electronic components, and the data analysis procedures for calculation of the material damping ratio. This section provides a summary of the background theory used in both resonant column devices.

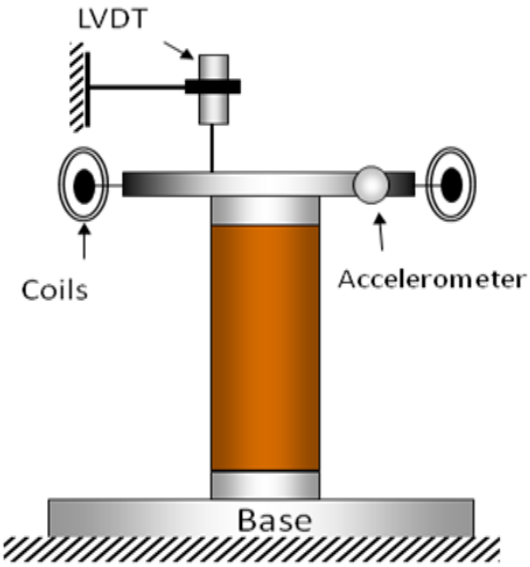

Figure 3.11: Basic schematic of fixed-free base resonant column device (Stokoe type).

The RCD-1 applies a sinusoidal chirp vibration with a wide range of frequencies to the soil specimen, and the resonant frequency is evaluated from the frequency response curve or transfer function of the system, which is represented as a single-degree-of-freedom system (SDOF). The applied torque (proportional to the current flowing through the coils) gives the input function; whereas the response function is given by the acceleration measured at the driving plate (Fig. 3.11). The damping ratio and the resonant frequency are determined by curve fitting the measured frequency response curve (Khan et al. 2008).

The instrumentation used in RCD-1 is illustrated in Figure 3.12. The input signal for the coils is generated by a built-in signal generator in a dynamic signal analyzer (HP-35670A). The low-power input signal is amplified by an audio power amplifier (Bogen

250W). The axial deformation of the specimen is measured with an LVDT (Schaevitz 500HR) mounted inside the resonant column device. The response of the specimen is measured with an accelerometer (PCB 353B65). The output signal of the accelerometer is monitored, processed, and stored in a digital oscilloscope (Agilent DSOX3014A), a dynamic signal analyzer (HP-35670A), and a computer. The cell and specimen pressures are controlled independently by a pneumatic pressure control panel (Brainard-Kilman E-400).

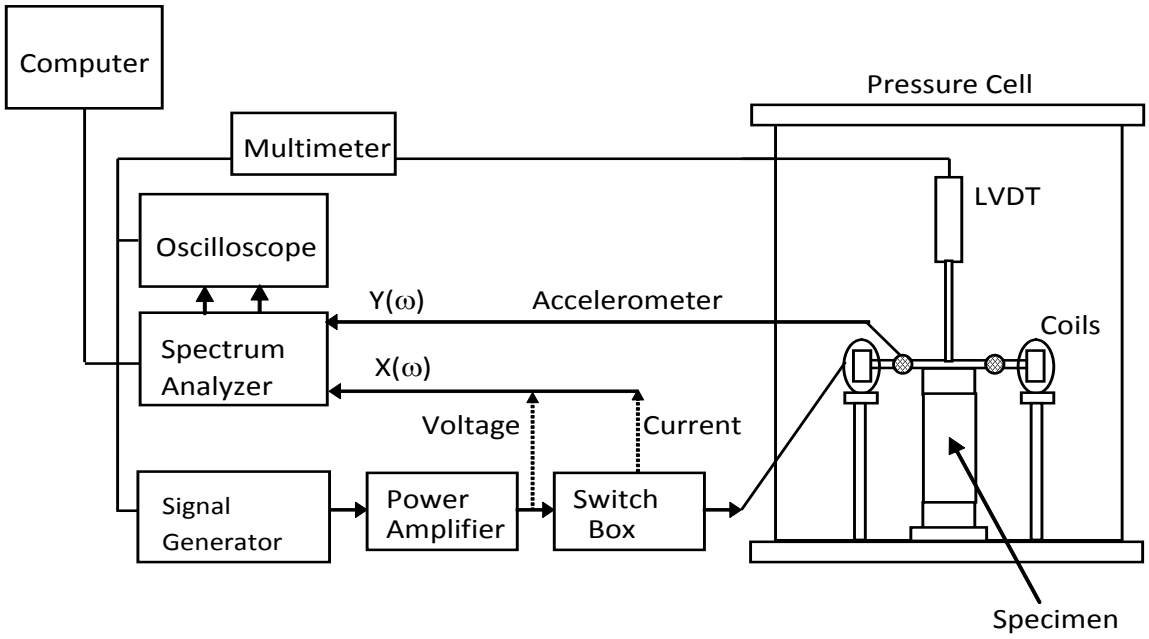

Figure 3.12: Typical instrumentation for resonant column device RCD-1.

The applied torque is computed from the measured current passing through the coils $I_C(\omega)$ at a given angular frequency (ω), and the distance from the magnets from the

center of the specimen (r_m). The experimentally measured magnetic coil factor (B_L) is used to convert current amplitude into torque amplitude as (Khan et al. 2008).

$$T_o(\omega) = B_L\, I_C(\omega)\, r_m \tag{3-15}$$

The spectral angular rotation of the specimen ($\varphi(\omega)$) is computed from the spectral acceleration measurement ($\ddot{X}(\omega)$) on the driving plate at a distance (r_a) from the axis of the specimen as

$$\varphi(\omega) = \frac{\ddot{X}(\omega)}{\omega^2\, r_a} \tag{3-16}$$

The phase lag between the torque and rotation is computed using the phase information from the cross-power Fourier spectrum of the input current and the output acceleration. The shear modulus and damping ratio as a function of frequency are computed by curve-fitting the transfer function between the applied torque, $T_o(\omega)$, and the induced angle of twist, $\varphi(\omega)$, as shown in Eq. 3-12 (Khan et al. 2008). This equation considers that the damping ratio (ξ) to be frequency independent.

The RCD-2 uses conventional methods for evaluation of shear modulus and damping ratio as outlined in ASTM D4015-2007. The instrumentation used in RCD-2 is illustrated in 3.13. The resonant frequency is assessed by applying different frequencies of excitation to the sample incrementally and selecting the frequency that corresponds to the maximum response in the measured frequency bandwidth. Once the resonant frequency is determined, the damping ratio is then computed using the free decay and the

logarithmic decrement method. At the resonant frequency, the amplitude of twist (or rotation angle) approaches infinity for a zero damping material; thus, the solution for the equation of motion for fixed-free RC is given by Eq. 3-6 (Richart et al. 1970). This equation is used in conventional RC testing to compute the shear wave velocity (V_S) of the material. The shear modulus G (kPa) is calculated from shear wave (V_S) and the bulk density (ρ) of the specimen as $G = \rho (V_S)^2$. The standard analysis of resonant column results is then based on the continuum theory of elastic wave propagation; only when $I_0 >> I$ the fundamental frequency predominates and the approximation of a SDOF model can be used. Therefore, to reduce data from the resonant column test, the mass polar moment of inertia of the drive system I_0 is required. As the drive system has a complex geometry, it is difficult to derive mathematically, its value is found experimentally. The mass polar moment of inertia of the specimen, I, is calculated from the mass (m) and the radius of the specimen (r) as $I = ½ m r^2$.

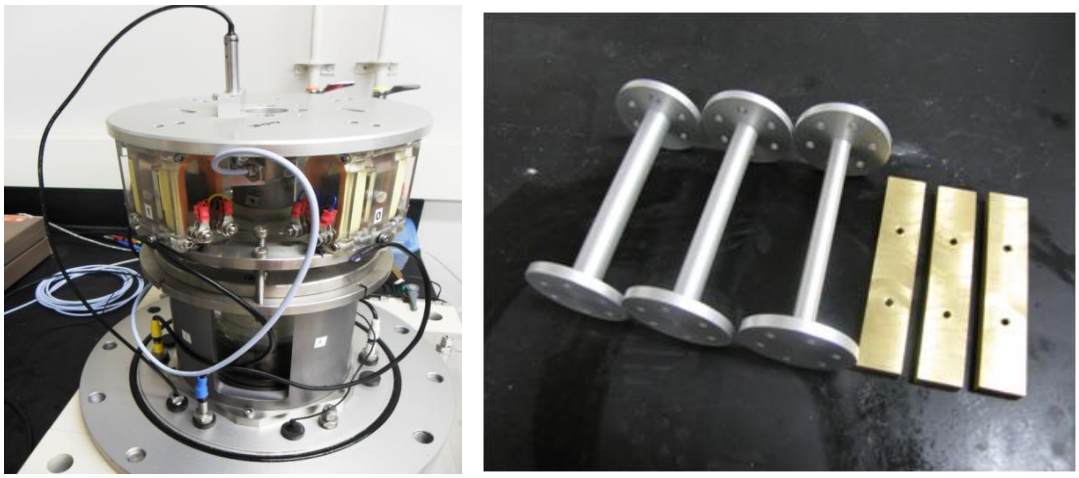

Figure 3.13: Typical instrumentation for resonant column device RCD-2.

The damping ratio, (ζ), is computed from the shape of free vibration decay curve. First, a sinusoidal wave is applied at the resonant frequency of the specimen, and then the excitation is shut off so the resulting free vibrations may be measured. The free vibration response ($x(t)$) of a SDOF system is given as function of the phase angle (θ) and the initial amplitude (A_0) as: (Humar, 2005)

$$x(t) = A_0 e^{-\xi \omega_0 t} \cos(\omega_D t + \theta) \tag{3-17}$$

where ξ is the damping ratio; ω_0, the circular resonant frequency; ω_D, the damped resonant frequency given by $\omega_D = \omega_0\sqrt{1-\xi^2}$; and A_0, the maximum amplitude of the displacement. For $\xi < 0.2$, $\omega_D \approx \omega_0$, whereas $\omega_D = 0.92\omega_0$ when ξ =0.4. The damping ratio can be estimated from the decrement logarithm method (Richart et al. 1970) as

$$\xi = \frac{1}{2\pi n} Ln\left(\frac{x(t_i)}{x(t_j)}\right) \tag{3-18}$$

where $x(t_i)$ and $x(t_j)$ are two peaks separated n cycles ($t_j = t_i + nT$). The full waveform of a free-decay response can be used to estimate a single value for the resonant frequency and damping ratio by curve-fitting the measured response with equation 3.17 the damping ratio is also calculated by plotting the Ln(peak amplitudes) against the phase angle (2π n). This plot should be straight line; and its slope represents the damping ratio. For the RCD-2, between 10 and 50 cycles are commonly used in the calculation.

CHAPTER 4

NEW METHOD FOR THE EVALUATION OF DYNAMIC PROPERTIES OF SOILS USING A STRAIN CONTROLLED EXCITATION

4.1 INTRODUCTION

The effects of intrinsic shear wave attenuation in rock have been of interest for many decades and the subject of study both in laboratory and in situ. While this effect in near surface soft soils (V_s< 250 m/s) has received less attention, it has important implications in the field of seismic hazard studies. Structures founded on soils with periods close to that of the thickness of the deposit may undergo more intense shaking due to a resonance effect setup between structure and soil. This building soil interaction is important because the amplification factors provided in the 2005 National Building Code of Canada (2005NBCC) may not be sufficiently high at the resonance period of a site, acknowledging the potential for de-amplification within then on-linear range. Hence, attenuation in soils is a particularly important property to understand, since the resonance effect in soft soils will be longer lasting if soil dissipation of wave strapped in then near surface is low (Crow, 2011).

The low and medium strain dynamic properties of soils are commonly measured in resonant column (RC) device (ASTM D4015-92, 2000). Conventional RC testing (RC

standard) is based on the determination of the resonant frequency by exciting the soil specimen at different frequencies (frequency sweep, random noise). The shear wave velocity is determined using the solution of the equation of motion for a column-mass system. The resonant frequency and the material damping ratio are typically computed by curve fitting the measured transfer function between the applied torque and induced angle of twist with the theoretical equations (e.g. Cascante et al. 2003).

The standard RC testing method is based on harmonic excitation, sweeping the frequency around resonance. The transfer function is determined with small frequency increments in order to get precise values of damping and resonant frequency. This procedure is time consuming, especially for low damping materials that present sharp resonant peak. To overcome this limitation, random noise and sinusoidal sweep excitations have been used (Prange 1981, Aggour et al. 1989, Cascante and Santamarina 1997). However, these excitations do not impose a constant strain on all frequencies; thus the reliability of the measurement rests on the definition of an equivalent strain level.

The effect of different strain levels in frequency sweep tests have been reported in previous studies (e.g. Cascante et al. 1997; Khan et al. 2008); which indicate that the error in the measured damping ratio increases with the increase in strain level because of the non-symmetrical shape of the measured transfer function. Although the measured transfer function can be curve fitted within acceptable error at low strain levels, the goodness of the fit deteriorates with the increase in shear strain level (Khan et al. 2008). Moreover, the effect of frequency on the dynamic properties is difficult to evaluate in conventional RC testing and recently proposed non-resonance (NR) method.

The non-resonance (NR) approach uses single frequency excitation instead of frequency sweep to measure the dynamic properties (Khan et al. 2008; Lai et al. 2001; Rix and Meng 2005). This method is based on the solution of the equation of motion governing the forced vibration of a continuous, homogeneous, and linear viscoelastic cylindrical specimen. The method allows for the simultaneous determination of the shear wave velocity and material damping ratio at the excitation frequency. The NR method is based on viscoelasticity theory and the application of the elastic-viscoelastic correspondence principle (Christensen, 1971).

Since the dynamic properties can be determined at different frequencies, the non-resonance (NR) method have been used to investigate the frequency dependence of dynamic properties (Lai et al. 2001; Rix and Meng 2005; Khan et al. 2008). The experimentally determined complex shear modulus is used to compute the shear wave velocity and damping ratio as a function of frequency. The use of linear viscoelasticity, however, forces one of the dynamic properties to vary with frequency. NR results from two cohesive soils presented by Meza and Lai (2006) showed that the data is well described by the Kramers-Kronig relationships (Booij and Thoone, 1982); however, the results are presented for low frequencies ($f < 30$ Hz). The NR method is appropriate for the evaluation of dynamic properties as function of the shear strain level because it uses the same frequency of excitation at all shear strain levels.

The main objective of this study is to present a simple testing technique, alternative to the NR method, to measure the transfer function and dynamic properties of soils as a function of frequency at constant strain levels. The proposed technique, called

the FN method, (sinusoidal + random excitation) is based on exciting the specimen simultaneously with a sinusoidal function (carrier frequency) and a relatively small amplitude random noise. The sinusoidal excitation controls the shear strain level and hence the resonant frequency of the specimen; whereas the small amplitude random noise excitation provides the required frequency bandwidth to compute the transfer function around resonance.

The proposed FN method has several advantages. Firstly it allows a better control of the shear strain level imposed in random-noise resonant column testing. Secondly, the errors in curve fitting the transfer function are reduced especially at large strain levels because at a constant strain level the transfer function matches the theoretical equation and thirdly, the dynamic properties can be evaluated as function frequency using conventional solution to the equation of motion used in resonant column testing.

To evaluate the potential of the proposed methodology, resonant column tests are performed on sand and clay specimens. The sand is tested at two isotropic confinements using the conventional (RC), non-resonance (NR), and the proposed (FN) methods. The error in the curve fitting of transfer functions decreased up to 30% at large strain levels, the dynamic properties of sand computed from the FN method show limited variation with frequency within the studied bandwidth.

4.2 EXPERIMENTAL SETUP AND EXPERIMENTAL PROGRAM

A modified, Stokoe-type resonant-torsional column apparatus is used in this study. The driving plate has a radius of 15 cm. The input signal to the driving coils is generated by a dynamic signal analyzer (HP-35670A) and amplified through a power amplifier (Bogen, GS-250). The response of the sample is acquired using an accelerometer (PCB 352A78) attached to the driving plate. The output signal from the accelerometer and the current through the coils are measured with a digital oscilloscope (HP-54645A) and recorded in the dynamic signal analyzer (HP-35670A). The mass polar moment of inertia (*MPMI*) of the driving plate (I_o = 6.9 x 10^6 g-mm^2) was measured by testing an aluminum (f_o = 29.7 Hz) and a PVC probe (f_o = 29.4 Hz). The calibration probes of lower resonant frequencies were selected to avoid the effects of base fixidity (Khan et al. 2008b).

RC tests were performed on a sand specimen at a confinement of σ_o = 50 kPa and 120 kPa. The tests were performed using conventional RC method, NR method, and the proposed methodology (FN Method) at different shear strain levels. The details of testing procedure for each method are presented in following.

4.2.1 RC Method

A broad-band frequency sweep (100 Hz) was used to approximately locate the resonance before a narrow band frequency sweep (25 Hz) was used to measure the transfer function, the induced current through the coils, and the acceleration response of the specimen. The equation of the transfer function (Eq. 3-7) was used to curve fit the

measured TF to determine the resonance and damping ratio. The shear strain was computed from Eq. 3-8 after measuring the largest peak-to-peak response of the specimen from the oscilloscope. The procedure was repeated at different shear strain levels to obtain the variation of dynamic properties with shear strain level.

4.2.2 NR Method

The specimen was excited with a fixed sine function at or very close to the resonant frequency and the corresponding value of transfer function was recorded (TF). The amplitude of the fixed sine was adjusted until the TF value matched the TF value obtained from RC method. The TF (e.g. Fig. 3.2) was then reconstructed around resonance by changing the frequency of fixed sinusoids but keeping the shear strains constant by controlling the amplitudes. Only one equal strain transfer function is generated for a certain shear strain level. The dynamic properties were then evaluated with Eq. 3-4 (e.g. Lai et al., 2001) using the discrete measurements of the equal strain transfer function.

4.2.3 FN Method

The new methodology (FN Method) is based on exciting the specimen at certain frequency with a fixed sine using the desired shear strain level; which controls the position of resonant frequency in the tested frequency bandwidth. A single frequency excitation produces one peak in the TF; hence, a small amplitude random noise excitation is added to the main sinusoid (carrier) to measure the transfer function around resonance.

The coupling of the signals is achieved by designing and constructing an in phase signal coupler. A typical transfer function obtained by using this method is presented in Figure 4.1. The effect of frequency is evaluated by changing the frequency of the carrier signal (shear strains kept constant). Since the shear strains are constant at all frequencies of the carrier signal, the position of transfer functions do not change for frequency independent behaviour. The dynamic properties are obtained by curve fitting the measured transfer functions with Eq. 3-7.

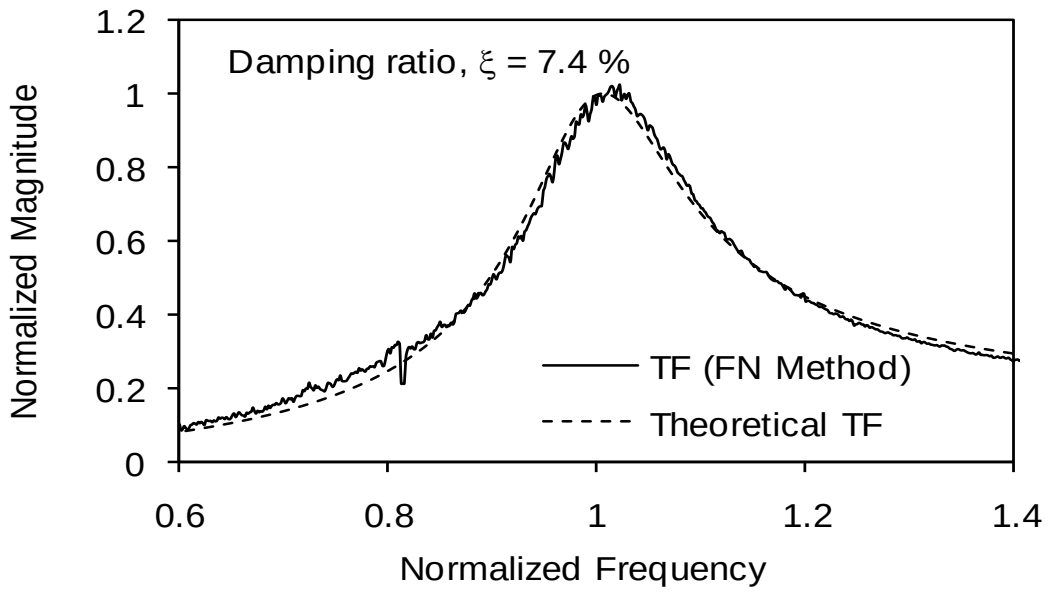

Figure 4.1: Transfer functions from FN measurements fitted with theoretical TF (*fo* = 42 Hz, $\gamma = 5.27 \times 10^{-4}$).

Finally the variation of dynamic properties with shear strain level is obtained by increasing the amplitude of the fixed sinusoid both in NR and FN methods. Although any frequency can be chosen for the carrier, a frequency close to resonance is preferred. The

use of the same excitation frequency at all shear strain levels eliminates the effect of frequency on the measurements if present. Moreover, the estimation of imposed shear strain level in the specimen is very accurate when using single frequency excitations.

4.3 RESULTS AND DISCUSSIONS

Dynamic properties of a dry-sand specimen were evaluated using conventional RC method, NR method and the proposed methodology (FN method). The new methodology is proposed to better evaluate the dynamic properties as function of frequency and shear strain level. Typical results and discussion are presented in the following sections.

The FN method produces transfer functions that have symmetrical shapes even at large strains that results in better fit of theoretical transfer function. Comparison of Figure 3.1 and Figure 4.1 (same shear strain level) indicates a 48 % overestimation in damping ratio when the transfer function is evaluated by conventional RC method (ξ = 11% and 7.4 %). The goodness of fit also improves significantly in the curve fitting of TF obtained from FN method.

Figure 4.2 presents the comparison of transfer functions obtained from RC, equal strain, and FN methods at an isotropic confinement of σ_o = 120 kPa. Transfer functions from FN method using two different carrier sinusoids are also presented. Figure 4.2 indicates excellent matching among the transfer functions obtained from different methods at low strain levels. The ability of this method to evaluate dynamic properties at

different frequencies of excitations can be used to study the frequency dependent behaviour of soils especially at low strain levels.

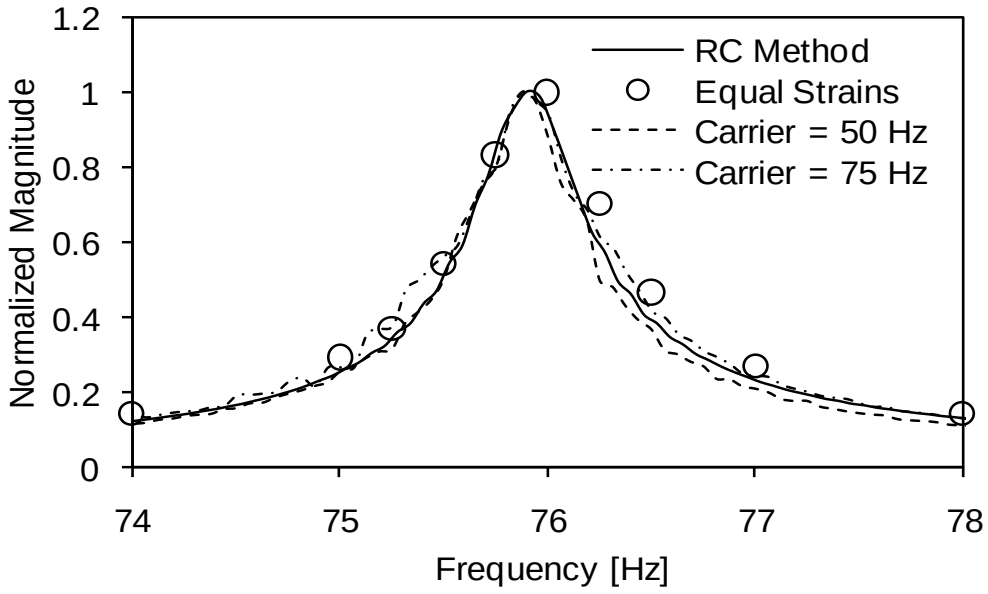

Figure 4.2: Comparison of transfer functions from RC, equal strains, and FN measurements ($\gamma = 9 \times 10^{-6}$).

Figures 4.3 and 4.4 show the typical results from the NR and FN methods for the variation of dynamic properties with frequency. The results from FN method are in agreement with previous results that show a practically frequency-independent damping ratio and wave velocity for sands at low strain levels (Hardin and Black 1966; Iwasaki et al. 1978; Bolton and Wilson 1989; Kim and Stokoe 1995; Khan et al. 2008). The NR method; however, forces shear wave velocity to increase with frequency as noted earlier. NR method is sensitive to the phase difference between the applied torque and resulting rotation; these small phase differences produce significant errors in damping even with small participation of flexural mode. This is evident from very large damping value at

about 35 Hz (Fig. 4.3) and 60 Hz (Fig. 4.4). The slight decrease in shear wave velocity (Fig. 4.3) with frequency is insignificant but requires further investigation. The damping ratio; however, becomes unstable in the FN method when the specimen is excited with a carrier frequency close to resonant frequency. A similar but smaller decrease is also evident in the measurements at σ_o = 120 kPa (Fig. 4.4). Although the exact mechanism is still being investigated, the significant reduction in the net current (excitation) going through the coils because of the EMF damping could generate inaccurate measurements close to resonance (EMF damping increases for lower frequencies). The jump in damping ratio at resonance is expected to decrease with increase in shear strain level due to relatively larger damping ratios and the reduction of EMF damping with strain level (Cascante et al. 2005).

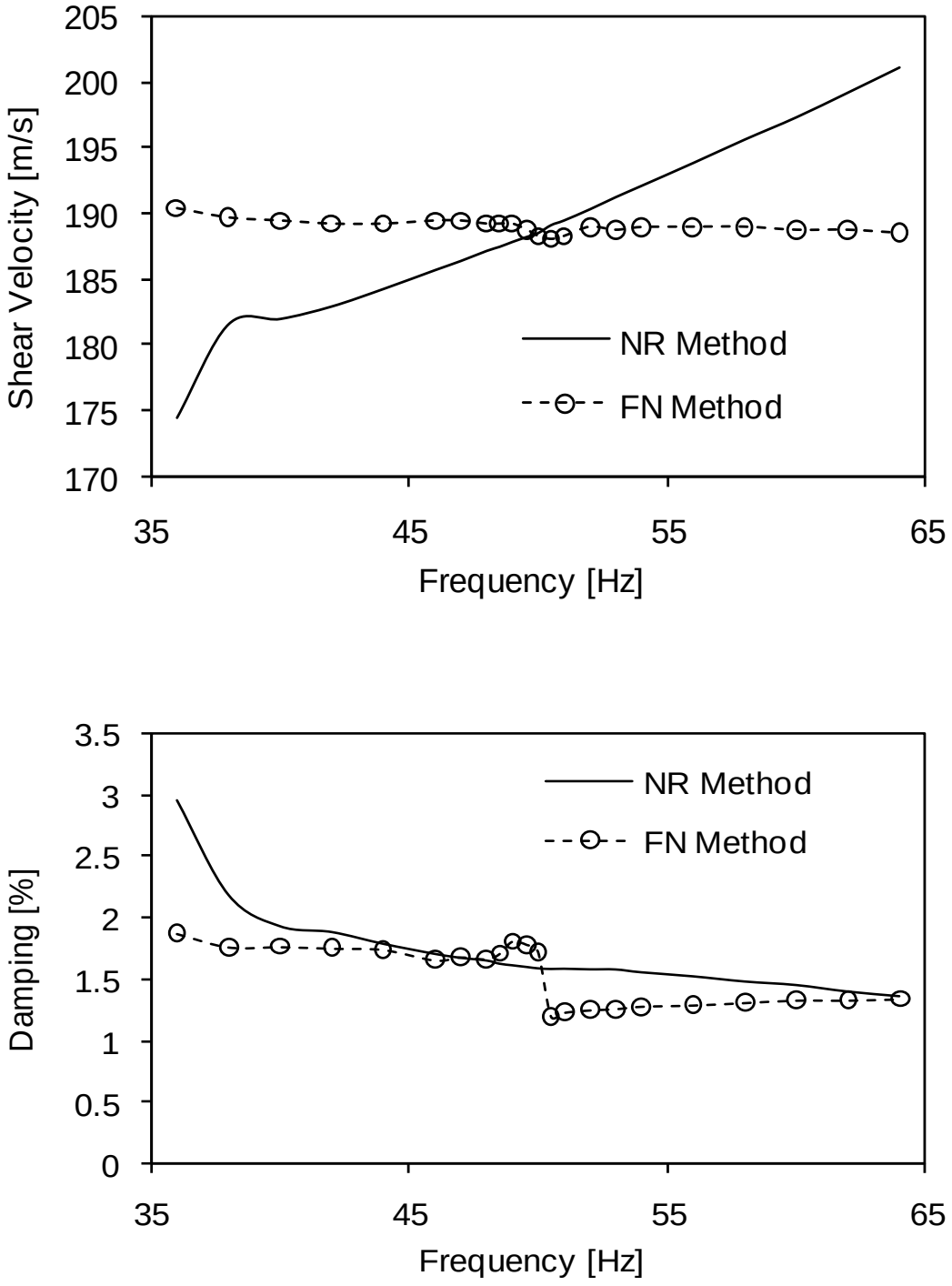

Figure 4.3: Evaluation of dynamic properties as function of frequency from NR and FN method (σ_o = 50 kPa, γ= 9.5 x 10^{-6}).

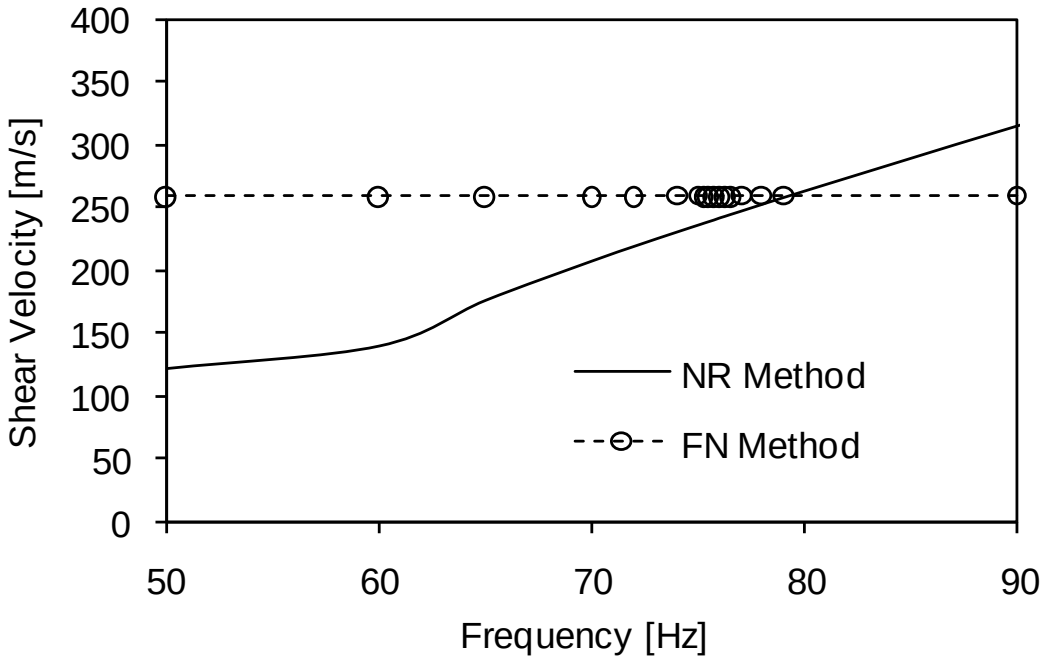

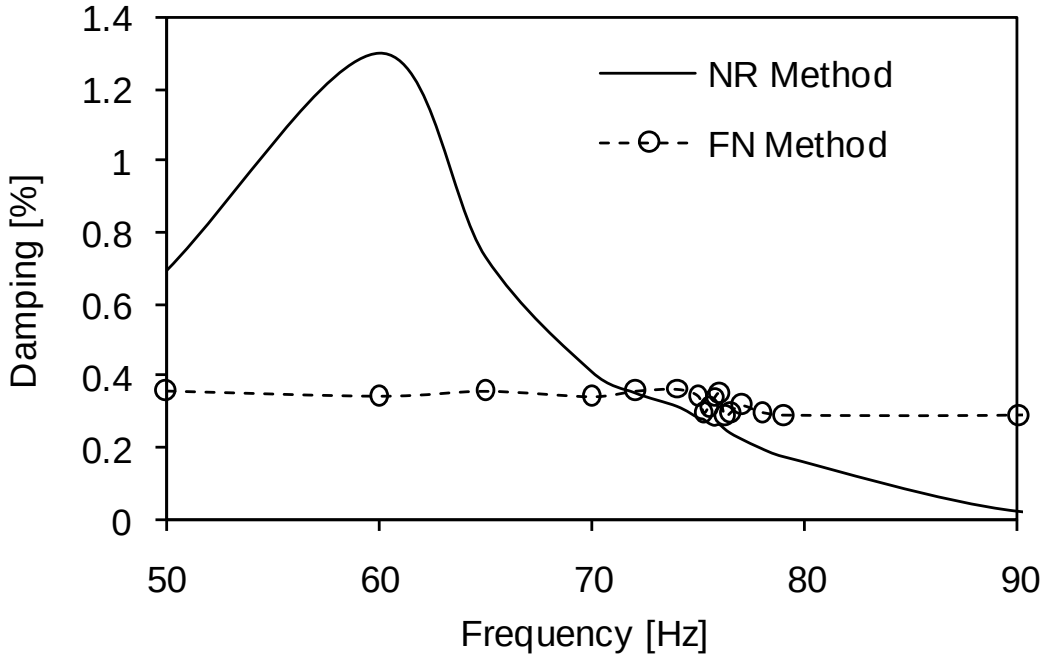

Figure 4.4: Evaluation of dynamic properties as function of frequency from NR and FN method (σ_o = 120 kPa, γ= 9 x 10^{-6}).

The variation of dynamic properties with shear strain level is presented in Figure 4.5 for the RC, NR, and FN methods at σ_o = 50 kPa. The results indicate that the variation of shear modulus is similar for all the methods. These findings are in agreement with literature (Khan et al. 2008). The damping ratio on the other hand shows larger difference among the methods. The difference increases with the increase in shear strain level. As noted earlier (Fig. 3.1 and Fig. 3.2), the damping ratio from RC method is overestimated because of the distorted shape of transfer function due to unequal strains. At low shear strain levels, the damping ratios from FN and RC measurements are in good agreement.

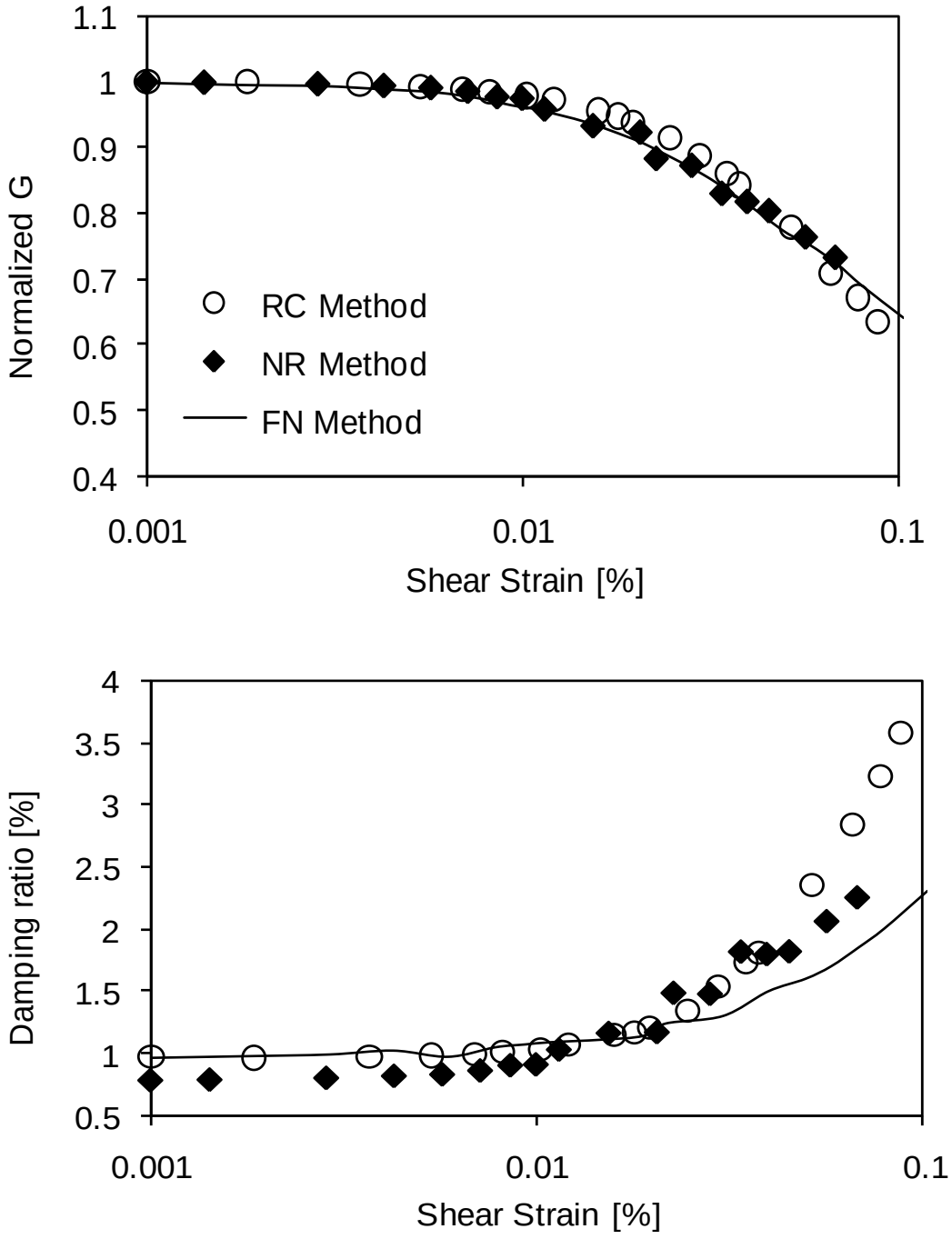

Figure 4.5: Evaluation of dynamic properties as function of shear strain from RC, NR and FN methods (σ_o = 50 kPa).

At shear strain level of 0.1 %, difference between FN and NR measurements is 20 % whereas the difference between NR and RC measurements is 45 %. The damping ratios measured from NR method at large strains are more reliable because the larger phase difference can be measured with greater accuracy. The detailed results of our different method (RC, NR and FN) are presented in appendix B. Although the shape of TF is symmetrical, FN method possibly does not produce enough shear strains at frequencies other than the carrier frequency and hence the damping ratios are slightly underestimated at large strains. The damping ratios measured from FN method are however more reliable in terms of accuracy.

4.4 CONCLUDING REMARKS

Resonant column tests were performed on a sand specimen at two isotropic confinements of 50 kPa and 120 kPa. The dynamic properties were evaluated by conventional RC, NR, and newly proposed FN methods. Dynamic properties were evaluated as a function of frequency and shear strain levels. The main conclusions from the study are:

The damping ratios from RC measurements are overestimated at large strains. A reconstruction of TF using tedious approach of equal strain method provides better estimate of damping ratio. The representative shear strains estimated from RC Method are less accurate than the NR and FN methods.

The variation of dynamic properties with frequency is better estimated by newly proposed FN method compared to NR method. NR method is sensitive to slight

variations in phase difference especially at low strain levels and the results become highly unreliable.

The variation of dynamic properties with shear strain level is better characterized by using either NR or FN methods. The degradation of shear modulus is practically similar from RC, NR, and FN methods. Damping ratio is overestimated by RC method due to distorted shape of transfer function at large strains. The FN method slightly underestimates the damping ratios at large strains but the difference is smaller compared to errors produced by RC Method. Table 4.1 summarizes the advantage and disadvantage of each method.

Table 4.1 Characteristic of different resonant column testing methods

METHOD	EXCITATION	ADVANTAGE	LIMITATION
RC	Broad-band frequency (20-175 Hz)	• Quick solution to find the resonant frequency in a broad band frequency range	• Over estimate the damping ratio because of distorted shape of transfer function due to unequal strain level
NR	Fix Sine (10- 200 Hz)	• Equal strain • Allows for simultaneous determination of shear wave velocity and damping at excitation frequency	• Sensitive to phase different between applied torque and resulting rotation
FN	Fix sine + Random Noise (20-200 Hz) + 20 mV	• Better evaluation of dynamic properties as function of frequency • Have symmetrical shape in large strain level	• Damping ratio becomes unstable in this method when the specimen is excited with carrier frequency close to natural frequency

CHAPTER 5

EQUIPMENT EFFECTS ON DYNAMIC PROPERTIES OF SOILS IN RESONANT COLUMN

5.1 INTRODUCTION

Shear modulus and damping ratio are important soil properties that influence the response of soils to dynamic loads. Both shear modulus and damping ratio can be evaluated in the laboratory using devices such as cyclic triaxial, bender elements (BE), or a resonant column device (RCD); which is the ASTM standard for dynamic characterization of soils (ASTM D4015-92 2000). The cyclic triaxial test is used for high shear strain levels ($> 10^{-3}$), whereas bender elements and the RCD are used for low strain levels ($<10^{-3}$). Bender element tests are economical and fast; however, the results can be affected by many variables and they require careful interpretation ; On the other hand, BE can only be used to measure the shear modulus at low strain levels (G_{max}). The evaluation of material damping in the BE test is complex and there is no standard procedure (Camacho et al. 2008). The RCD provides more consistent test results; and it is considered one of the most accurate ways to determine the dynamic properties of soils at low to mid shear strain levels. Resonant column (RC) tests are accurate and reliable; however, the effect of different equipment in making the measurements on the results has not yet been evaluated. This is especially true of the damping measurements, which are

significantly affected by the electro-motive force (EMF). (Cascante et al. 2003; Wang et al. 2003).

The RC tests can vary in their configuration and the analytical methods used for the computation of the dynamic properties. While many testing programs have been performed to measure the dynamic properties of soils on a single resonant column apparatus (Stokoe et al. 1994, Dobry and Vucetic 1987; Cascante and Santamarina 1997, Khan et al. 2005, Camacho et al. 2008), very few have evaluated the dynamic properties of the same soils on different RCDs. In most cases in which a soil was tested on two different RCDs the tests were for calibration purposes, when the RCD had been modified to accommodate different samples (e.g. stiffened base, Avramidis and Saxena 1990). In this case, however, the same test method and data analysis are used in the initial and modified state of the RCDs. Fewer comparisons have been done with two RCDs that use different testing methods and different data analysis. The main objective of this part of our study is to measure the dynamic properties of a typical silica sand using two different RCDs and provide a comparison of the results. The effect of the equipment and the use of different data analysis procedures for the calculation of damping are discussed.

5.2 EXPERIMENTAL PROGRAM

For the accurate measurement of the equipment effects on the test results, it is critical to ensure that the same testing procedures were used for both RCDs. While developing the testing procedure, practice tests were performed with all members of the testing teams present to ensure that samples would be prepared and tested similarly. Three

aluminum specimens were used to calibrate the resonant-column systems. The aluminum specimens are made of a vertical aluminum pipe with two horizontal aluminum bars or disks. The bars or disks were attached at each end of the pipe to allow assemblage of the probe with the resonant column (Figures 5.1a, 5.1b). The main characteristics of the calibration specimens tested are given in Table 5.1.

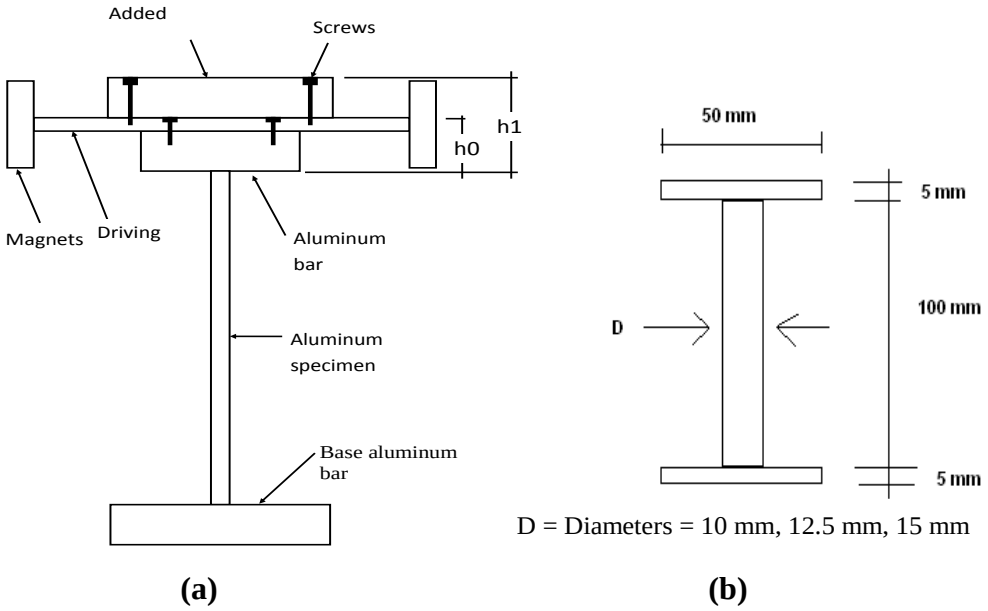

Figure 5.1: Calibration bar for systems (a) RCD-1 and (b) RCD-2.

Table 5.1: Characteristics of the aluminum probes.

Device	Prob	Diameter (cm)		Length (cm)	Resonant Frequency (Hz)
		Outside	Inside		
RCD - 1	AL 1	0.955	0.701	22.54	12
RCD - 1	AL 2	2.534	1.901	22.54	97
RCD - 2	AL 3	1	0	10	40.7
RCD - 2	AL 4	1.5	0	10	90

Four different Ottawa sand specimens were tested in this study. Sands 1 and 2 (S1, S2) were tested in the RCD-1; whereas, sands 3 and 4 (S3, S4) were tested in the RCD-2. At each confinement and shear strain level, the dynamic properties were computed using the analytical procedures described before. To reduce the effects of large-strain cyclic loading, the specimens are compacted before testing to an average relative density $D_R \approx 77$ %. The main characteristics of the sand specimens are given in Table 5.2.

Table 5.2: Change in height and void ratio during the test.

Property of Specimen	S1	S2	S3	S4
Initial diameter D0 (mm)	69.97	70.32	50.17	49.84
Height during loading (mm)	146.44	144.23	97.69	96.56
Height after Unloading (mm)	146.47	144.14	97.61	96.55
Residual axial strain (%)	0.02	0.06	0.08	0.02
Void ratio during loading	0.521	0.496	0.531	0.561
Void ratio after Unloading	0.520	0.493	0.530	0.561
Max change in Void Ratio (%)	0.21	0.60	0.24	0.05
Average Density (kg/m3)	1741	1749	1736	1702

All sand specimens were tested at confining pressures of 30, 60, 120, and 240 kPa, with 0 kPa back pressure. For each pressure, the resonant frequency and damping ratio were measured over a range of shear strains ($10^{-6} < \gamma < 10^{-3}$). Vertical displacements were measured throughout the tests and after unloading with the use of an LVDT. After unloading each sample, the residual vertical strain was required to be less than 0.2% to ensure that the samples did not change significantly throughout the testing.

5.3 SAMPLE PREPARATION

Ottawa silica sand was chosen for testing because it is well characterised in the literature and is uniformly graded, which should enhance the reproducibility of samples. The geotechnical properties of the silica sand were determined in the laboratory; its grain size distribution is shown in Fig. 5.2 (D_{50}=0.279 mm, e_{max}=0.727, e_{min}=0.476, SiO^2 content 99.6% and Gs=2.66 g/cm^3). Samples were prepared in a split mold by the dry pluviation and tamping technique. Once the upper platen was set in place, vacuum was applied to hold the sample and the split mold was removed. Then, the connections for the driving plate, LVDT, and accelerometer were arranged, and the chamber was assembled. Sample vacuum was gradually released while increasing the cell pressure, until an effective confinement. Isotropic loading was applied to all samples tested in this study, increasing the confining pressure from 30 kPa to 240 kPa.

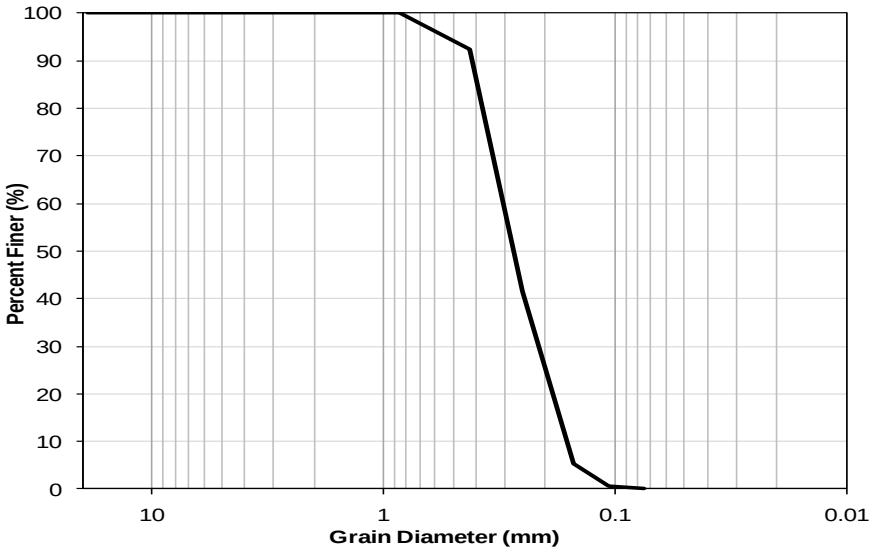

Figure 5.2: Grain size distribution of silica sand used (Barco sand #49).

The diameter of the cylindrical specimens for the RCD-1 is 70 mm; whereas the diameter is 50 mm for the RCD-2. All sand samples were tested in dry conditions. Each sample was built in five layers; each layer was tamped 70 times with a plastic tamper at a constant height. To achieve the same void ratio for both sample sizes, a tamper with a smaller tamping area was used for the 50 mm diameter samples than for the 70 mm diameter samples.

5.4 RESULTS AND DISCUSSION

Figure 5.3 shows the variation of damping ratio with shear strain level for the calibration specimens. The results for the low frequency probes at low strains levels (Fig. 5.3a, Table 5.1) indicate that the damping in the RCD-1 is 1.6 times larger than the damping measured with the RCD-2; and that the damping ratio increases almost linearly

with the strain level. The damping ratio in aluminum specimens at the testing frequencies of the resonant column is practically zero (Zemanek, and Rudnick 1961); thus the observed increase in damping with strain level could be generated by the radiation of energy through the base of the resonant column. The base of the resonant column was assumed to be fixed; however, it has been demonstrated that for the evaluation of shear modulus, the base is not perfectly fixed and a correction factor should be applied to the measured values especially for stiff specimens (Khan et al. 2008, Avramidis and Saxena 1990). The results for the high frequency probes (Fig. 5.3b) show an increase in the damping values measured with the RCD-1 compared to the corresponding values using the RCD-2 (5 times larger). This increase in attenuation confirms the non-fixed conditions of the base; as the stiffness ratio of the probes tested in the RCD-1 is 65; whereas, the ratio is equal to five for the RCD-2 probes. For the low and high frequency probes (Fig. 5.3), the damping measurements from the RCD-1 are higher than the measured values using the RCD-2 because different base fastening conditions. The RCD-1 was mounted on a flexible bench; whereas the RCD-2 was attached to a stiffer bench. The radiation damping in the RCD-1 increases with the increase the stiffness of the aluminium probe as expected. However, further studies are required to better characterize the radiation damping. The increase in radiation damping with shear strain and frequency is observed on aluminum probes because of their low damping in comparison with typical soils.

Figures 5.4, 5.5 and 5.6 show typical results for the dynamic properties measured at σ'_o=30, σ'_o=60 and σ'_o=120 kPa. The results from the two devices are in good agreement.

The maximum difference in damping ratio, at low strain levels, is 31%; whereas the maximum difference in the normalized shear modulus is 20%. The shear modulus is normalized to remove the effect of void ratio using the correction factor proposed by Hardin and Drnevich (1972). Table 5.3 shows that the difference in shear modulus and damping ratio for σ'_o=240 kPa (Fig. 5.7) are only 2% and 12% respectively. These differences could be related to the different sizes of the specimens and the coupling conditions between the top and bottom caps with the specimen. The platens of the RCD-2 provide better coupling conditions than those of the platens of the RCD-1 because they have deeper grooves. The difference in the damping ratios measured with the two systems is expected to increase with shear strain because of the different testing procedures used. However, these differences are not significant up to the maximum strain levels achieved in this study. The variation of shear modulus and damping ratio with shear strain level are in good agreement and follow the hyperbolic model (Fig. 5.8). Figure 5.8b shows typical results for the normalized values of the shear modulus with respect to G_{max}.

Table 5.3: Summary of Ottawa sand results for low shear strain levels ($2.7*10^{-6} < \gamma < 1.0*10^{-5}$).

Confinement (Kpa)	Sample	Void ratio	Resonanat frequency (Hz)	Damping (%)	Shear Velocity (m/s)	Shear Modulus (Gpa)	G /F(e)*
30	S1	0.521	48.9	0.71	176.1	54.3	30.3
30	S2	0.496	50.0	0.52	163.7	47.7	25.4
30	S3	0.532	48.3	0.49	179.9	56.2	32.1
30	S4	0.563	45.2	0.45	171.3	50.0	30.2
Difference Avg (%)		7.72	5.44	23.66	3.35	4.08	11.90
60	S1	0.521	57.1	0.42	205.8	74.1	41.4
60	S2	0.495	58.7	0.37	192.0	65.6	35.0
60	S3	0.532	61.1	0.72	227.6	89.9	51.4
60	S4	0.563	58.1	0.33	220.0	82.4	49.9
Difference Avg (%)		7.81	2.92	32.18	12.50	23.35	32.47
120	S1	0.520	69.3	0.29	249.5	108.9	60.8
120	S2	0.495	76.9	0.39	251.5	112.6	59.9
120	S3	0.533	73.3	0.60	273.1	129.4	73.9
120	S4	0.563	70.0	0.29	264.9	119.4	72.3
Difference Avg (%)		7.99	1.93	30.99	7.40	12.33	21.11
240	S1	0.520	92.8	0.27	334.1	195.3	109.0
240	S2	0.494	93.2	0.31	325.0	188.1	99.9
240	S3	0.533	87.9	0.44	327.4	186.1	106.3
240	S4	0.563	85.0	0.21	321.4	175.8	106.4
Difference Avg (%)		8.09	7.01	12.46	1.55	5.60	1.82

* $F(e) = (2.17 – e)^{2} / (1 + e)$ Hardin and Drnevich (1972)

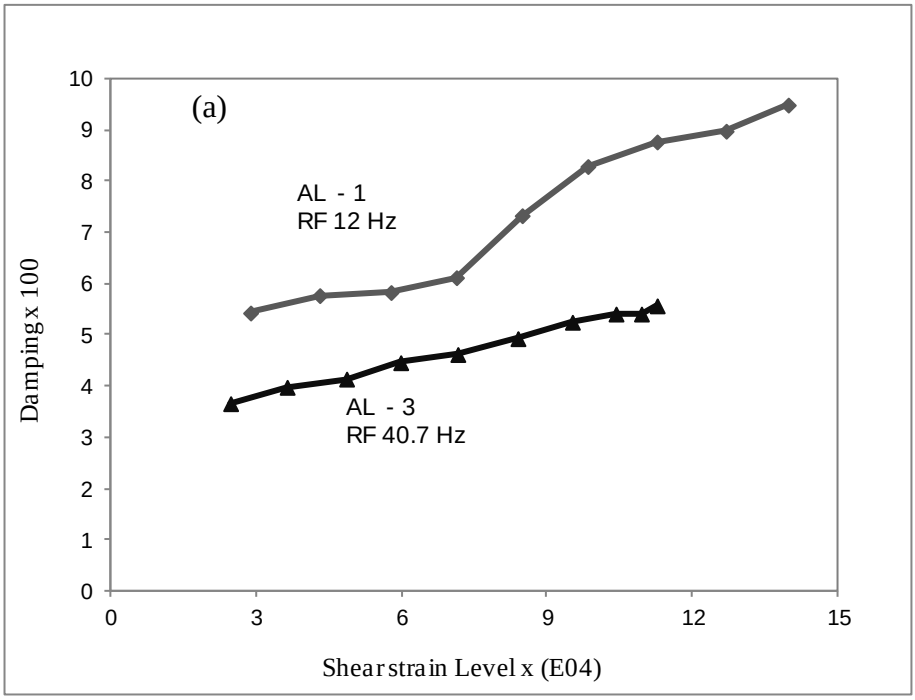

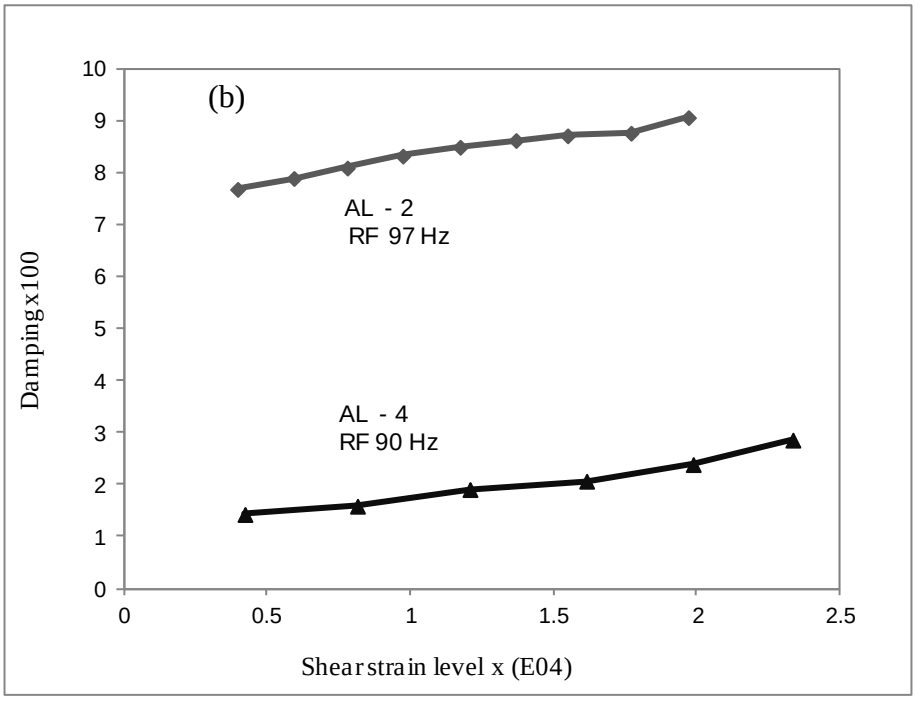

Figure 5.3: Damping vs. shear strain level for aluminum probes.

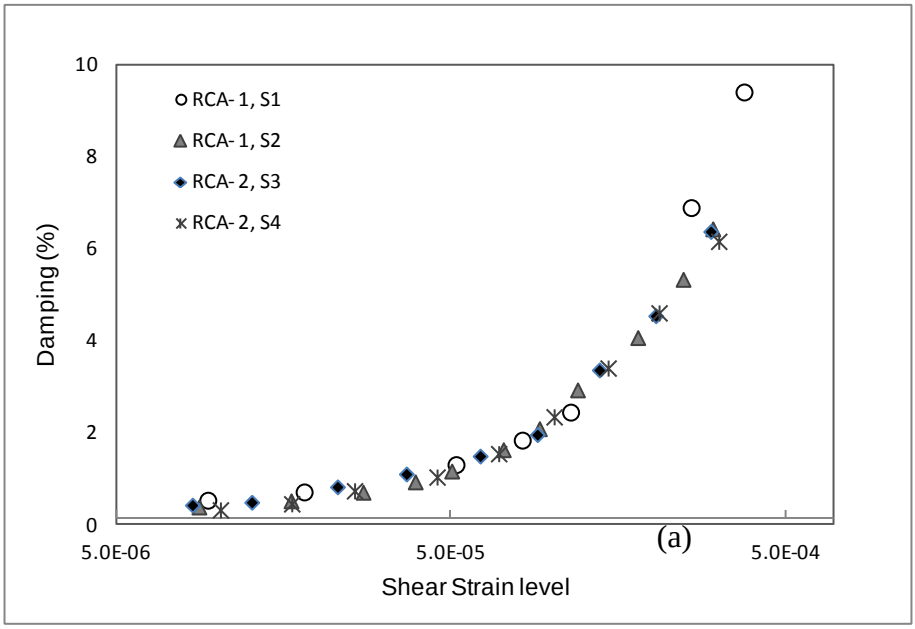

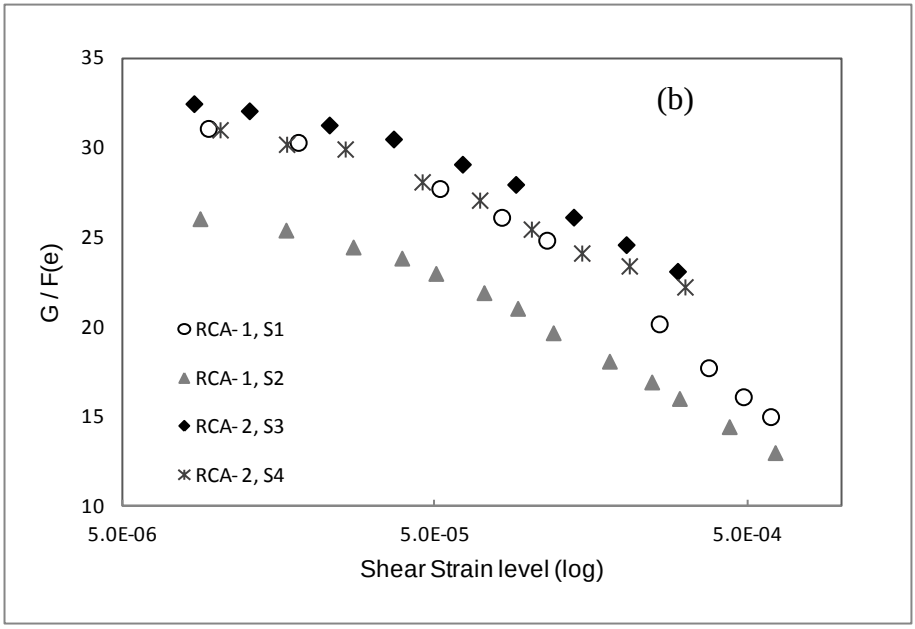

Figure 5.4: (a) Damping vs. shear strain level and (b) shear modulus vs shear strain leve,l at σ' = 30 KPa.

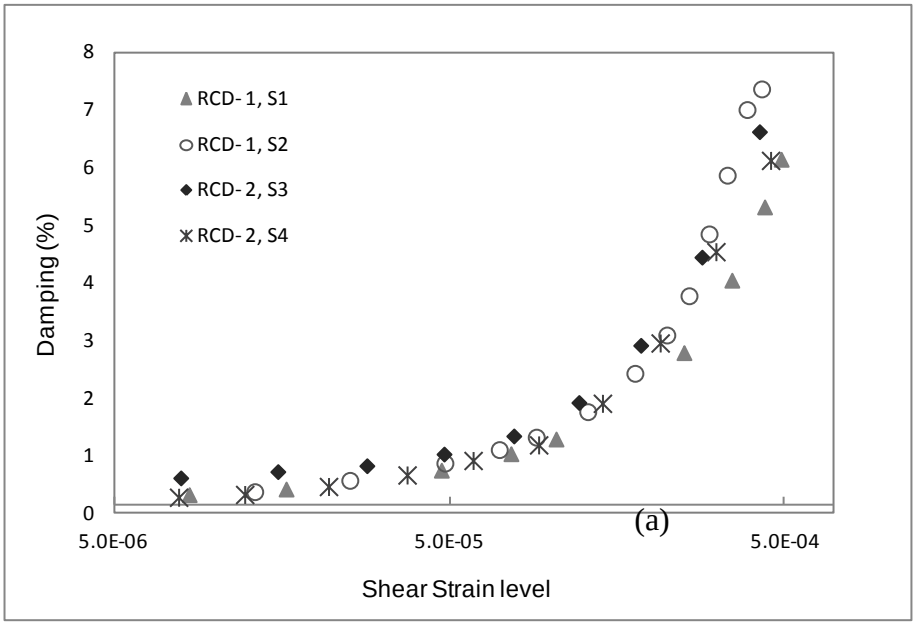

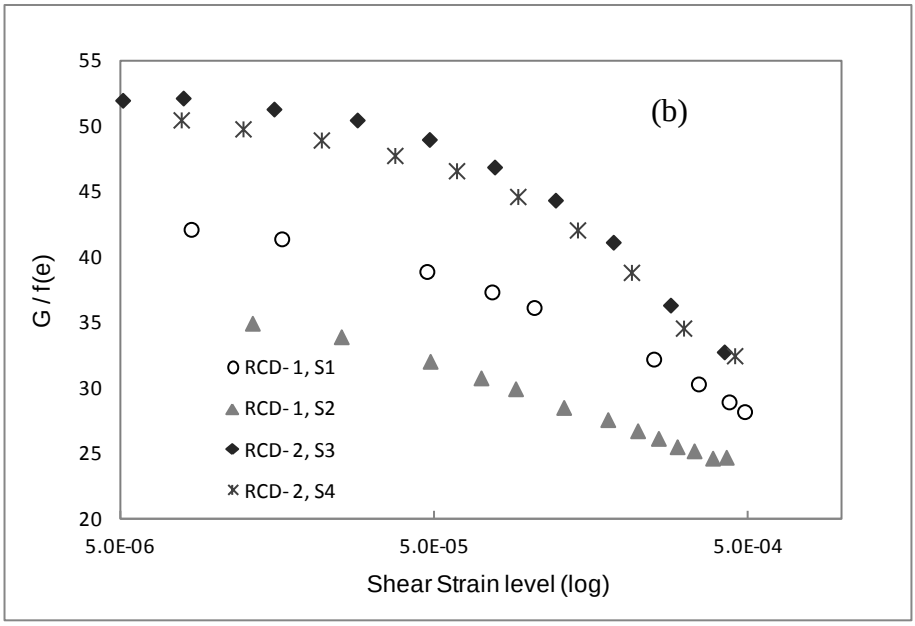

Figure 5.5: (a) Damping vs shear strain level and (b) shear modulus vs shear strain level at $\sigma' = 60$ KPa.

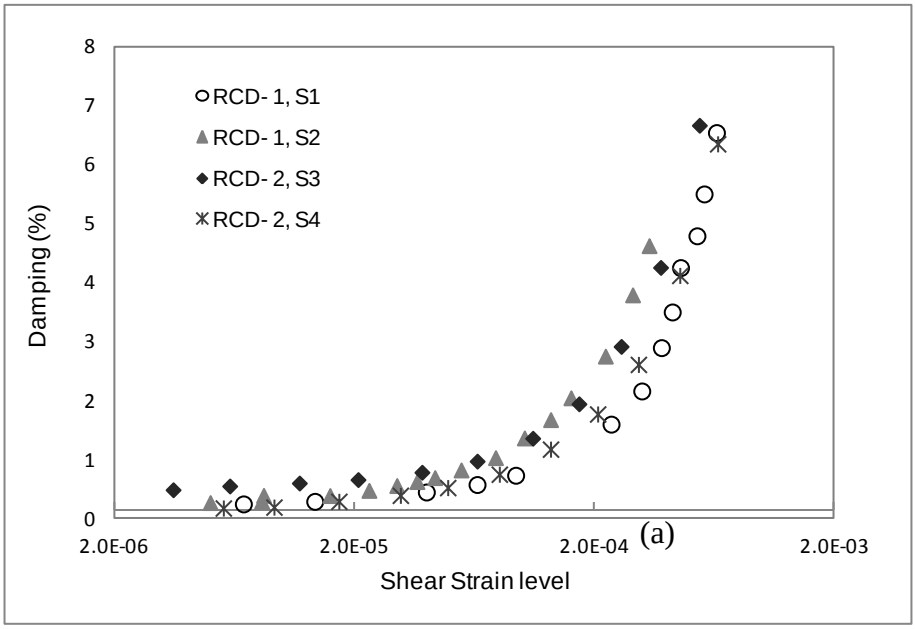

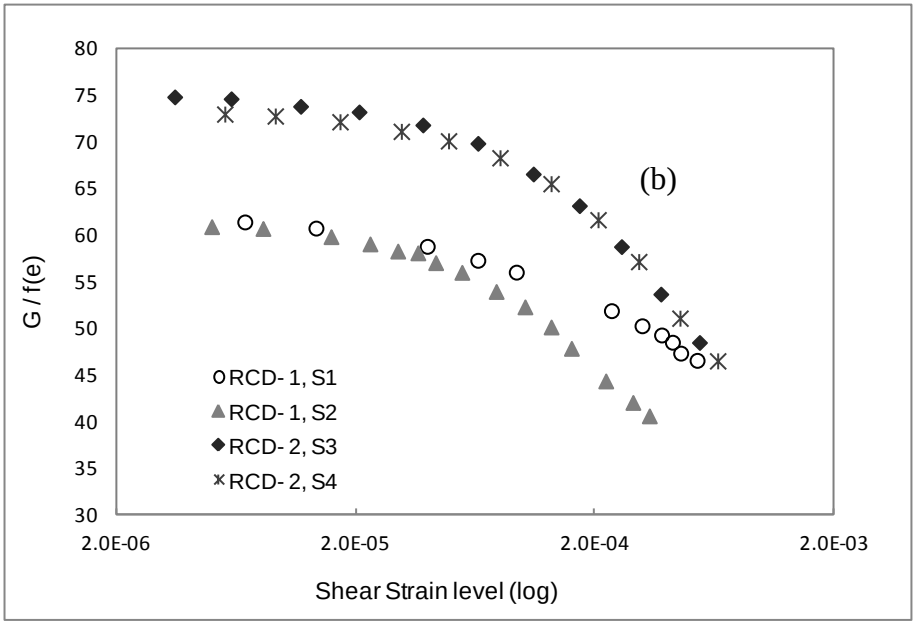

Figure 5.6: (a) Damping vs shear strain level and (b) shear modulus vs shear strain level at $\sigma' = 120$ KPa.

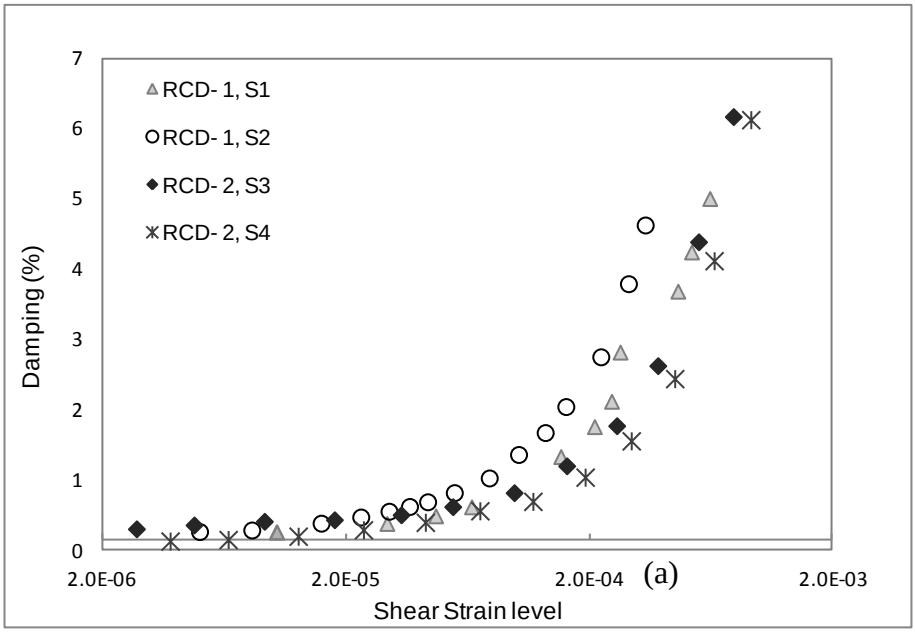

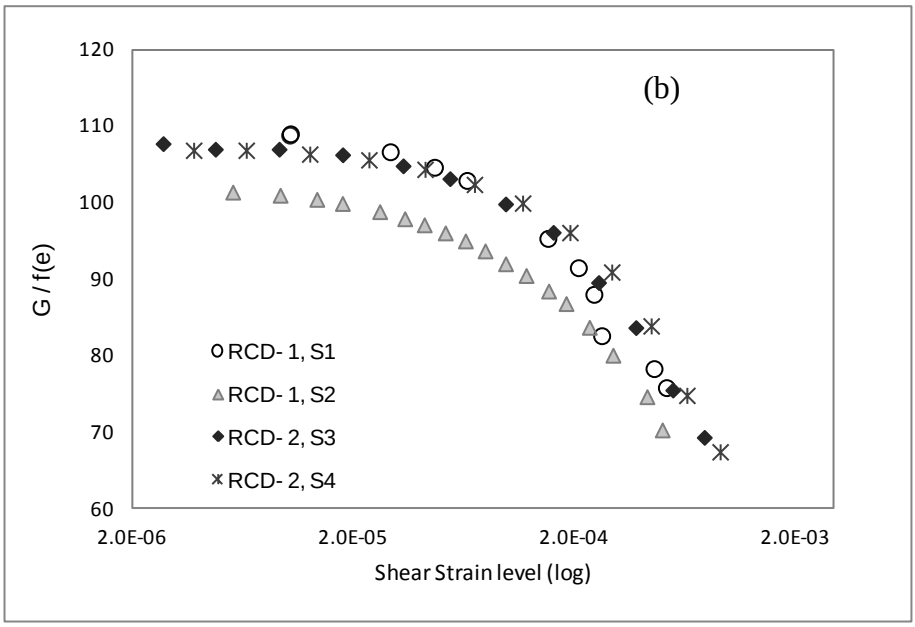

Figure 5.7: (a) Damping vs shear strain level and (b) shear modulus vs shear strain level at σ' = 240 KPa.

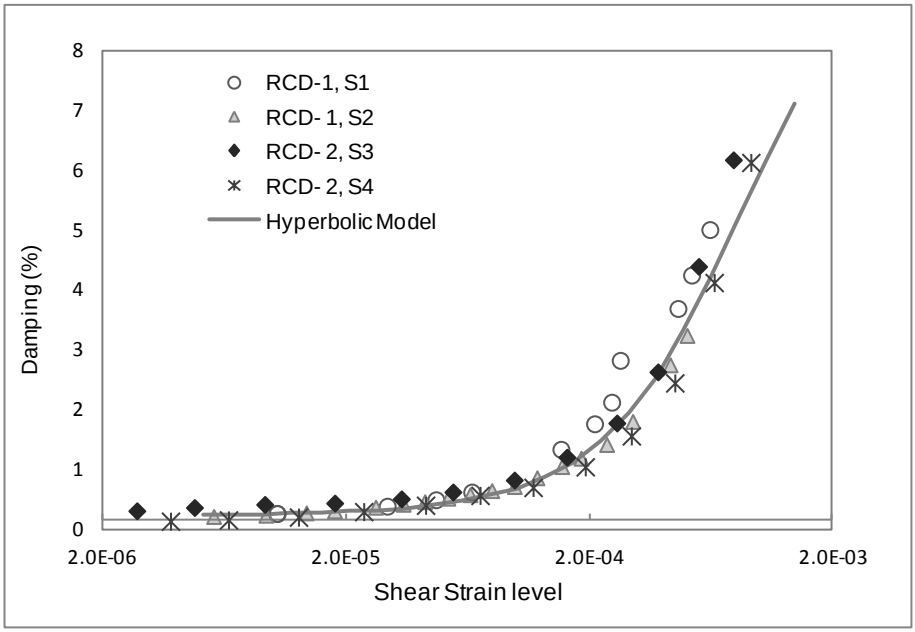

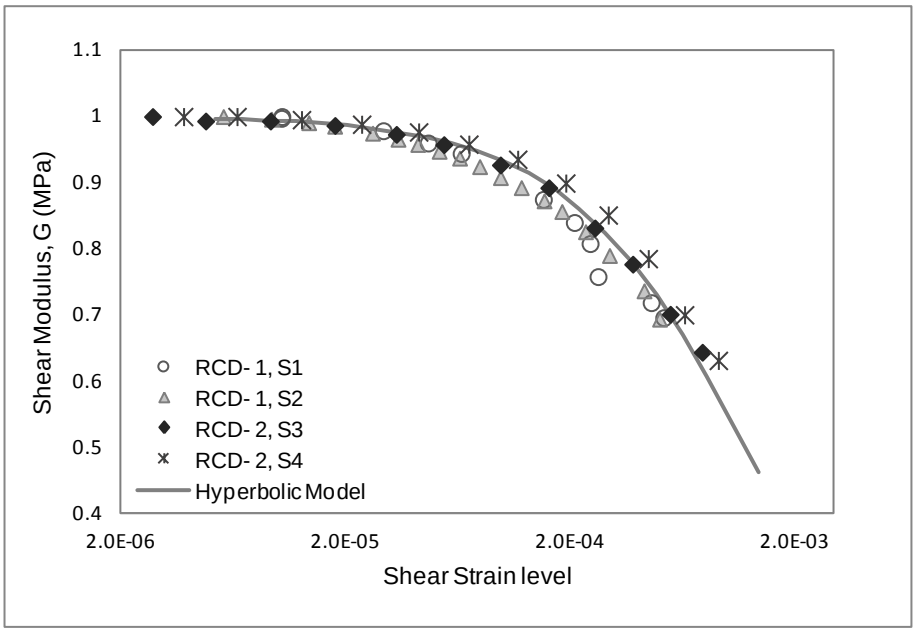

Figure 5.8: (a) Damping vs shear strain level and (b) shear modulus vs shear strain level at σ' = 240 KPa, with hyperbolic model.

5.5 CONCLUDING REMARKS

The results of an experimental study using two different resonant columns are presented. RC tests are performed on calibration aluminum probes and on dry sands (Ottawa silica sand). The results from the calibration probes show that the base of the RC cannot be considered fixed as the damping ratio increases with the excitation frequency. This trend suggests that radiation damping should be considered in the data analysis, especially at low strain levels where the damping ratio of the tested dry sands is smaller than 1%. The measured damping ratio of the aluminum probes differed by up to an order of magnitude for the different types of equipment used. The damping ratio and shear modulus at low strains measured with the two devices differed by up to 32% for the dry sand specimens. This difference could have been generated by the different coupling between the top caps and the specimens or by the different geometry of the specimens. However, the results are in good agreement with the predictions of the standard hyperbolic model once that the curves are normalized with respect to G_{max}.

CHAPTER 6

CONCLUSIONS AND RECOMMENDATIONS

6.1 CONCLUSIONS

Shear modulus and damping ratio are the most important material properties that determine the behavior of soils under dynamic loadings. Laboratory determination of these properties is convenient but presents several challenges in terms of testing bias, invalidated assumptions and analysis techniques. Reliable measurement of dynamic properties is important for successful analysis of an important class of geotechnical problems such as seismic design and machine foundations. This thesis investigates the experimental determination of dynamic properties using resonant column. Different sources of errors are identified, models for analysis are presented, testing methodologies are developed, and comparison of results from different equipment is presented. My research had contribution to the geotechnical community in three different categories as follow:

6.1.1 Equipment Modification

The research involves modifications to the resonant column testing device at University of Waterloo. The modification includes achieving higher torque in order to increase the level of strain in the test setup. Also, the testing equipment (Amplifier) was modified so that a constant excitation could be used during the test.

6.1.2 Development of New Methods for the Evaluation of Dynamic Properties

These properties can be measured from the transfer function between the excitation and the response using the resonant column device. The force function generated by a sinusoidal sweep excitation induces different shear strain levels at different frequencies. Consequently, the shape of the measured transfer function is distorted and differs from the theoretical transfer function for an equivalent single-degree-of-freedom system. The difference between the measured and assumed transfer functions becomes more pronounced with the increase in shear strain levels. This study presents a new methodology for the evaluation of dynamic properties from an improved transfer function. In this methodology, the soil specimen is excited using a fixed sine at the required strain level along with a simultaneous excitation of small amplitude random noise. The strain level induced by the fixed sine controls the resonant frequency and damping coefficient of the specimen whereas the random noise controls the shape of transfer function. The new methodology also shows a good potential for the evaluation of dynamic properties of soils as function of frequency in resonant column testing.

6.1.3 Effect of Resonant Column Properties on Dynamic Soils characteristics

In other part of my research an experimental study using two different resonant columns is presented. RC tests are performed on calibration aluminum probes and on dry sands (Ottawa silica sand). The measured damping ratio and shear modulus was different in each resonant column device. This difference could have been generated by the

different coupling between the top caps and the specimens or by the different geometry of the specimens. However, the results are in good agreement with the predictions of the standard hyperbolic model once that the curves are normalized with respect to G_{max}.

6.2 RECOMMENDATIONS AND FUTURE STUDIES

Non-resonance methods have been used in torsional mode only; however, modified resonant columns such as the one used in this study have the capability to operate in axial mode. Comparison of non-resonance method in axial and torsional mode can provide insight on the effect of mode of excitation on the dynamic properties using the same specimen and device at very low strain levels. Besides measurement of dynamic Poisson ratio, relationships between the damping ratios and elastic moduli from two modes can be verified.

Non-resonance methods can provide better evaluation of the dynamic properties as a function of the number of cycles than the conventional resonance method. The present research presented suggests the feasibility of engineered fills with high damping and stiffness characteristics. Further research is required to design cheaper materials and verification of their performance in mitigating ground vibrations due to cyclic loading.

REFERENCES

Achenbach, J.D. 1984, "Wave Propagation in Elastic Solids", North Holland, Amsterdam, Netherlands, pp. 425

Alarcon-Guzman, A. 1986. Cyclic Stress-Strain and Liquefaction Characteristics of Sands. PhD. Thesis, Purdue University, Indiana.

ASTM D4015-92, 2000. "Standard Test Methods for Modulus and Damping of Soils by the Resonant-Column Method," American Society for Testing and Materials, Annual Book of Standards.

Avramidis, A.S. and Saxena, S.K. 1990. The Modified "Stiffened" Drnevich Resonant Column Apparatus. Japanese Society of Soil Mechanics and Foundation Engineering. Vol. 30, No. 3, 53-68.

Bar, Y. S., Bay, J.A. 2009. Modifications of resonant column and torsional shear device for the large strain. Computers and Geotechnics 36 (2009) 944–952.

Badali J.P., and Santamarina, J.C. 1992. Damping of Waves in Soils. Experimental Geomechanics Group, University of Waterloo, Ontario, June.

Bellotti, R., Ghionna, V.N., Jamiolkowski, M., and Robertson, P.K., 1989, "Design Parameters of Cohesionless Soils from In-situ Tests", Specialty Session, Sponsored by Committee A2L02-Soil and Rock Properties, National Research Council, Transportation Research Board, Washington, USA

Biot, M. A., 1956. Theory of Propagation of Elastic Waves in Fluid-Saturated Porous Solid. Journal of the Acoustical Society of America, 28, 168-191.

Blair, D. P. 1990. A direct comparison between vibrational resonance and pulse transmission data for assessment of seismic attenuation in rock. Geophysics, 55(1): 51-60.

Bolton, M. D., and Wilson, J. M. R. 1989. An Experimental and Theoretical Comparison between Static and Dynamic Torsional Soil Tests. Géotechnique, 39(4), 585-599.

Booij, H. C., and Thoone, G. P. C. M. 1982. Generalization of Kramers-Krönig Transforms and Some Approximations of Relations between Viscoelastic Quantities. Rheologica Acta, 21, 15-24.

Bratsin, D. 2009. Soils Nonlinearity Effects On Dominant Site Period Evaluation. Proceedings of the Romanian Academy, Series A.

Brocanelli, D., and Rinaldi, V. 1998. Measurement of low-strain material damping and wave velocity with bender element in the frequency domain. Canadian Geotechnical Journal, 35: 1032-1040.

Bourbie, T., Coussy, O., Zinszner, B., 1987. Acoustics of Porous Media. Gulf Publishing Company. Houston, Texas.

Campanella, R. G., Stewart, W. P., Roy, D., and Davies, M. P. 1994. Low strain dynamic characteristics of soils with the downhole seismic peizocone penetrometer. Dyn. Geotech. Test. II, ASTM STP 1213, Philad., pp. 73-87.

Cao, X., He, Y., & Xiong, K. 2010. Confining pressure effect on dynamic response of high rockfill dam. Frontiers of Architecture and Civil Engineering in China , 116-126.

Cevik, A. c. 2009. Modelling damping ratio and shear modulus of sand–mica mixtures using genetic programming. Expert Systems with Applications , 36 (4), 7749-7757.

Cascante, G., Vanderkooy, J., and Chung, W. 2005. "A new mathematical model for resonant-column measurements including eddy-current effects." Canadian Geotechnical Journal, 42:(1) 121-135, 10.1139/t04-073

Cascante, G., Vanderkooy, J., and Chung, W., 2003, "Difference between current and voltage measurement in resonant column testing," Canadian Geotechnical Journal, 40(4): 806-820.

Cascante, G. and Santamarina, J. C. 1997. Low Strain Measurements Using Random Noise Excitation, Geotechnical Testing Journal, 20(1): 29-39.

Cascante, G., Santamarina, J.C., and Yassir, N., 1998. Flexural Excitation in a Standard Resonant Column Device. Canadian Geotechnical Journal, 35(3): 488-490.

Christensen, R. M. 1971. An Introduction to Theory of Viscoelasticity, Academic Press, New York, pp. 245.

Crow, H. Hunter, J. A., Motazedian, D. 2011. Monofrequency in situ damping measurements in Ottawa area soft soils. Soil dynamics and Earthquake Engineering 31 (2011) 1669 – 1677.

Das, B. M., & Ramana, G. (2011). Principles of Soil Dyanmics. Cengage Learning.

Delépine, N., Lenti, L., Bonnet, G., & and Semblat, J.-F. (2009). Nonlinear Viscoelastic Wave Propagation: An Extension of Nearly Constant Attenuation Models. Journal of Engineering Mechanics , 10.

Dobry, R. 1970, "Damping in Soils: Its Hysteretic Nature and Linear Approximation", Research Report R70-14, Massachusetts Inst. of Tech.

Dobry, R. and Vucetic, M. (1987). "Dynamic Properties and Seismic Response of Soft Clay Deposits." International Symposium on Geotechnical Engineering of Soft Soils, Vol. 2, Mexico City, 51-87.

Drnevich, V. P., 1967. "Effects of strain history on the dynamic properties of sand," Ph.D. Thesis, University of Michigan, 151 pp.

Drnevich, V.P. 1978. Resonant-Column Problems and Solutions. Dynamic Geotechnical Testing, ASTM STP 654, p 384-398.

Drnevich, V.P. and Richart, F.E., Jr. 1970. Dynamic Prestraining of Dry Sand. Journal of Soil Mechanics and Foundations Divisions, ASCE, Vol. 96, No.SM2 pp 453-469.

Drnevich, V.P., 1985. Recent Developments in Resonant Column Testing. Richart Commemorative Lectures, Edited by R.D. Woods, Proceedings of a Session

sponsored by the Geotechnical Engineering Division in conjunction with the ASCE Convention, Detroit, Michigan, p 79-107.

Du Tertre, A., Cascante, G., and Tighe, S. Combining PFWD and Surface Wave Measurements for Evaluation of Longitudinal Joints in Asphalt Pavements. The Transportation Research Board (TRB) 89th Annual Meeting. Washington, D.C., January, 3319-3327. (Accepted 2010).

Electric Power Research Institute, 1991, Proceedings: NSF/EPRI Workshop on Dynamic Soil Properties and Site Characterization. Report NP-7337, Vol 1, Research Project 810-14.

Fratta, D. and Santamarina, J. C., 1996, "Wave propagation in soils: Multi-mode, wide band testing in waveguide device" Geotechnical Testing Journal, ASTM, 19(2): 130-140.

Frost J.D., 1989. Studies on the Monotonic and Cyclic Behaviour of Sands. PhD. Thesis, Purdue University, Indiana.

Fung, Y.C. 1965, "Foundations of Solid Mechanics", Prentice-Hall, New Jersey, pp. 525

Groves, P., Cascante, G., Chatterji, P.K., Dundas, D., 2011. Use of Geophysical Methods for Soil Profile Evaluation. Canadian Geotechnical Journal.

Groves, P., Cascante, G., Knight, M. 2011. Ultrasonic Characterization of Exhumed Cast Iron Water Pipes Geotechnical Journal. Smart Structures & Systems Journal.

Hardin, B. O., and Drnevich, V. P. (1972). "Shear Modulus and Damping in Soils: Measurement and Parameter Effects." Journal of the Soil Mechanics and Foundations Division, Proceedings of the ASCE, 98(SM6), 603-624.

Hardin, B. O. and Drnevich, V. P., (1972). "Shear Modulus and damping in soils: Design equations and curves." Journal of soil mechanics and foundations division, ASCE, Vol. 98, No. SM7, pp. 667.

Hardin, B.O., 1965. The Nature of Damping in Sands. Journal of the Soil Mechanics and Foundations Division, ASCE, Vol. 91, No. SM1, pp. 63-97.

Hardin, B.O. and Richart, F.E. Jr. 1963. Elastic Wave Velocities in Granular Soils. Journal of the Soil Mechanics and Foundations Division, ASCE, 89(SM1): 33-63.

Hardin, B.O. and Scott G.D. 1966. Generalized Kelvin-Voigt Used in Soil Dynamics Study. Journal of the Engineering Mechanics Division, ASCE, February, 143-156.

Humar, L. 2005. Dynamics of Structures (2nd Edition ed.). New York: Taylor & Francis.

Hauge, P. S. 1981. Measurements of attenuation from vertical seismic profiles. Geophysics, 46: 1548-1558.

Isenhower, W.M., 1980. Torsional Simple Shear/Resonant Column Properties of San Francisco Bay Mud. MS. Thesis, The University of Texas at Austin

Ishihara, K. 1986. Evaluation of Soil Properties for Use in Earthquake Response Analysis. In Geomechanical Modelling in Engineering Practice, Edited by R. Dungar and J.A. Studer, A.A. Balkema Publishers, Rotterdam, Netherlands.

Ishihara, K. 1996. Soil Behavior in Earthquake Geotechnics, Oxford University Press Inc., New York.

Iwasaki, T., Tatsuoka, F., and Takagi, Y. 1978. Shear Modulus of Sands under Cyclic Torsional Shear Loading. Soils and Foundations, 18(1), 39-56.

Jafarzadeh, F. Sadeghi, H. 2011. Experimental study on dynamic properties of sand with emphasis on the degree of saturation. Soil Dynamic sand Earthquake Engineering 32 (2012) 26 – 41.

Jiang, Z. Ponniah, J., and Cascante, G., Haas, R., 2011. Innovative Nondestructive Test Method for Condition Assessment of Hot Mix Asphalt Mixtures. Canadian Journal of Civil Engineering.

Johnston, D.H. 1981. Seismic Wave Attenuation. Geophysics Reprint Series, No. 2. Society of Exploration Geophysicists. Tulsa, Oklahoma, p. 123-135.

Jones, T.D. 1986. Pore Fluids and Frequency-Dependent Wave Propagation in Rocks. Geophysics, v. 51, p. 1939-1953.

Kallioglou, P., Tika, T., Koninis, G., & St.Pitilakis, K. (2009). Shear Modulus and Damping Ratio of Organic Soils. Geotechnical and Geological Engineering , 217-235.

Khan, Z. H., Cascante, G., and El Naggar, M.H. 2011. Frequency dependent dynamic properties from resonant column and cyclic triaxial tests. Journal of the Franklin Institute 348 2011 1363 – 1376

Khan, Z. H., Cascante, G., and El Naggar, M.H., 2008a. Linearity of the first torsional mode of vibration and base fixidity in resonant column. ASTM, Geotechnical Testing Journal, 31(1): 587 - 606.

Khan, Z. H., Cascante, G., El Naggar, M.H., and Lai, C. 2008b. Measurement of frequency-dependent dynamic properties of soils using the Resonant-Column device. Journal of Geotechnical and Geoenvironmental Engineering, ASCE, 134(9): 1319-1326.

Kim, D.S., 1991. Deformational Characteristics of Soils at Small to Intermediate Strains from Cyclic Tests. PhD. Thesis, The University of Texas at Austin.

Kim, D.-S., and Stokoe, K. H. 1995. Deformational Characteristics of Soils at Small to Medium Strains. Earthquake Geotechnical Engineering, Tokyo, Japan, 89-94.

Kjartansson, E., 1979, “Constant Q-wave Propagation and Attenuation”, Journal of Geophysical Research, 84: 4737-4748

Kramer, S. L. 1996. Geotechnical Earthquake Engineering, Prentice Hall, New Jersey.

Lai, C. G., Meza-Fajardo, K. C., 2007, On the implications of the principle of physical causality in the propagation of seismic waves in geomaterials. Rivista Italiana Di Geotecnica.

Lai, C. G., Pallara, O., Lo Presti, D. C. and Turco, E. (2001). "Low-strain stiffness and Material Damping Ratio Coupling in Soils." Advanced Laboratory Stress-strain

Testing of Geomaterials, Tatsuoka, T., Shibuya, S., and Kuwano, R. Eds, Balkema, Lisse, pp: 265-274.

Liu, H.P., Anderson, D.L., and Kanamori, H. 1976, "Velocity Dispersion due to Anelasticity: Implications for Seismology and Mantle Composition", Geophysical Journal Royal Astronomical Society, 47: 41-58

LIU, F., 2010. Research on consolidation pressure correlated dynamic properties model of clay and its application. Rock and Soil Mechanics .

Lodde, P.F., 1982. Dynamic Response of San Francisco Bay Mud. M.S. Thesis, The University of Texas at Austin.

Lo Presti, D.C.F., and Pallara, O. 1997, "Damping Ratio of Soils from Laboratory and In-situ Tests", Proceddings, 14th International Conference on Soil Mechanics and Foundation Engineering, Hamburg, Germany, pp: 6-12

Lo Presti, D.C.F., Jamiolkowski, M., Pallara, O., and Cavallaro, A. 1996, "Rate and Creep Effect on the Stiffness of Soils", Proc. Conference on Measuring and Modeling Time Dependent Soil Behavior, Held in Conjunction with the ASCE National Convention, Washington D.C., USA.

Lovelady, P. L. and Picornell, M. 1990, "Sample coupling in resonant column testing of cemented soils." Dynamic Elastic Modulus Measureemnt in Materials, ASTM STP 1045, Philadelphia.

Malagnini, L., 1996, "Velocity and Attenuation Structure of Very Shallow Soils: Evidence for Frequency Dependent Q", Bulletin of Seismological Society of America, 86(5): 1471-1486.

Mott, G. and Wang, J., 2010, The effects of variable soil damping on soil-structure dynamics. Journal of Vibration and Control 2011 17: 365.

Murphy, W.F. 1982. Effects of Partial Water Saturation on Attenuation in Massilon Sandstone and Vycor Porous Glass. Journal of the Acoustical Society of America 71(6), June, p. 1458-1467.

Murphy, W.F., Winkler K.W. and Kleinberg R.L. 1984. Frame Modulus Reduction in Sedimentary Rocks: The effect of Adsorption on Grain Contacts. Geophysical Research Letters. v. 1, p. 805-808.

Naggar, M. H. 2008. Dynamic Properties of Soft Clay and Loose Sand from Seismic Centrifuge Tests. Geotechnical and Geological Engineering, 593-602.

NBCC, 2010. National Building Code of Canada 2010. National Research Council of Canada, NRCC 38726, Ottawa, 571 pp.

O'Connell, R.J., and Budiansky, B. 1978, "Measures of Dissipation in Viscoelastic Media", Geophysical Research Letters, 5: 5-8

Pak, J. C. 2010. Application of Random Vibration Techniques to Resonant Column Testing. GeoFlorida 2010: Advances in Analysis, Modeling, & Design. Proceedings of the GeoFlorida 2010 Conference.

Pipkin, A.C. 1986, "Lectures on Viscoelasticity Theory", 2nd Edition, Springer-Verlag, Berlin, pp. 188.

Raptakis, D. G., 2011, Pre-loading effect on dynamic soil properties: Seismicmethods and their efficiency in geotechnical aspects, Soil Dynamics and Earthquake Engineering 34 (2012) 69 – 77.

Read, W. T. J. 1950. "Stress Analysis for Compressible Viscoelastic Materials", Journal of Applied Physics, 21, 671-674.

Richart F. E., Hall J. R. and Woods R. D. 1970. Vibrations of soils and foundations. Prentice Hall, Englewood Cliffs, pp: 414.

Rix, G. J., and Meng, J. 2005. A non resonance method for measuring dynamic soil properties., Geotechnical Testing Journal, 28(1), pp.1-8.

Santamarina, J. C., Klein, K. A., and Fam, M. A. 2001. Soils and Waves. John Wiley & Sons, New York.

Schuettpelz, C. C., Fratta, D., 2010. Mechanistic Corrections for Determining the Resilient Modulus of Base Course Materials Based on Elastic Wave Measurements. Geotechnical and Geoenvironmental Engineering, 1086–1094.

Shibuya, S., Mitachi, T., Fukuda, F., and Degoshi, T. (1995). "Strain-Rate Effects on Shear Modulus and Damping of Normally Consolidated Clay." Geotechnical Testing Journal, 18(3), 365-375.

Stokoe, K.H. II, Hwang, S.K., Lee, J.N.-K, and Andrus, R.D. 1994. Effects of various parameters on stiffness and damping of soils to medium strains, Proceedings, International Symposium on Prefailure Deformation Characteristics of Geomaterials, Vol. 2, Japanese Society of Soil Mechanics and Foundation Engineering, Sapporo, Japan, September, 785-816.

Stokoe, K., and Isenhower M., 1980. Dynamic Properties of Offshore Silty Samples. Proceedings of the 12th Annual Offshore Technology Conference. Houston, Texas.

Stoll, Robert D., 1978. Damping in Saturated Soil. Proc. Specialty Conf. on Earthquake Engineering and Soil Dynamics, ASCE, New York, p. 969-975.

Stoll, Robert D., 1979. Experimental Studies of Attenuation in Sediments a). Acoustical Society of America 66(4), October, p. 1152-1160.

Stoll, Robert D., 1984. Computer-Aided Measurements of Damping in Marine Sediments. Computational Methods and Experimental Measurements. 3.29-3.39.

Stoll, Robert D., 1985. Computer-Aided Studies of Complex Soil Moduli. Measurement and Use of Shear Wave Velocity for Evaluating Dynamic Soil Properties, Richard W. May, p. 18-33.

Tallavo, F., Cascante, G. and Pandey, M. D., 2011. Estimation of the Probability Distribution of Wave Velocity in Wood Poles, Journal of Materials in Civil Engineering, ASCE.

Toksöz, M. N., Johnston, D. H., and Timur, A. 1979. Attenuation of seismic waves in dry and saturated rocks: I. Lab. Meas. Geophysics, 44(4): 681-690.

Toll, J.S. 1956. Causality and the dispersion relation: logical foundations. Physical Review, 104(6): 1760-1770.

Tschoegl, N. W. 1989. The Phenomenological Theory of Linear Viscoelastic Behavior, An Introduction, Springer-Verlag, Berlin Heidelberg, pp: 769.

Tsui, Y.-H. W.-Y. 2009. Experimental Characterization of Dynamic Property Changes in Aged Sands. Journal of Geotechnical & Geoenvironmental Engineering , 12.

Turan, A., Hinchberger, S., & El Naggar, M. (2009). Mechanical Characterization of an Artificial Clay. Journal of Geotechnical & Geoenvironmental Engineering , 11.

Vinod, T. G. 2010. Evaluation of Shear Modulus and Damping Ratio of Granular Materials Using Discrete Element Approach. Geotechnical and Geological Engineering, 28 (5), 591-601.

Vucetic, M. 1994. "Cyclic Threshold Shear Strains in Soils." Journal of Geotechnical Engineering, ASCE, 120(12), 2208-2228.

Vucetic, M., and Dobry, R. 1991, “Effect of Soil Plasticity on Cyclic Response”, Journal of Geotechnical Engineering, ASCE, 117(1): 89-107

Wang, Z., and Nur, A. 1992. Elastic Wave Velocities in Porous Media: A Theoretical Recipe. Seismic and Acoustic Velocities in Reservoir Rocks. vol. 2, 1-35.

White, J.E., 1975. Computed Seismic Speeds and Attenuation in Rocks with Partial Gas Saturation. Geophysics, v. 40, p. 224-232.

Wilson, S.D., and Dietrich, R.J., 1960. Effect of Consolidation Pressure on Elastic and Strength Properties of Clay, Proceedings of the ASCE, Soil Mechanics and Foundations Division, Research Conference on Shear Strength of Cohesive Soils, Boulder, CO.

Winkler, K., Nur, A., and Gladwin, M. 1979. Friction and seismic attenuation in rocks. Nature, 227: 528-531.

Winkler, K., and Nur, A., 1982. Seismic Attenuation: Effects of Pore Fluids and Frictional Sliding. Geophysics. v. 47, p. 1-15.

Woods, R.D., 1978, "Measurement of Dynamic Soil Properties", Proceedings, ASCE Specialty Conference on Earthquake Engineering and Soil Dynamics, Pasadena, California. Vol.1, pp. 91-178.Dobry, R. and Vucetic, M. (1987) State of the art report: Dynamic properties and response of soft clay deposits. Proc. Int. Symp on Geotechnical Engineering of Soft Soils, Vol. 2, 51- 87.

Wu, R., and Aki, K. 1988. Introduction: Seismic wave scattering in three-dimensionally heterogeneous earth. In Scattering and Attenuation of Seismic Waves, Part 1. Edited by K. Aki and R. Wu. Birkhäsuer Verlag. Pp: 1-6.

Yang, Y., Cascante, and Polak, M., 2010. Damping measurements in construction materials using the wavelet transform. Journal of Geotechnical and Geoenvironmental Engineering, ASCE.

Zemanek, J., Jr., and Rudnick, I. 1961. Attenuation and dispersion of elastic waves in a cylindrical bar. The Journal of the Acoustical Society of America, 33: 1283-1288.

APPENDIX A

TRANSFER FUNCTION METHOD

The equation of motion for a specimen subjected to torsional excitation in the resonant column device can be expressed in terms of the displacement, x.

$$J_1 \frac{\ddot{x}}{r_a} + c\frac{\dot{x}}{r_a} + k\frac{x}{r_a} = F\, r_m \qquad \text{[A1]}$$

where F is the force induced by current in the coils, J_1 is the mass polar moment of inertia of the specimen and driving plate ($J_1 = I_o + I/3$), c is the viscous damping coefficient, r_m is the distance of magnets from the center of the specimen, I_o and I are the mass polar moment of inertia of the driving plate and specimen respectively, and r_a is the radial distance of accelerometer from the center of the specimen. Time derivatives are expressed by the dots on top of the appropriate variables.

The force ($F = B_L\ I_C$) applied to the driving plate is proportional to the current (I_C) amplitude in the coils and the magnetic force factor of the coils. Defining the stiffness of the specimen (k) as the product of ω_o^2 and J_1, Eq. A1 can be written as;

$$J_1 \frac{x}{r_a}(i\omega)^2 + c\frac{x}{r_a}(i\omega) + \omega_o^{\,2} J_1 \frac{x}{r_a} = B_L\, I_C\, r_m \qquad \text{[A2]}$$

$$\frac{x}{r_a}\left[-J_1\,\omega^2 + c(i\omega) + \omega_o^{\,2} J_1\right] = B_L\, I_C\, r_m \qquad \text{[A3]}$$

The angular rotation ($\varphi(\omega)=x/r_a$) can be expressed in terms of displacement (x) and r_a as

$$\varphi(\omega) = \frac{B_L I_C r_m}{\left[-J_1 \omega^2 + c(i\omega) + \omega_o{}^2 J_1\right]} \qquad [A4]$$

$$\frac{B_L I_C r_m}{\varphi(\omega)} = -J_1 \omega_o{}^2 \left[\frac{\omega^2}{\omega_o{}^2} - \frac{c(i\omega)}{J_1 \omega_o{}^2} - \frac{\omega_o{}^2}{\omega_o{}^2} \right] \qquad [A5]$$

$$\frac{B_L I_C r_m}{\varphi(\omega)} = J_1 \omega_o{}^2 \left[1 - \frac{\omega^2}{\omega_o{}^2} + \frac{c(i\omega)}{J_1 \omega_o{}^2} \right] \qquad [A6]$$

Viscous damping coefficient is expressed in terms of material damping ratio (ξ) and mass polar moment of inertia of the system as $c = 2 J_1 \omega_o \xi$. Substitution in Eq. A6 yields;

$$\frac{B_L I_C r_m}{\varphi(\omega)} = J_1 \omega_o{}^2 \left[1 - \left(\frac{\omega}{\omega_o} \right)^2 + i \frac{2 J_1 \omega_o \xi(\omega/\omega_o)}{J_1 \omega_o} \right] \qquad [A7]$$

$$\frac{T_o(\omega)}{\varphi(\omega)} = \left(I_o + \frac{I}{3} \right) \omega_o{}^2 \left[1 - \left(\frac{\omega}{\omega_o} \right)^2 + i2 \xi \left(\frac{\omega}{\omega_o} \right) \right] \qquad [A8]$$

where $T_o(\omega)$ is the applied torque to the system.

APPENDIX B

COMPARISON OF DIFFERENT METHODS OF RC TESTING

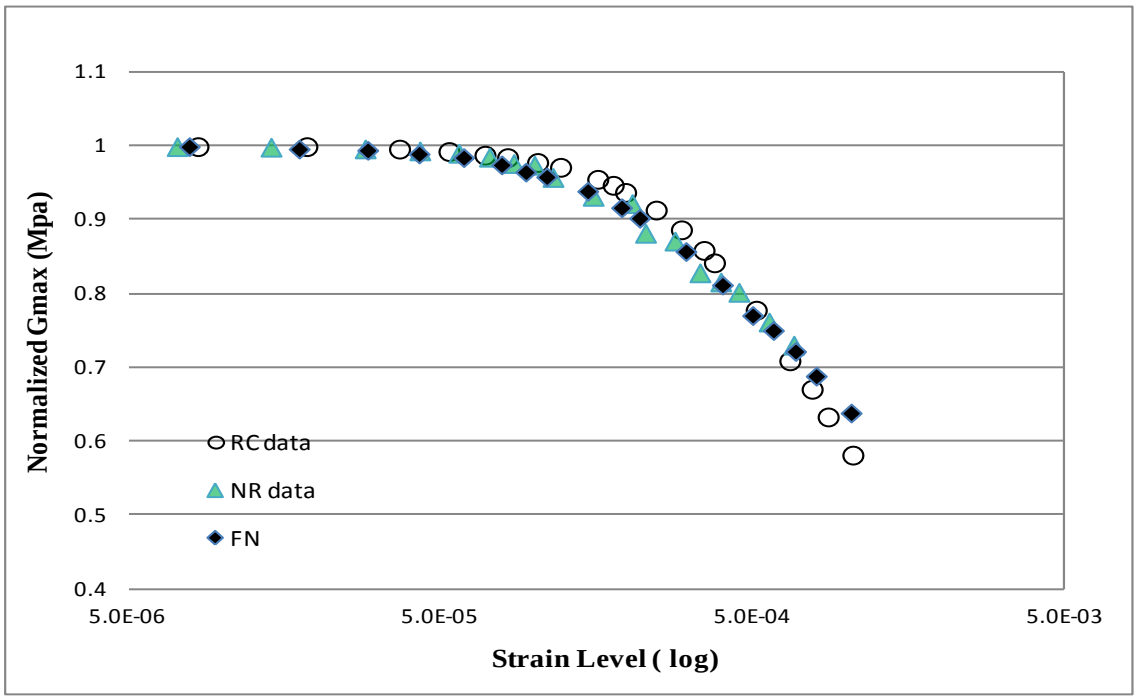

Figure B1. Comparison of Shear modulus calculated by FN, NR and RC Method In Leda Clay.

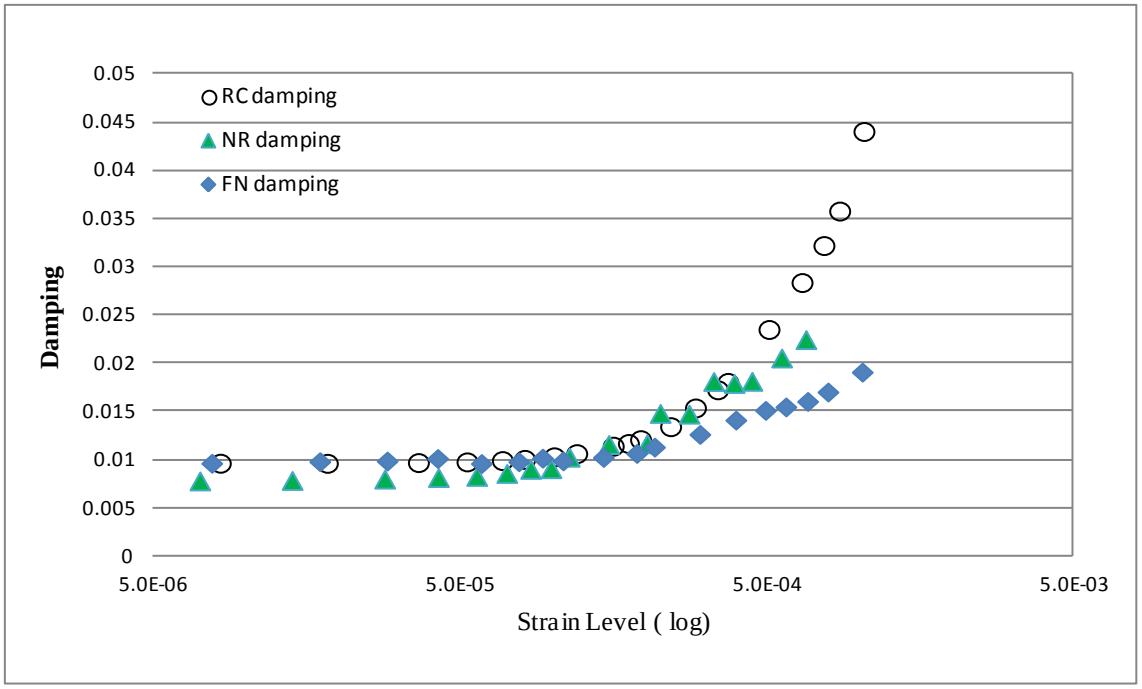

Figure B2. Comparison of Damping calculated by FN, NR and RC Method in Leda Clay.

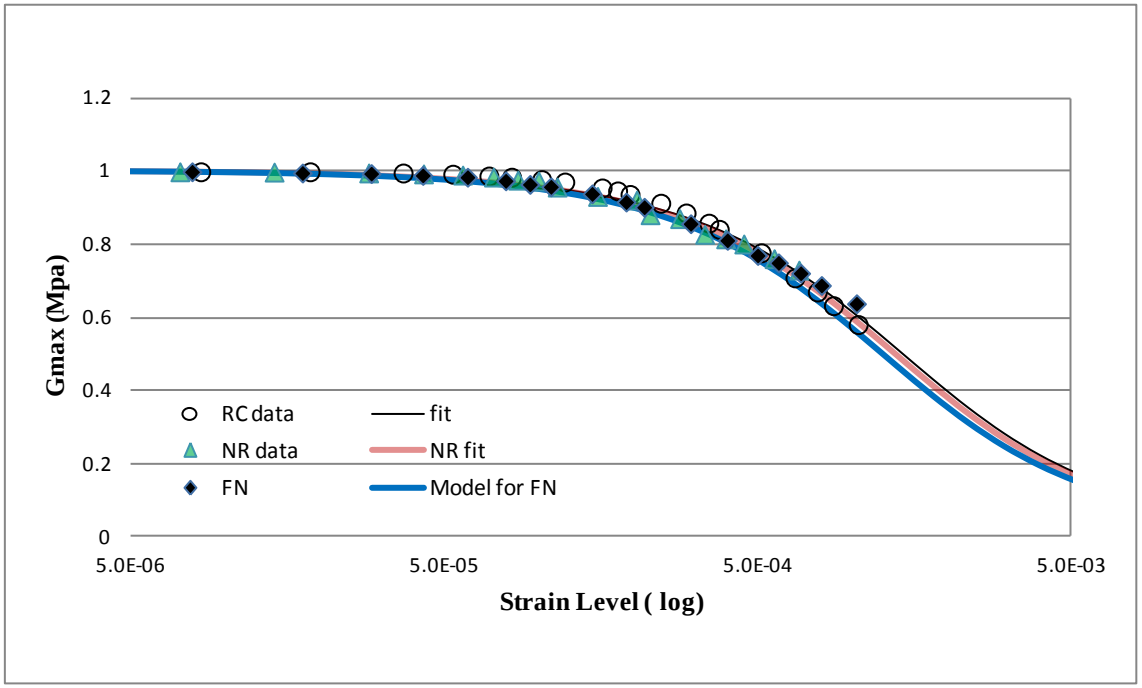

Figure B3. Comparison of Shear modulus calculated by FN, NR and RC Method In Leda Clay and curve fit with theoretical TF for each one.

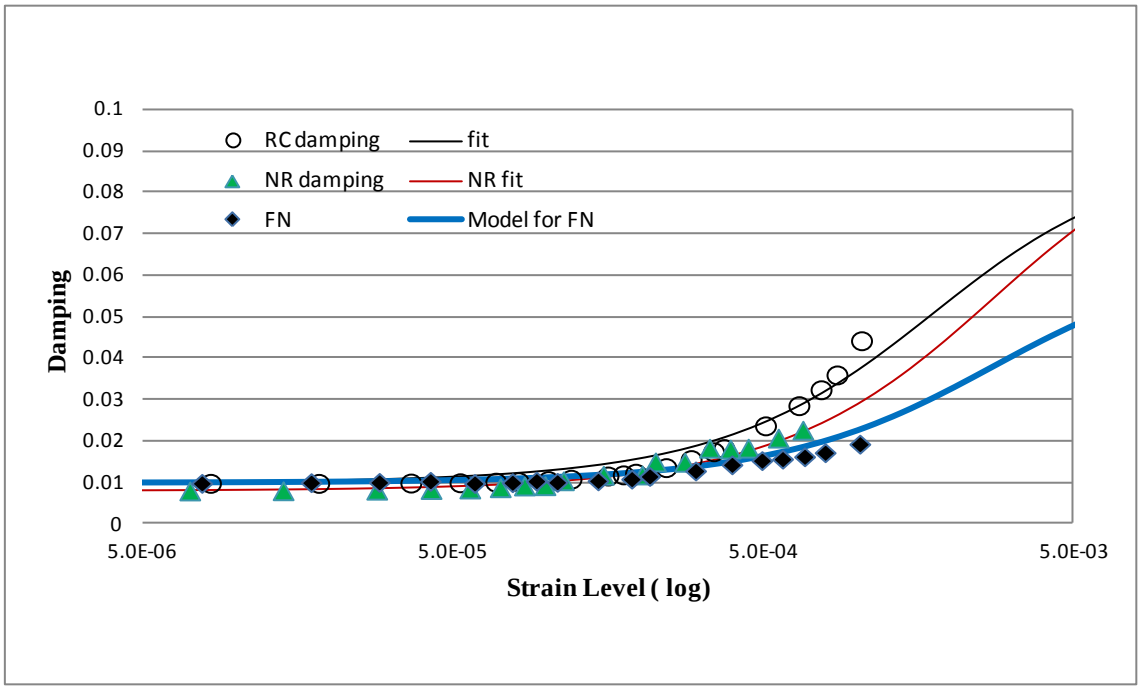

Figure B4. Comparison of Shear modulus calculated by FN, NR and RC Method In Leda Clay and curve fit with theoretical TF for each one.

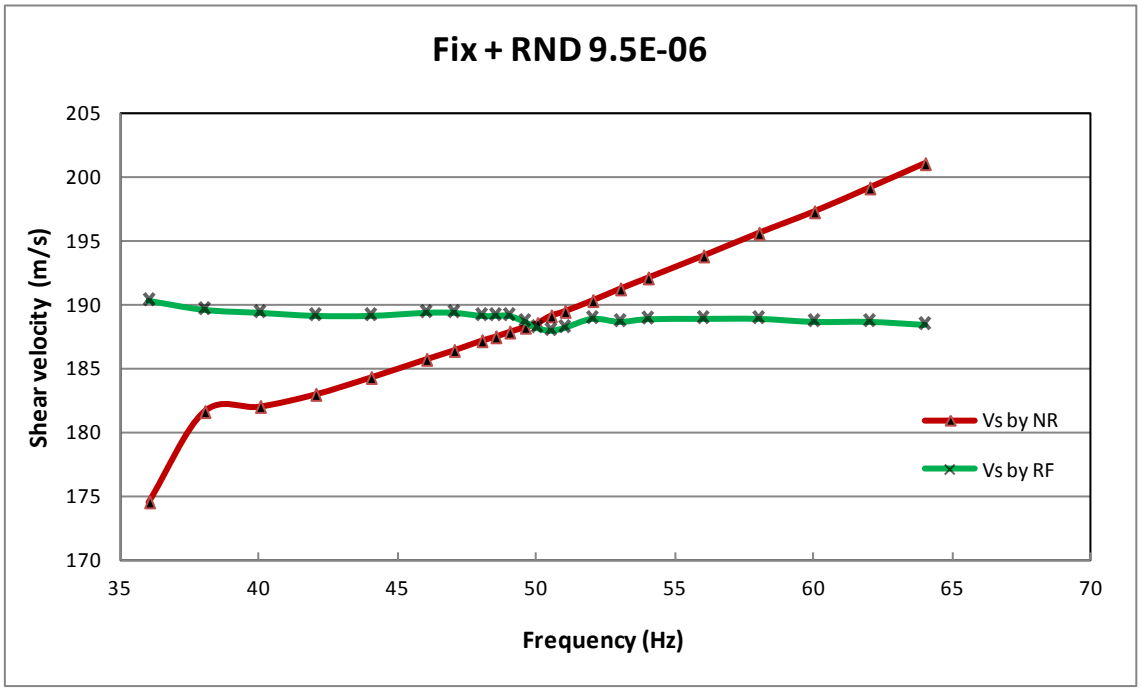

Figure B5. Comparison of Shear modulus calculated by NR and FN Method In Sand.

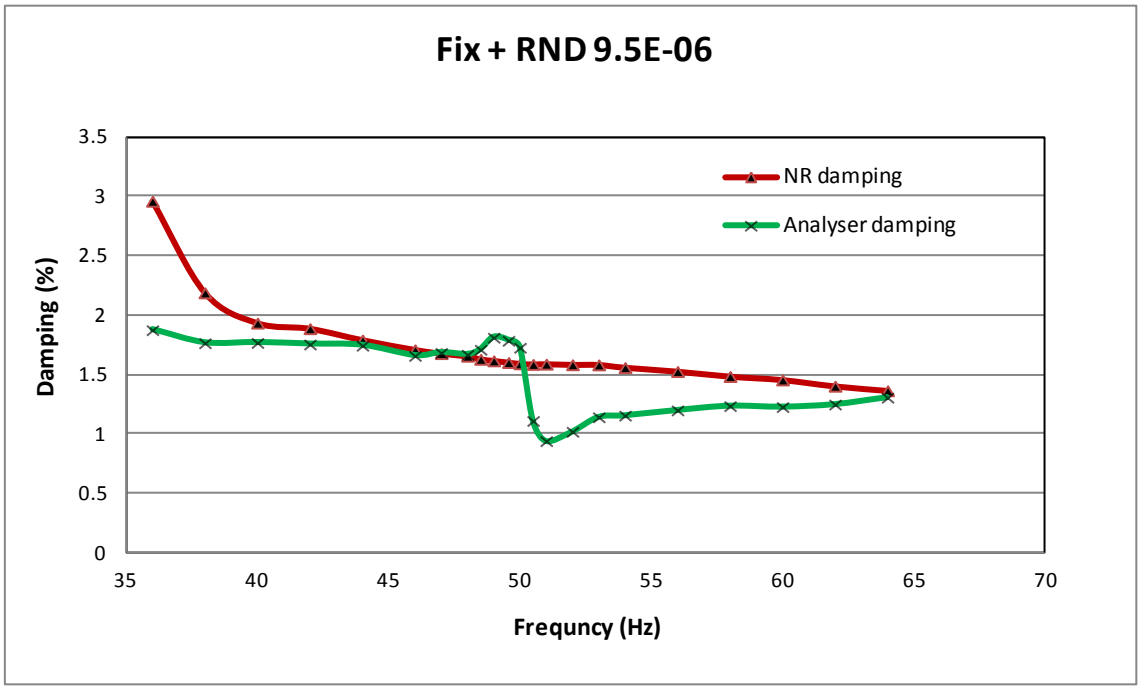

Figure B6. Comparison of Damping calculated by FN, NR and RC Method in Sand.

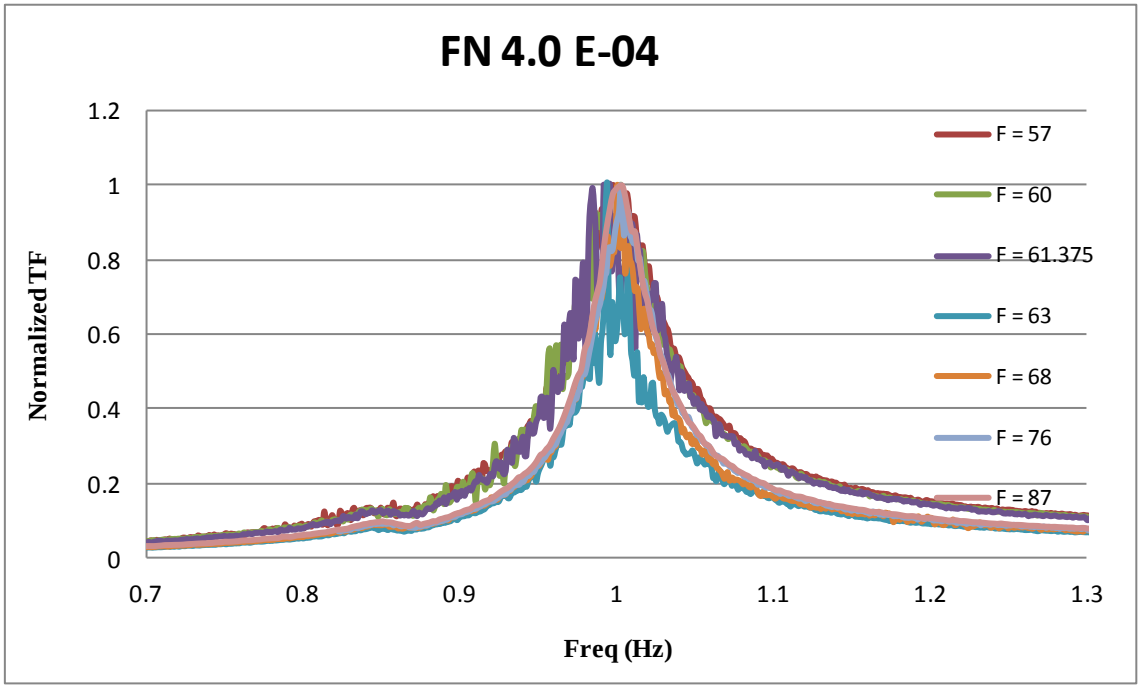

Figure B7. Normalized TF at different frequency in high strain level using FN method.

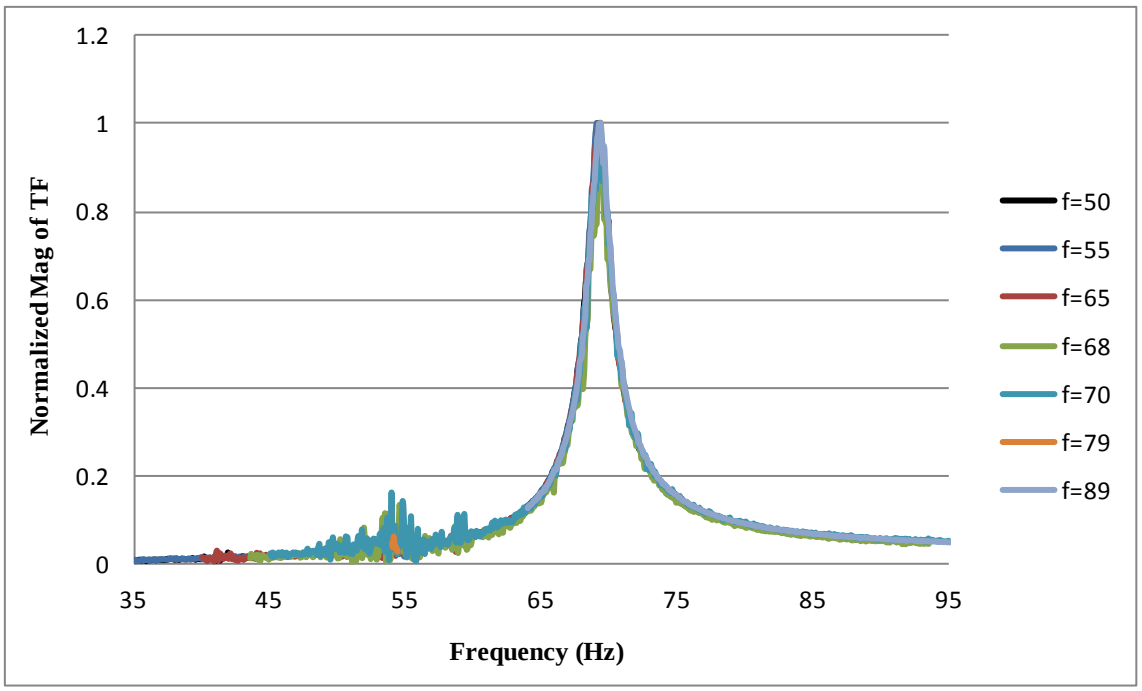

Figure B8. Normalized TF at different frequency in Low strain level using FN method

APPENDIX C

SOLUTION FOR NON RESONANCE (NR) METHOD

Shear stress on the element in a cylindrical specimen with negligible damping coefficient is given by

$$\tau(z,r,t) = G\, r\, \frac{d\theta}{dz} \qquad \text{[C1]}$$

$d\Theta/dz$ is angle of twist per unit length, r is radial distance from center, and G is shear modulus

$$T(z,t) = G\, J\, \frac{d\theta}{dz} \qquad \text{[C2]}$$

J is area polar moment of inertia. Applying Newton's 2nd law of motion to element with length *dz*

$$\frac{dT}{dz} = \rho\, J\, \frac{d^2\theta}{dt^2} \qquad \text{[C3]}$$

where ρ is the mass density. Taking derivative of Eq. C2 w.r.t. z and substituting in Eq.C3

$$\frac{d^2\theta}{dt^2} = \frac{G}{\rho}\, \frac{d^2\theta}{dz^2} \qquad \text{[C4]}$$

The displacement function can be assumed as

$$\theta(z,t) = u(z)\left[\cos(\omega t) + \sin(\omega t)\right] \qquad \text{[C5]}$$

where *u(z)* is spatial function defined by boundary conditions. By differentiating Eq. C5 w.r.t. z and t and substituting in Eq. C4, following relationships are obtained.

$$-\omega^2 \left[u(z)\left(\cos(\omega t)+\sin(\omega t)\right)\right]=\frac{G}{\rho}\left[u''(z)\left(\cos(\omega t)+\sin(\omega t)\right)\right]$$

$$\left(\frac{G\,u''(z)}{\rho\,\omega^2}+u(z)\right)\left(\cos(\omega t)+\sin(\omega t)\right)=0$$

Let u(z) = $e^{\lambda z}$, then the taking the double derivative w.r.t. z and substitution can be solved for the two roots of λ.

$$\frac{G}{\rho}u''(z)+\omega^2\,u(z)=0$$

$$G\,\lambda^2\,u(z)+\rho\,\omega^2\,u(z)=0$$

$$G\,\lambda^2+\rho\,\omega^2=0$$

$$\lambda\ =\left(\pm i\frac{\omega}{Vs}\right)$$

Then u(z) can be defined as Eq. C6 and can be rewritten as Eq. C7.

$$u(z)=A_1\,e^{i\frac{\omega}{Vs}z}+A_2\,e^{-i\frac{\omega}{Vs}z} \qquad \text{[C6]}$$

$$u(z)=C_3\,\cos\left(\frac{\omega}{Vs}z\right)+C_4\sin\left(\frac{\omega}{Vs}z\right) \qquad \text{[C7]}$$

The first boundary condition is that the displacement at fixed end is zero (z=0) Then Eq. C5 becomes:

$$\theta(0,t)=u(0)\left[\cos(\omega t)+\sin(\omega t)\right]=0$$

By applying this boundary condition we know that u(0)=0 and hence c_3=0. Hence the equations for u(z) can be simplified to

$$u(z) = C_4 \sin\left(\frac{\omega}{Vs} z\right) \qquad \text{[C8]}$$

The second boundary condition is that the forces at top should satisfy the the equation of motion, hence,

$$T(L,t) = -I_o \frac{d^2\theta(L,t)}{dt^2} + T_o \sin(\omega t)$$

Substituting T(L,t) from Eq. C2

$$I_o \frac{d^2\theta(L,t)}{dt^2} + G\ J\ \frac{d\theta}{dz} = T_o \sin(\omega t)$$

$$I_o \frac{d^2\theta(L,t)}{dt^2} + \frac{G\,I}{\rho\,L} \frac{d\theta}{dz} = T_o \sin(\omega t) \qquad \text{[C9]}$$

By differentiating Θ(z,t) with respect to z and t and setting z = L Eq. C9 becomes

$$\frac{G\,I}{\rho\,L} u'(L) - I_o\,\omega^2\,u(L) = T_o$$

$$\frac{G\,I}{\rho\,L} \frac{\omega}{Vs} \cos\left(\frac{\omega L}{Vs}\right) - I_o\,\omega^2 \sin\left(\frac{\omega L}{Vs}\right) = \frac{T_o}{C_4} \qquad \text{[C10]}$$

At resonance the amplitude of twist C_4 should approach to infinity and therefore

$$\frac{G\,I}{\rho\,L} \frac{\omega_o}{Vs} \cos\left(\frac{\omega_o L}{Vs}\right) - I_o\,\omega_o{}^2 \sin\left(\frac{\omega_o L}{Vs}\right) = 0$$

$$\frac{I}{I_o} = \left(\frac{\omega_o L}{Vs}\right) \tan\left(\frac{\omega_o L}{Vs}\right) \qquad \text{[C11]}$$

Similarly Eq. C10 can be rearranged and by setting $\beta = \omega\,L/Vs$

$$\frac{T_o}{C_4} = \frac{G\,J\,\omega}{Vs}\left[\cos(\beta) - \frac{I_o}{I}\frac{\omega\,L}{Vs}\sin(\beta)\right]\frac{\sin(\beta)}{\sin(\beta)}$$

$$\frac{T_o}{C_4\sin(\beta)} = Vs\,\rho\,J\,\omega\left(\cot(\beta) - \frac{I_o\,\beta}{I}\right)$$

$$\frac{T_o}{u(L)} = Vs\,\rho\,\omega\,J\cot(\beta) - Vs\,\rho\,\omega\,J\frac{I_o\,\beta}{I}$$

$$\frac{T_o}{u(L)} = Vs\,\rho\,\omega\,J\cot(\beta) - Vs\,\rho\,\omega\frac{I}{\rho\,L}\frac{I_o\,\omega\,L}{I\,Vs}$$

$$\frac{T_o}{u(L)} = Vs\,\rho\,\omega\,J\cot(\beta) - I_o\,\omega^2$$

$$\frac{T_o}{u(L)} = \frac{\omega\,L}{\omega\,L}Vs\,\rho\,\omega\,J\cot(\beta) - I_o\,\omega^2$$

$$\frac{T_o}{u(L)} = \frac{\pi\,R^4}{2}\,\frac{\rho\,\omega^2\,L}{\beta\tan(\beta)} - I_o\,\omega^2 \qquad \text{[C12]}$$

Equation C12 is the non-resonance frequency equation which can be solved for complex b. Equation C12 should be also approach 0 at resonance for negligible damping and yield Eq. C11.